A RESEARCH STUDY ON INTERNAL CORROSION OF HIGH-PRESSURE BOILERS

• • • •

FINAL REPORT

by

P. GOLDSTEIN, Senior Project Engineer
Steam and Water Division

C. L. BURTON, Senior Project Engineer
Mechanical Division
Kreisinger Development Laboratory
Combustion Engineering, Inc.
Windsor, Connecticut

This is the final report on an investigation performed under the sponsorship of the American Society of Mechanical Engineers with joint financial support by the Edison Electric Institute, Industry, and others concerned with the operation of high pressure boilers.

[Nobs-94516]

Presented at

ASME - EEI CORROSION SEMINAR

Hartford, Connecticut

May 21-22, 1968

ABSTRACT

The following report is the last in a series of four describing the progress and results of "A Research Study on Internal Corrosion of High Pressure Boilers." The first three reports described the background, scope, and organization of the program, as well as the test facility and the results of Phases I, II, and III. This final report includes the results of the eight Phase IV tests and a discussion of the results and conclusions from the entire program.

Phase IV test results include data and observations on plug-type corrosion and hydrogen damage. The discussion of results describes the mechanisms involved in these types of attack, as well as the causes of caustic gouging. Observations on chemical hideout and deposition are discussed in addition to the heat transfer and fluid flow phenomena involved in nucleate boiling and departure from nucleate boiling.

The American Society of Mechanical Engineers
United Engineering Center/345 E. 47th St., New York, N.Y. 10017/212-752-6800

RESEARCH COMMITTEE ON
BOILER FEEDWATER STUDIES

June 28, 1968

TO: Sponsors

SUBJECT: Final Report - Research Study on Internal Corrosion in High Pressure Boilers

The Steering Committee is pleased to present this final report to the Sponsors.

The goal of this study was to determine the cause and practical preventive solution for the type of internal corrosion commonly experienced in units operating at pressures between 800 and 2600 psig. It is the opinion of the Steering Committee that this goal has been met in every sense.

We believe that the results obtained by Combustion Engineering during the study are reliable and are applicable to modern power plant practice. We wish to emphasize that the conclusions presented in the attached report are unanimously endorsed by the Steering Committee and that we place a great confidence in the work that supports them.

Sincerely,

J. K. Rice

J. K. Rice, Chairman
Steering Committee

JKR/cr

INTRODUCTION

Previous progress reports (1, 2, 3) describe the background and results of the original three-phase research program. Based upon these results and the success of the short duration screening test concept, plans for conducting longer term tests were set aside. Phase IV was, therefore, conducted as a series of short duration tests. This final report defines the results of Phase IV, summarizes the previous research, and presents conclusions drawn from the entire program.

Table I summarizes the experimental conditions for Phases II, III, and IV in terms of boiler water treatment and contaminants employed, as well as other key variables which were studied. Throughout Phase IV, a review of test results and modification of test conditions were carried out in order to obtain the most meaningful data within the general framework of program goals. For this reason, the Phase IV conditions listed in Table I vary from the projected conditions included in a previous report (3). In addition, the program was expanded by one test.

The first progress report (1) defined the goal of the corrosion studies as: "to determine the cause and practical preventive solutions for the type of internal corrosion commonly experienced in units operating at pressures between 800 to 2600 psig". Three categories of attack were listed as being of major interest:

1. Ductile gouging or pitting attack
2. Hydrogen damage or embrittlement
3. Plug-type oxidation

All three types of attack were reproduced and studied during testing. Causes have been defined and preventive solutions are suggested by the data. In addition, pertinent data on and observations relating to deposition, chemical hideout, heat transfer, and the physical chemistry of high-temperature boiler water solutions have been made.

TEST APPARATUS

The heat transfer and corrosion test loop shown in Fig. 1 was described in the first progress report (1). Modifications to the make-up water supply system, horizontal preheat furnace, and the addition of a reflux condenser were discussed in the second progress report (2). The apparatus used for Phase IV testing was unchanged, with the exception of the power control system.

TABLE I

PROGRAM ORGANIZATION

Phase No.	Group	Test No.	Treatment	Boiler Condition	Boiler Water Contamination
II	—	1	Volatile	Clean	None
		2	Phosphate	Clean	None
		3	Caustic	Clean	None
III	A	1	Volatile	Dirty—Fe_3O_4 + Cu	None
		2	Phosphate	Dirty—Fe_3O_4 + Cu	None
		3	Caustic	Dirty—Fe_3O_4 + Cu	None
	B	1	Volatile	Dirty—Fe_3O_4 + Cu	Fresh water salts
		2	Phosphate	Dirty—Fe_3O_4 + Cu	Fresh water salts
		3	Caustic	Dirty—Fe_3O_4 + Cu	Fresh water salts
	C	1	Volatile	Dirty—Fe_3O_4 + Cu	Seawater salts
		2	Phosphate	Dirty—Fe_3O_4 + Cu	Seawater salts
		3	Caustic	Dirty—Fe_3O_4 + Cu	Seawater salts
IV	—	1	Volatile	Dirty—Fe_3O_4 + Cu	Fresh water salts
		2	Phosphate	Dirty—Fe_3O_4 + Cu	Fresh water salts
		3	Caustic	Dirty—Fe_3O_4 + Cu	Fresh water salts
		4	Phosphate	Dirty—Fe_3O_4 + Cu	Magnesium chloride
		5	Caustic	Dirty—Fe_3O_4 + Cu	Magnesium chloride
		6	Phosphate	Dirty—Fe_3O_4 + Cu	None (Test in DNB)
		7*	Phosphate	Dirty—Fe_3O_4 + Cu	Magnesium chloride
		8	Phosphate	Dirty—Fe_3O_4 + Cu	Calcium sulfate Calcium chloride

* Continuous $MgCl_2$ injection and PO_4 treatment.

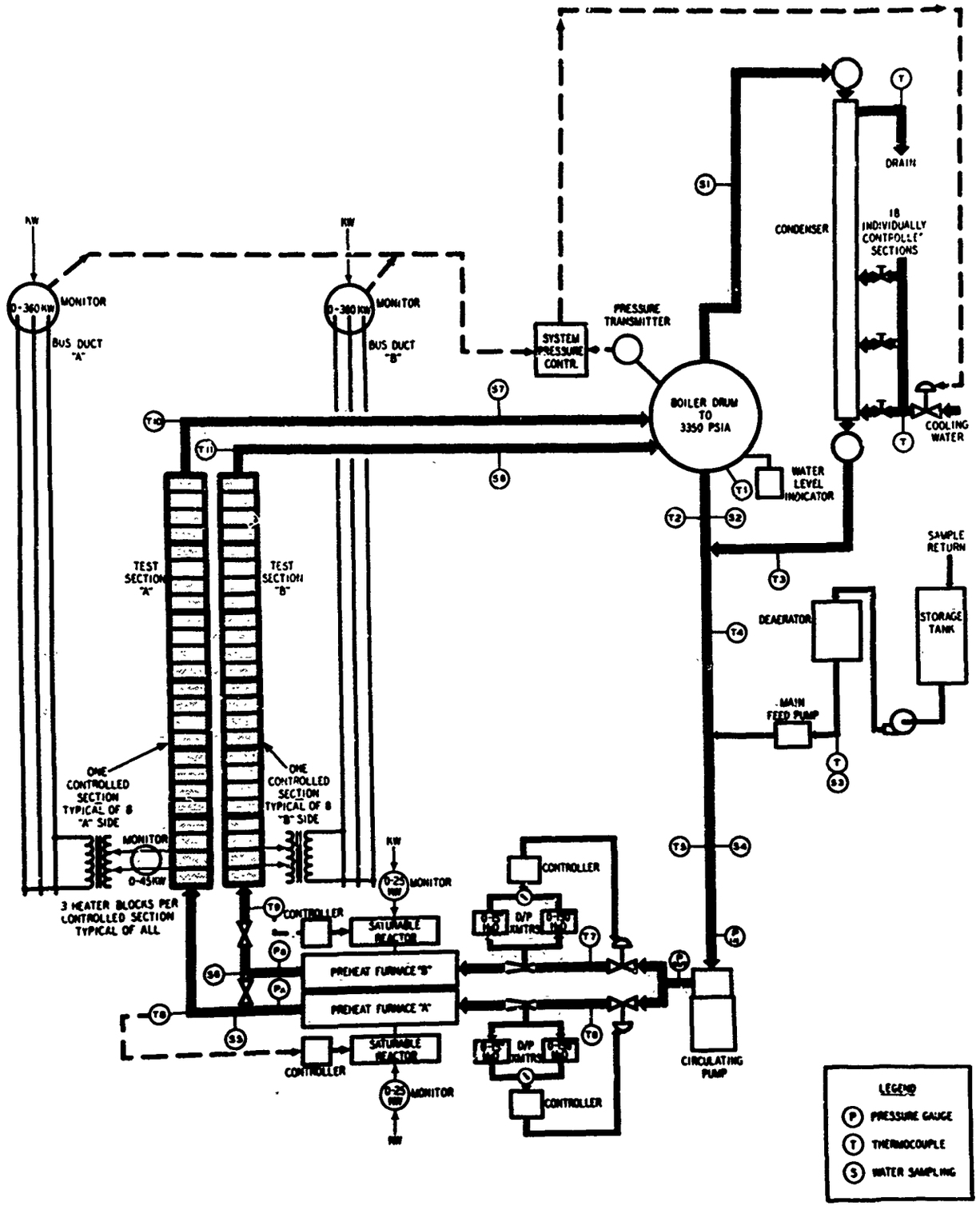

Fig. 1: Schematic of test loop employed for heat transfer and corrosion research

Test objectives required that at least one test be conducted in departure from nucleate boiling (DNB). The previous arrangement for controlling electrical power input is shown in Fig. 2. Total power and local heat transfer rates were controlled using manually operated, tapped secondary transformers for both the vertical preheat and test sections. Manually operated saturable reactors were used for controlling the horizontal preheat furnace. Normal line voltage variations produced slight changes in fluid enthalpy and local flux rates during testing with this arrangement.

Satisfactory operation of the test loop in DNB required that line voltage variations be stabilized. A relatively new and unique technique employing silicon controlled rectifiers (SCR) was used to accomplish this. Figure 3 illustrates the application of SCR control to the "A" loop power supply. Total power to the test section is monitored and recorded by a strip chart recorder-controller. The instrument set point is manually adjusted to obtain the proper power level for the desired heat flux. A signal from the controller to the SCR cells and firing networks subsequently adjusts the power output of the SCR to maintain constant flux by automatically compensating for variations in line voltage.

Similarly, the total power of the horizontal and vertical preheaters is measured and fed to another recorder-controller. Compensation for line voltage variations to obtain constant enthalpy at the test section entrance is automatically achieved in this sub-system by set-point control of the power output of the saturable reactors.

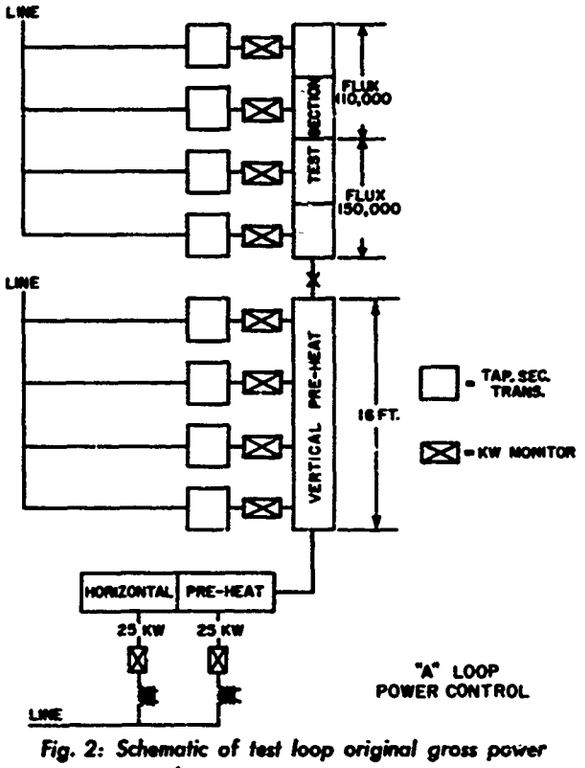

Fig. 2: Schematic of test loop original gross power control

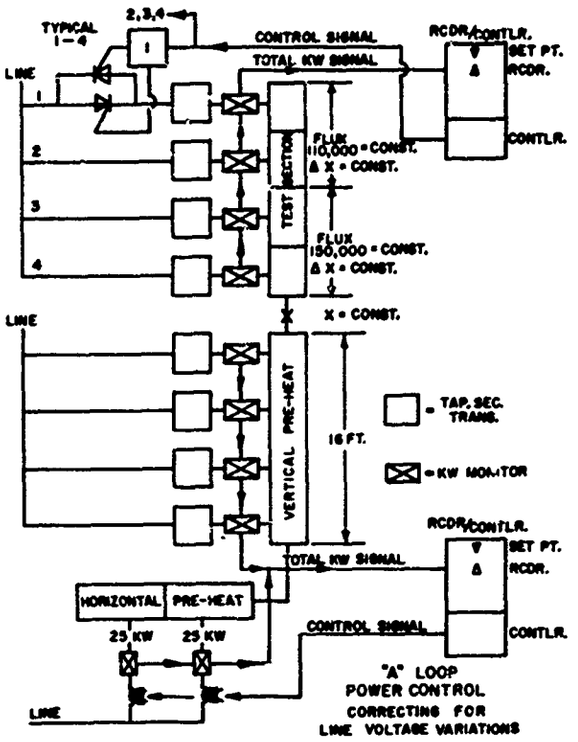

Fig. 3: Schematic of test loop modified power control

TEST CONDITIONS

Test Sections — Commercial, 1½-in., 0.200-in. wall, SA-192 carbon steel tubing was used for corrosion testing. Details relating to the composition and structure of this material were included in the second progress report (2).

Water Chemistry — Control chemistry specifications are listed in Table II. These specifications were maintained when simulated condenser leakage solutions were not being injected into the boiler water. They were applicable to all tests, with the exception of Test 7,

TABLE II

CONTROL CHEMISTRY SPECIFICATIONS

Name Treating Chemical	pH Value at 25 C	Hydroxide ppm OH	Phosphate ppm PO_4
Volatile (NH_3)	8.6 - 9.0	—	—
Phosphate (Na_3FO_4)	9.8 - 10.0	0	9 - 11
Caustic (NaOH)	10.5 - 10.7	As required to maintain pH	2 - 4

Phase IV which was conducted with continuous injection of magnesium chloride solution and continuous phosphate control chemistry. Specifications were relaxed for this test as follows:

$$pH = 9.5 \text{ to } 10.0$$

$$PO_4 = 5 \text{ to } 10 \text{ ppm}$$

Heat Transfer — One of the key concepts of this corrosion research program was the use of relatively short-term screening tests. Thermal and hydraulic test conditions were selected to accelerate corrosion. Heat-transfer rates represented a range of average to maximum values found in operating boilers. The variables employed as accelerating parameters were mass velocity and steam quality.

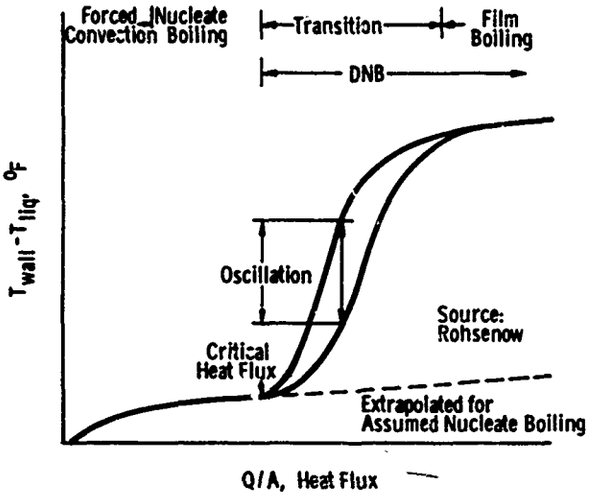

Fig. 4: DNB tube metal temperature history with increasing heat flux compared to an assumed extension of nucleate boiling

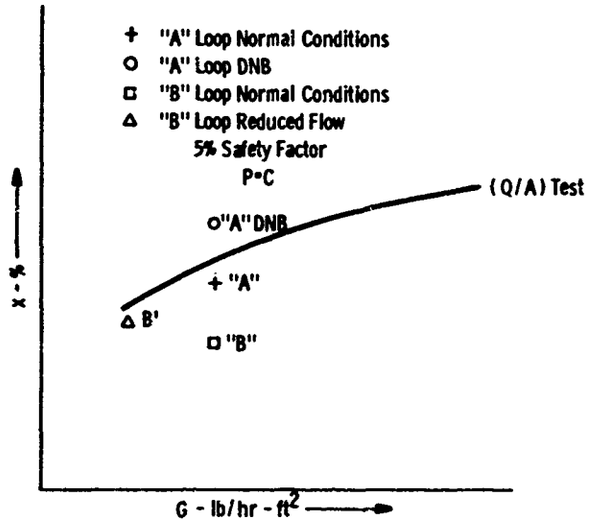

Fig. 5: Loop test conditions shown on a plot of critical parameters

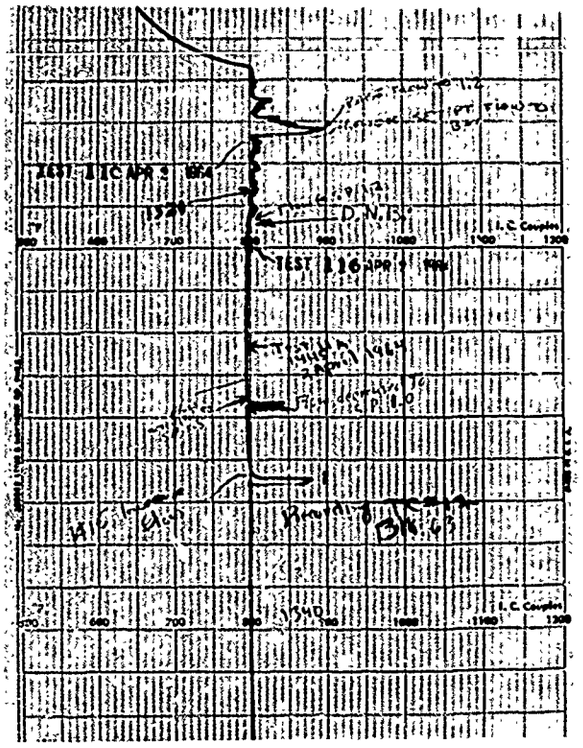

Fig. 6: Typical temperature response to various levels of DNB

The first progress report (1) described Phase I of the program. Briefly, Phase I consisted of a series of tests which defined various combinations of low-mass-flow rates, high steam qualities, and heat-transfer rates which produce departure from nucleate boiling (DNB). Figure 4 illustrates the effects of DNB on tube-metal temperature as a function of local-heat-transfer rate (Q/A). Actual evaluation of the Phase I data and selection of parameters for corrosion testing were made from plots (Fig. 5). In this format, the critical heat flux is shown as the Q/A curve and the critical variables are mass-flow rate (G) and steam quality (X). Values on and above the curve represent DNB conditions and values below the curve nucleate boiling. Plotted points represent the operating conditions employed for this program as specified in the legend.

Figure 6 is a reproduction of a strip chart from a tube metal temperature recorder. Both the temperature increase and instability of DNB operation are shown. The sensitivity of tube metal temperature to both decreases in mass-flow rate and bulk steam quality are illustrated.

Phases II and III were conducted with "A" loop conditions as close to DNB as possible, allowing an operational tolerance of 5 percent quality to compensate for parametric changes induced by line-voltage variations. The same test conditions were employed in the "A" test loop for Phase IV. The "B" loop con-

TABLE III

NOMINAL TEST CONDITIONS

	II, III, IV A Loop	II, III B Loop	IV B Loop	IV (DNB Test) A Loop
Mass velocity (G), lb/hr-ft²	0.55×10^6	0.55×10^6	0.45×10^6	0.55×10^6
Flow rate (W), lb/hr	3,630	3,630	2,970	3,630
*Heat flux $(Q/A)_1$, Btu/hr-ft² (based on ID of tube)	150,000	150,000	150,000	150,000
Heat flux $(Q/A)_1$, Btu/hr-ft² (based on projected area)	173,000	173,000	173,000	173,000
**Approx. heat flux $(Q/A)_2$, Btu/hr-ft² (based on ID of tube)	110,000	110,000	110,000	110,000
Approx. heat flux $(Q/A)_2$, Btu/hr-ft² (based on projected area)	127,000	127,000	127,000	127,000
Approx. quality (X_0) entering test section, %	23	8	20	28
Approx. quality (X_1) leaving $(Q/A)_1$, %	30	15	29	35
Approx. quality (X_2) leaving $(Q/A)_2$, %	35	20	35	40

* $(Q/A)_1$—Heat flux in lower test section.
** $(Q/A)_2$—Heat flux in upper test section.

ditions for Phases II and III consisted of the same mass-velocity and heat-transfer rates as the "A" loop, but much lower steam-quality. Phase IV conditions placed the "B" loop as close to DNB as practical with reduced mass-flow rates and increased steam quality as shown in Table III.

These conditions apply to all Phase IV tests with the exception of Test 6 which was conducted in the unstable transitional boiling region of DNB. Parameters for this test are also listed in Table III ("A" loop only).

TEST PROCEDURES

In most cases, Phase IV test procedures were similar to those employed in Phase III. Briefly summarized, the normal routine for testing was as follows:

1. Thermal, hydraulic, and control chemistry test conditions were established.
2. A short test to determine the critical quality for DNB was run both to check out instrumentation and to establish that no unusual conditions existed at the test surfaces.
3. The loop was operated at normal control conditions until hydrogen concentrations in the steam approached equilibrium base values (passivation).
4. Injection of corrosion products and condenser leakage contamination was begun. The sequence of initial injections of the two types of contaminants was varied depending upon the individual test objectives.
5. Corrosion product contamination was normally added on a two-hour cycle until 2400 grams of iron oxide and copper powder was injected. (Details on the iron oxide and copper contaminants were included in the second progress report (2).)
6. Simulated condenser leakage was normally added to the test loop continuously for an eight-hour period each day. No attempts to maintain control chemistry were made during periods of injection. Table IV summarizes the composition of the condenser leakage contaminants employed, the rates of addition, and the total amounts added to the test apparatus during each test.
7. Control chemistry was re-established after each condenser leakage cycle. Control conditions were maintained for the remaining 16 hours of each test day.
8. Each test was run for two weeks unless unusual conditions caused early termination.

Significant deviations from the previously listed procedure were made in Tests 6, 7, and 8. Test 6 was operated in DNB for most of its two-week duration. The test was conducted in DNB with clean surfaces for three days. Nucleate boiling conditions were then re-established for the following 48-hour period of corrosion product injection. The remainder of the run was conducted in DNB with fouled surfaces.

Test 7 was run with continuous injection of magnesium chloride solution as well as the continuous maintenance of phosphate control chemistry.

Test 8 deviated from normal conditions since more than one type of condenser leakage was evaluated. The first half of the test was run with calcium sulfate and the remainder with calcium chloride.

Evaluation of test results was made on the basis of operating data, water analyses, analyses of material filtered from boiler water, deposit analyses, normal visual and microscopic examination, metallurgical testing, and metallography.

TABLE IV

PHASE IV CONDENSER LEAKAGE SUMMARY

Test No.	Test Day	Composition of Condonser Leakage—ppm								Quantity, liters/day	Wt. of Cont. Salts	
		Na	K	Mg	Ca	Cl	SO_4	HCO_3	SiO_2		gm/day	gm/test
1 (1)	3-15	55.0	5.25	19.3	79.3	66.7	257.5	37.4	6.5	120	63.23	759.
2	2-14	55.0	5.25	19.3	79.3	66.7	257.5	37.4	6.5	120	63.23	885.
	8-9 (2)	55.0	5.25	19.3	79.3	66.7	257.5	37.4	6.5	360	189.	
3	3-16	55.0	5.25	19.3	79.3	66.7	257.5	37.4	6.5	120	63.23	885.0
4	2-6	—	—	37.5	—	110.0	—	—	—	120	17.7	283.4
	7-11	—	—	75.0	—	220.0	—	—	—	120	35.4	
5	3-6	—	—	75.0	—	220.0	—	—	—	120	35.4	141.6
6	NO CONTAMINANT SALTS WERE INJECTED DURING THIS TEST											
7 (3)	4-6	—	—	37.5	—	110.0	—	—	—	240	35.4	818.9
	6-16	—	—	75.0	—	220.0	—	—	—	240	70.8	
8 (4)	3-4	—	—	—	122.5	—	295.0	—	—	120	50.1	250.4
	5-6 (3)	—	—	—	122.5	—	295.0	—	—	360	150.3	163.6
	7-10	—	—	—	122.5	218.3	—	—	—	120	40.9	

NOTES: 1. Salts used in Test 1, 2, and 3 were: Na_2SiO_3, $NaHCO_3$, Na_2SO_4, KCl, $MgSO_4$, $CaSO_4$, and $CaCl_2$.
2. During Test 2 and Test 8 contaminant salts were introduced continuously for 24-hr and 32-hr periods, respectively.
3. Contaminant salts were injected into the test loop continuously—(24 hr/day).
4. Salts used in Test 8 were $CaSO_4$ and $CaCl_2$.

RESULTS

The methods and conditions for testing during the entire program were designed to accelerate corrosion and thereby provide a basis for the evaluation of various environmental parameters upon corrosion processes within a limited period of time. These methods and conditions were intended to exaggerate high-pressure boiler operation.

Test results are presented in the form of individual "Test Logs" which include a representative description of each test, operating data, and analytical findings. Obviously it is impossible to include all of the data accumulated during Phase IV in this report. The entire collection of records and data from Phase IV, as well as Phases II and III, are being kept on file for the ASME at Combustion Engineering's Kreisinger Development Laboratory.

LOG-TEST 1, PHASE IV

Volatile (NH_3) Boiler Water Treatment — pH = 8.6 to 9.0

Dirty Boiler Conditions — Fresh Water Condenser Leakage

The test loop had been chemically cleaned prior to commencing operation. Approximately three days of seasoning were allowed at the beginning of the test to permit reduction of hydrogen concentrations. During this period, iron oxide and copper contaminants were added to the loop. Once hydrogen concentrations were sufficiently low, addition of simulated fresh water condenser leakage was begun.

Figure 7 shows the response of hydrogen concentration to the injections of condenser leakage which were started on the fourth test day and continued throughout the remainder of the test. During the first three days of condenser leakage addition, hydrogen values exceeded the 570 ppb full-scale capability of the analyzer, and hydrogen gas bubbles were noted in the reflux condenser sample. Although subsequent daily values were less than full scale, the variations in hydrogen concentration reveal an interesting upward trend of both the minimum peak and maximum peak values for each cycle. Injection of condenser leakage resulted in a reduction in boiler water pH to values of approximately 4.0 to 4.5 as shown in Fig. 8. During the last few days of operation, the boiler water pH

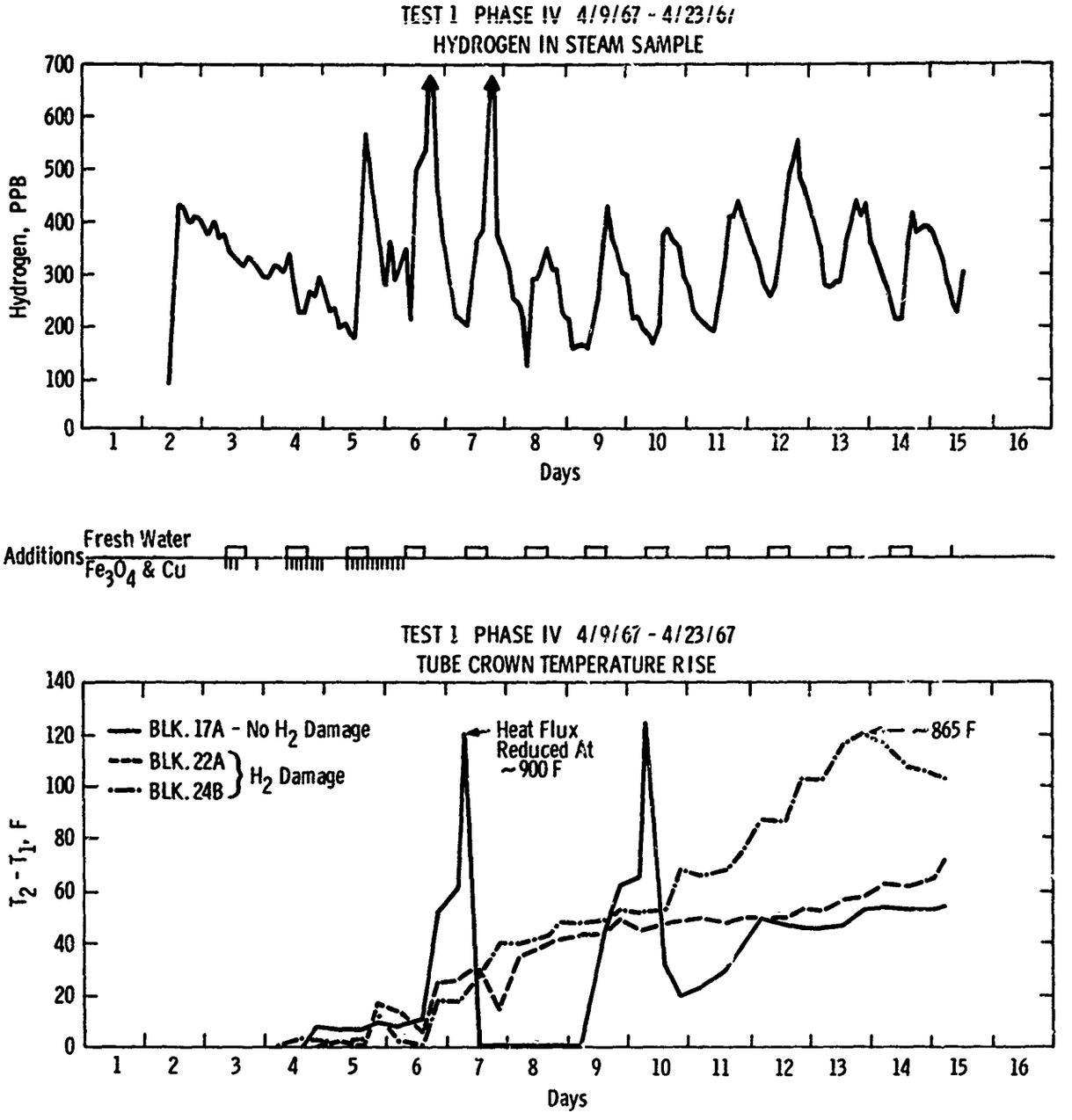

Fig. 7

was maintained with ammonium hydroxide. Control with ammonia had no effect upon the corrosion rate during this period. Increases in conductivity also accompanied the injection of condenser leakage. The changes in water chemistry throughout a daily cycle are shown in Tables V and VI.

Increases in tube-metal temperature were noted (Fig. 7) with the injection of condenser leakage throughout the duration of the test. The greatest rate of increase was noted in the 150,000-Btu per hr-sq ft test section with lesser rates of increase in the upper 110,000-Btu per hr-sq ft section. Rapid erratic changes in metal temperature, superimposed on the general increases, were observed during this test. As individual readings exceeded 900 F, reductions in heat-flux were made to retain control of local temperature. Some adjustments to operating quality were also required when iron oxide and copper contaminants were being added. Bulk quality was reduced to avoid operation beyond the threshold of departure from nucleate boiling.

TABLE V

TEST 1, PHASE IV

BOILER WATER ANALYSIS

TEST DAY No. 10

Time	pH**	pH	Cond.** umhos	Total Alkalinity "P" Epm	Total Alkalinity "MO" Epm	SO_4 ppm	Cl ppm	Na ppm	Ca ppm	Mg ppm	Cu ppm	Fe ppm	H_2** ppb	SiO_2** ppm
0100	8.9	6.2	22	—	.06	—	3.37	3.1	—	—	*—	*—	260	.140
0200	8.9	4.3	36	—	—	—	5.03	3.1	—	—	.030	—	261	.140
0300	8.9	6.2	21	—	.04	.3	3.47	3.1	—	—	—	—	213	.135
0400	8.8	6.1	25	—	.04	.3	3.69	3.7	—	—	.004	—	218	.132
0500	8.8	4.7	25	—	.02	.7	4.47	3.3	—	—	—	—	209	.132
0600	9.0	3.9	67	—	—	.3	6.82	2.4	—	—	.014	—	195	.128
0700	9.0	8.4	16	—	.12	.3	2.13	2.6	—	—	—	—	191	.050
0800	9.0	4.2	35	—	—	.3	4.02	1.4	—	—	.004	.004	184	.050
0900	6.8	5.5	26	—	.04	—	3.64	2.7	.4	.3	—	—	188	.050
1000	5.2	5.7	46	—	.06	1.0	6.33	6.8	.4	.3	.084	.044	165	.050
1100	4.7	4.3	84	—	—	4.3	10.63	9.5	.4	.3	—	—	174	.050
1200	4.6	4.5	98	—	.02	5.0	12.99	12.3	.4	.3	.102	.050	200	.050
1300	4.4	4.5	112	—	—	3.5	14.53	14.3	.4	.3	—	—	256	.020
1400	4.6	4.7	92	—	.02	4.7	12.31	11.8	.4	.3	.100	.050	375	.220
1500	4.5	4.6	85	—	.02	5.5	11.08	11.8	.4	.3	—	—	387	.230
1600	4.4	4.3	95	—	.02	4.3	12.67	12.0	.4	.3	.130	.025	388	—
1700	8.6	5.0	84	—	.04	—	12.46	12.0	—	—	—	—	397	—
1800	9.0	5.7	68	—	.08	1.5	9.70	9.8	—	—	.022	.006	364	—
1900	9.0	7.9	48	—	.08	.7	6.60	7.3	—	—	—	—	365	.230
2000	9.0	4.7	39	—	.02	.7	5.75	4.2	—	—	.020	.006	359	.225
2100	9.1	8.3	22	—	.01	—	3.30	2.9	—	—	—	—	330	.220
2200	9.0	6.0	21	—	.06	—	3.41	2.6	—	—	.011	.006	297	.190
2300	9.0	4.7	27	—	.02	—	3.83	2.5	—	—	—	—	282	.380
2400	9.1	4.1	47	—	—	—	5.33	2.4	—	—	.012	.006	274	.370

* Samples taken on even hours only.

** Values determined at time of sampling. All other recorded values are from later lab analyses.

TABLE VI

TEST 1, PHASE IV

X-RAY DIFFRACTION ANALYSIS OF MATERIAL FILTERED* FROM BOILER WATER

Test Day	Time	Major	Minor	Trace
No. 10	0900	Fe_3O_4	—	—
	1000	Fe_3O_4	—	—
	1100	Fe_3O_4	—	—
	1200	Fe_3O_4	—	—
	1300	Fe_3O_4	—	—
	1400	Fe_3O_4	—	—
	1500	Fe_3O_4	—	—
	1600	Fe_3O_4	—	Cu
	1700	Fe_3O_4	—	—
	1800	—	Fe_3O_4, Cu	—
	1900	—	Fe_3O_4, Cu	—
	2200	—	Fe_3O_4, Cu	—

* 0.45 micron pore size.

Test specimens were removed for inspection and analysis. Figure 9 illustrates the appearance of tube surfaces. Deposit thickness ranged from 30 to 50 mils. Results of the analyses of these deposits are listed in Table VII. Some specimens were chemically cleaned with the standard hydrochloric acid, ammonium bifluoride, thiourea solvent. Inspection of the exposed metal surfaces revealed significant local attack (10 mils) in various areas of both the A and B test loops (Fig. 10).

Specimens were cut from each heater block location for a macro etch with hot ferric chloride solution and bend testing. The initial macro etch of these specimens was inconclusive, but suggested that some fissured metal might be present. Bend tests confirmed that many specimens had experienced varying degrees of

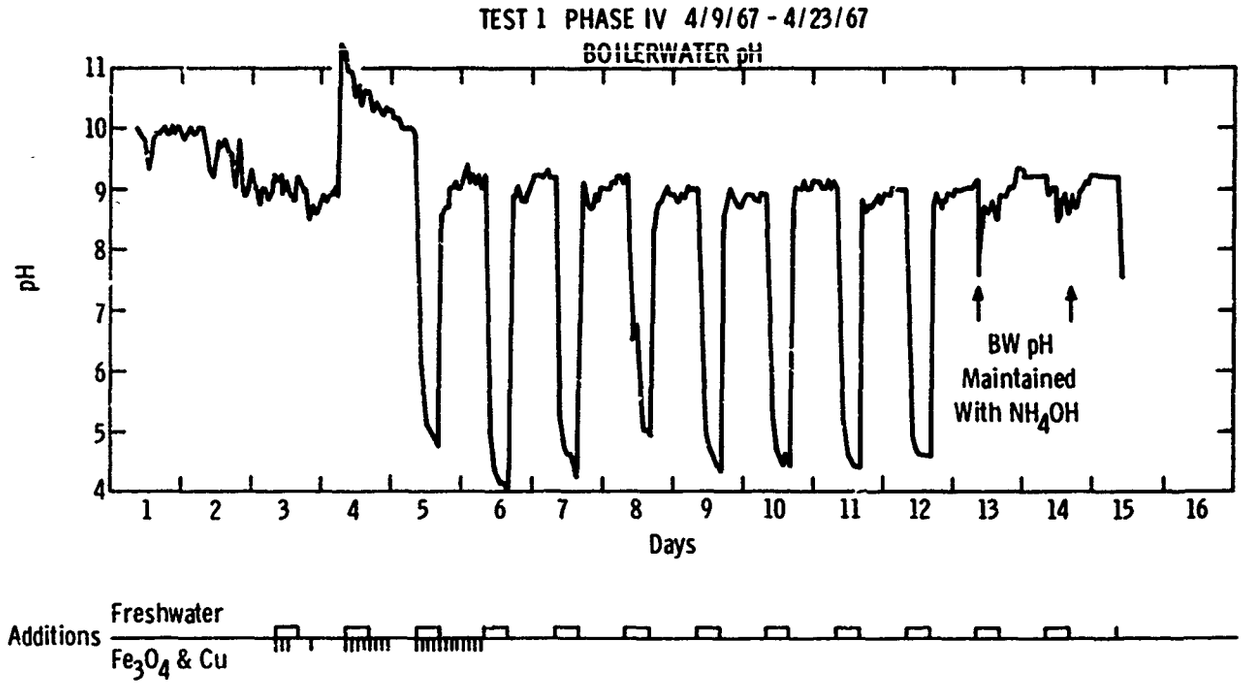

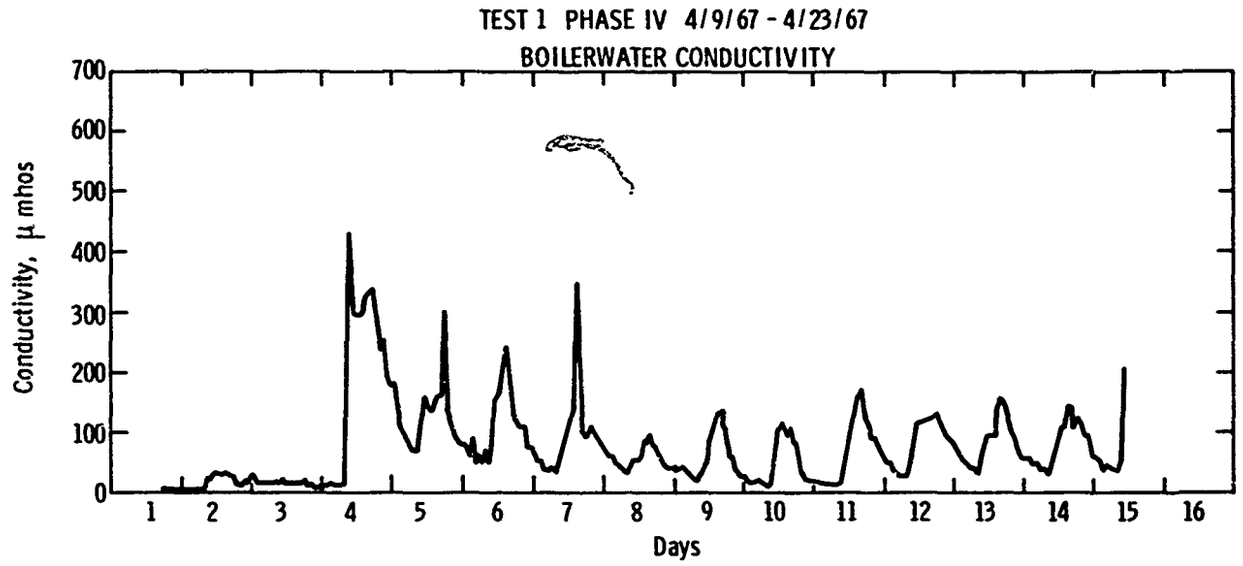

Fig. 8

TABLE VII
TEST 1, PHASE IV
DEPOSIT ANALYSIS

X-RAY DIFFRACTION ANALYSIS

Block No.	17A	22A	18B	21B
MAJOR	Fe_3O_4	Fe_3O_4	Fe_3O_4	Fe_3O_4
	$CaSO_4$	—	$CaSO_4$	—
MINOR	Cu	$CaSO_4$	Cu	$CaSO_4$
	CuO	—	CuO	—
	Cu_2O	—	—	—
	SiO_2	—	—	—

* ND—none detected.

CHEMICAL ANALYSIS

Block No.	17A	22A	18B	21B	24B
IGNITION	GAIN	GAIN	GAIN	GAIN	GAIN
SiO_2, %	5.0	3.0	4.0	5.1	2.9
Fe_3O_4, %	80.2	89.1	59.6	94.3	88.1
Cu, %	2.5	0.4	2.4	—	0.4
CaO, %	8.1	2.1	16.2	—	1.7
MgO, %	ND*	ND	ND	ND	ND
SO_3, %	7.0	4.2	17.5	—	2.9

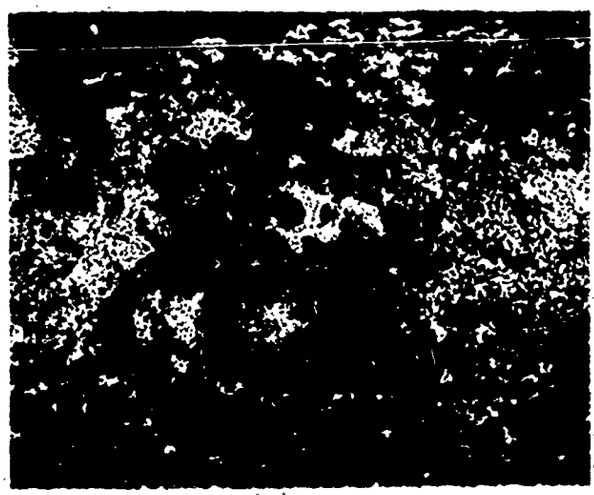

Fig. 9: Deposits on tube surface—Test 1

Fig. 10: Cleaned tube surface—Test 1

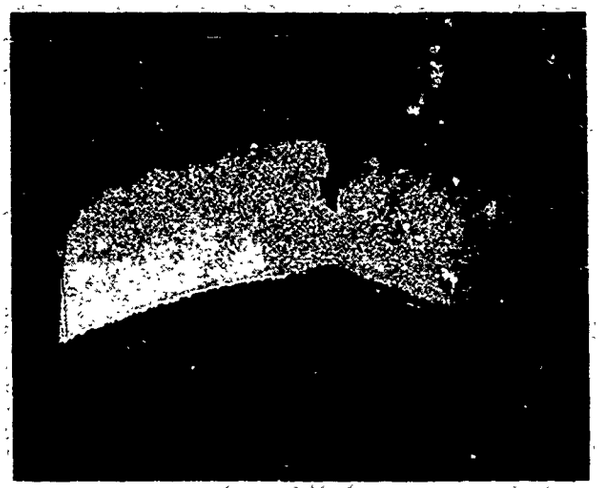

Fig. 12: Cross section of hydrogen damaged bend-test specimen—Test 1

hydrogen damage (Fig. 11). Figures 12 and 13 illustrate the cracking of a bend test specimen and the ductility of normal tube metal, respectively. Hydrogen-damaged metal was noted at blocks 21B, 24B, 19A, 19B, 21A, and 22B. The most severely damaged specimens appeared to have occurred in the low-heat-flux region of the B test loop.

Figures 14, 15, and 16 are photomicrographs of fissured specimens. It has been found that fissuring of the metal is most clearly evidenced in highly polished unetched specimens (Fig. 14). These photos show the significant fissuring which occurred close to the internal surface and the gradient in damage outward through the metal. Damage is less evident in Fig. 15 which is a specimen after a standard nital etch. Decarburization may, however, be observed. Figure 16 illustrates the characteristic layered deposit structure over the cor-

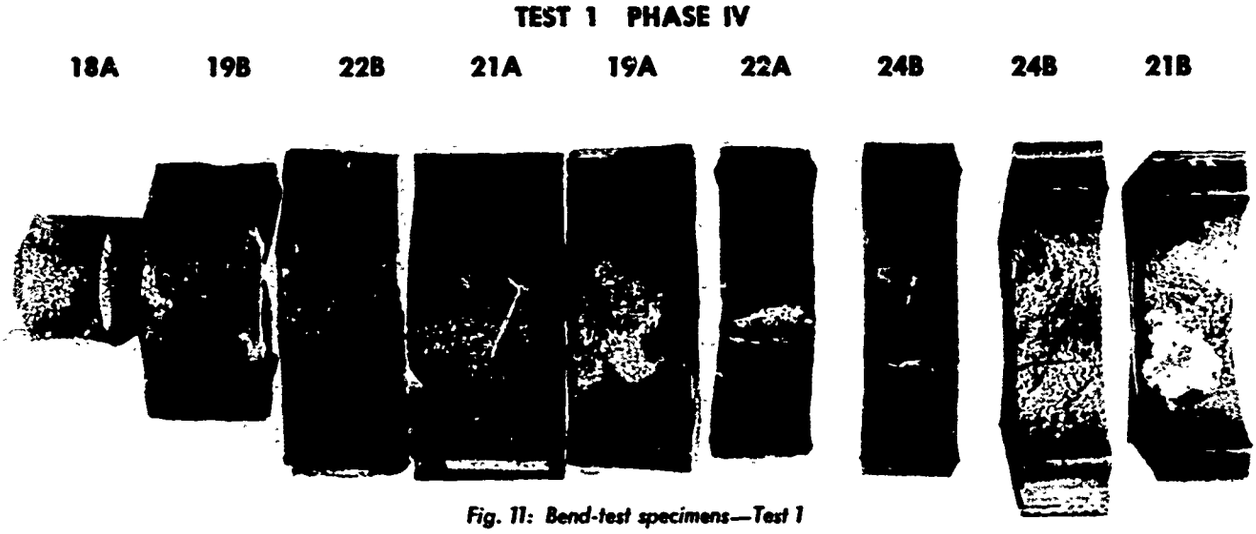

Fig. 11: Bend-test specimens—Test 1

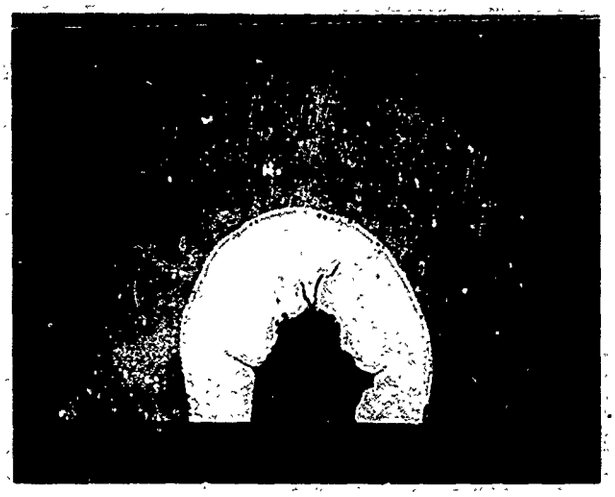

Fig. 13: Cross section of normal ductile tube specimen after bend test

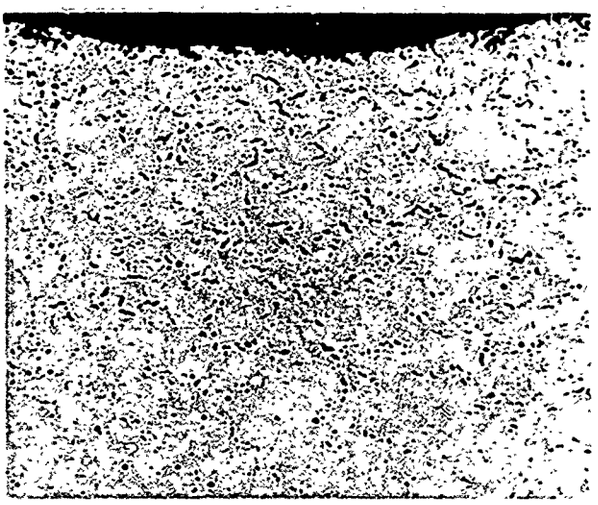

Fig. 14: Photomicrograph of fissured tube metal—unetched—Test 1

roded surface. Deposits in the areas of attack consisted of approximately 90 percent magnetic iron oxide.

LOG-TEST 2, PHASE IV

Coordinated Phosphate Boiler Water Treatment — pH = 9.8 to 10.0

Dirty Boiler Conditions — Fresh Water Condenser Leakage

Equilibrium hydrogen concentrations were reached shortly after start-up. Thereafter, contamination of the system with iron oxide and copper was begun. Injections of fresh water condenser leakage were simultaneously started.

As shown by Figs. 17 and 18, the injection of fresh water contaminants resulted in pH excursions to values between 4.0 to 4.5. Corresponding excursions in hydrogen concentrations were experienced during the first four days of injection. However, no corrosion was indicated by the hydrogen data during subsequent excursions in pH. Hydrogen values increased on the ninth day of testing as a result of continuous injection of condenser leakage over a 24-hour period, which was not the normal mode of operation. Hydrogen values

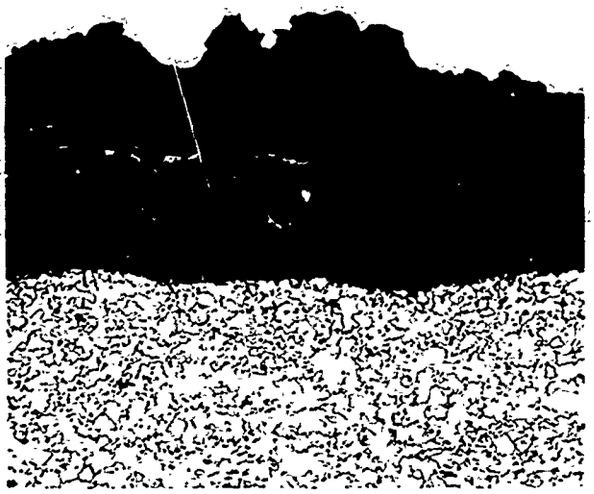

Fig. 15: Photomicrograph of deposit cross section and tube metal—Test 1—nital etch (original mag = 100x)

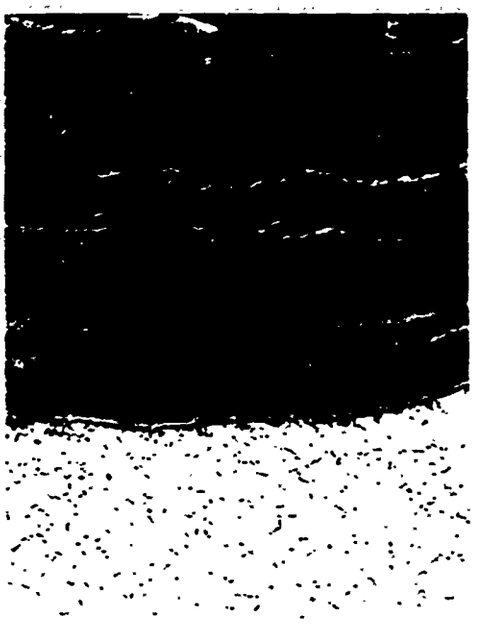

Fig. 16: Photomicrograph of deposit cross section at site of hydrogen damage—Test 1—unetched (original mag = 100x)

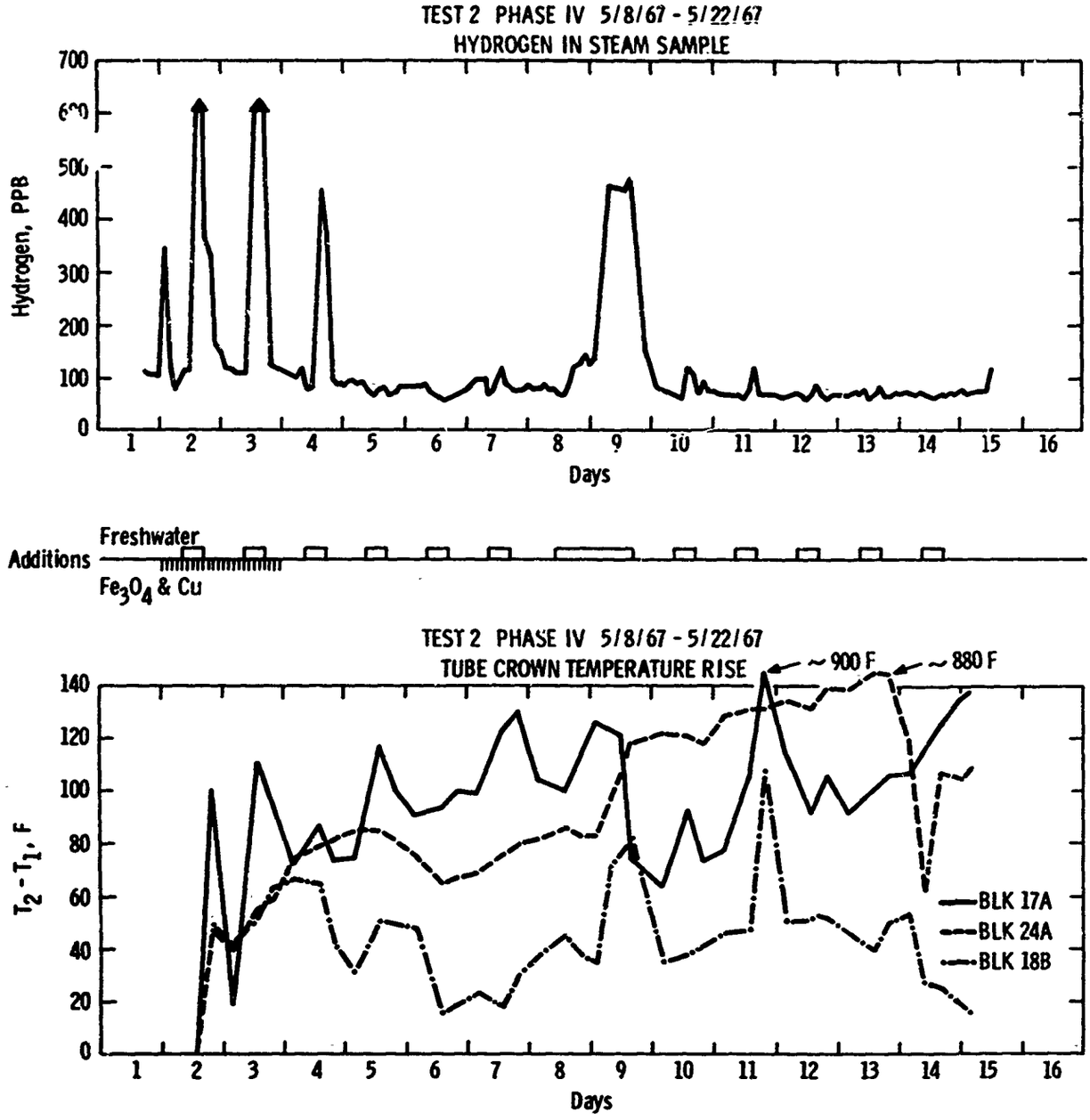

Fig. 17

began to increase only after an extended period of low pH (approxim tely 16 hours). These effects have been attributed to the reaction of phosphate hide-out. The same phenomenon had previously been observed during Phase III of the program.

Tables VIII and IX illustrate the typical dissolved and suspended solids concentrations in the boiler water through a period of fresh water contaminant injection, pH excursion, and restoration of normai operating conditions.

Tube metal temperatures increased very rapidly during this test. Figure 17 illustrated the temperature increases resulting from the deposition of contaminants. The characteristic of the increase was rapid and steady, although the temperature plots do not clearly show this. This discrepancy results from modifications of heat flux made to prevent overheating of the tube metal. Generally speaking, heat-flux reductions were made when tube-metal temperatures entered the 900 to 920 F temperature range.

During shutdown operations, water samples were taken to measure chemical hide-out. Phosphate, sulfate,

TABLE VIII
TEST 2, PHASE IV
BOILER WATER ANALYSIS
TEST DAY No. 5

Time	pH**	pH	Cond.** umhos	Total Alkalinity "P" Epm	Total Alkalinity "MO" Epm	SO_4 ppm	Cl ppm	PO_4** ppm	PO_4 ppm	Na ppm	Ca ppm	Mg ppm	Cu ppm	Fe ppm	H_2** ppb	SiO_2** ppm
0400	10.0	8.2	91	—	.24	10.5	6.0	10.8	7.9	18.50	—	—	.01	.02	91	.26
0825	9.8	9.2	124	.04	.22	23.5	6.5	9.5	7.1	21.0	—	—	*—	*—	90	—
0900	8.9	7.0	133	—	.14	29.0	7.0	6.1	4.5	23.25	—	—	.001	.06	73	—
1000	5.2	5.4	145	—	.10	32.5	8.7	2.5	2.6	24.50	2.0	.6	—	—	71	—
1100	4.9	5.1	146	—	.08	32.5	9.4	2.2	2.4	23.25	1.4	.4	.20	.05	70	—
1200	4.2	4.4	191	—	.02	40.0	12.1	1.1	1.1	28.50	2.0	.6	—	—	62	1.70
1300	4.0	4.2	239	—	—	47.5	16.8	0.3	—	32.75	1.0	1.0	.35	.21	63	2.50
1400	3.9	4.1	270	—	—	56.5	18.5	0.5	—	38.50	—	—	—	—	74	2.50
1500	3.9	4.1	269	—	—	52.5	16.7	0.9	—	36.75	—	—	.24	.17	85	2.60
1600	3.9	4.1	260	—	—	50.0	18.1	1.0	—	36.0	—	—	—	—	80	3.00
1700	6.7	4.6	203	—	.06	43.0	15.5	2.4	1.2	33.50	—	—	.16	.10	80	2.90
1800	8.8	8.8	149	.02	.22	30.5	9.0	2.5	5.1	26.50	—	—	—	—	64	2.80
1900	9.8	9.2	107	.04	.22	23.0	6.8	6.5	5.0	20.50	—	—	.42	.24	80	1.50
2000	9.8	8.5	107	.02	.20	17.0	7.1	7.0	5.4	18.50	—	—	—	—	70	1.50
2100	9.9	9.2	90	.04	.24	16.0	5.8	7.0	3.9	16.25	—	—	.002	.04	72	1.30
2200	9.8	8.7	70	.02	.20	12.5	4.2	8.0	6.0	13.75	—	—	—	—	80	1.00
2300	9.8	7.8	61	—	.22	10.0	1.4	6.0	5.1	11.75	—	—	.003	.03	80	.74
2400	9.7	7.9	61	—	.24	9.5	1.0	9.0	7.9	12.00	—	—	—	—	80	.65

* Samples were taken every other hour.
** Values determined at time of sampling. All other recorded values are from later lab analyses.

TABLE IX
TEST 2, PHASE IV
X-RAY DIFFRACTION ANALYSIS OF MATERIAL FILTERED* FROM BOILER WATER

Test Day	Time	Major	Minor	Trace
No. 5	0200	Fe_3O_4	Cu	Fe_2O_3
	0500	Fe_3O_4	Cu	Fe_2O_3
	0700	Fe_3O_4	Cu, Fe_2O_3	—
	0900	Fe_3O_4	Cu, CuO	Fe_2O_3
	1000**	—	—	Fe_3O_4, Cu_2O
	1100**	—	Fe_3O_4	—
	1300**	—	—	Fe_3O_4
	1500**	—	—	Fe_3O_4
	1600	Fe_3O_4	—	Fe_2O_3
	1700	Fe_3O_4, Cu_2O	Cu	Fe_2O_3
	2000	Cu	Fe_3O_4, Cu_2O	Fe_2O_3

* 0.45 micron pore size.
** X-ray analysis showed no diffraction pattern for major portions of deposit. The major portion was amorphous.

chloride, and sodium concentrations increased during shutdown. Phosphate increased from 8 to 50 ppm, sulfate from 28 to 275 ppm, chloride from 6 to 10 ppm, and sodium from 26 to 175 ppm when power was turned off the two 8-ft test sections. No change in pH occurred.

Inspection of the internal surfaces revealed that heavy deposits (approximately 60 mils) were present on the heated portion of the tubing (Fig. 19). Analyses of these deposits are shown in Table X. It should be noted that a major unidentified compound was found in each of the deposits analyzed. Considerable time and effort were expended in attempting to make an identification. Chemical analysis indicated that the unidentified phase was probably some complex sodium,

TABLE X
TEST 2, PHASE IV
DEPOSIT ANALYSIS

X-RAY DIFFRACTION ANALYSIS

Block No.	Loop "A" Composite	18A	19A	20B
MAJOR	Fe_3O_4	Fe_3O_4	Fe_3O_4	Fe_3O_4
	Unidentified	Unidentified	Unidentified	Unidentified
	—	—	—	Fe_2O_3
MINOR	Fe_2O_3	Fe_2O_3	Fe_2O_3	$NaFeSiO_6$
	Cu	Cu	Cu	$Cu_5(PO_4)_3OH$
	$Cu_5(PO_4)_2(OH)_4$	—	—	Cu
	—	—	—	SiO_2
TRACE	Fe_2O_3	Fe_2O_3	Fe_2O_3	Fe_2O_3
	SiO_2	SiO_2	SiO_2	$Ca_5(PO_4)_3OH$
	$Ca_5(PO_4)_3OH$	$Ca_5(PO_4)_3OH$	$Ca_5(PO_4)_3OH$	—
	$NaFeSiO_6$	$NaFeSiO_6$	$NaFeSiO_6$	—
	—	$Cu_5(PO_4)_3OH$	$Cu_5(PO_4)_3OH$	—

CHEMICAL ANALYSIS

Block No.	"A" Composite	"B" Composite	19A	19B
IGNITION	GAIN	GAIN	GAIN	GAIN
SiO_2, %	2.4	3.5	3.4	4.5
Fe_3O_4, %	38.5	46.8	59.0	55.6
Cu, %	9.2	23.5	2.2	2.9
CaO, %	14.6	7.0	1.4	1.9
MgO, %	1.4	3.7	1.9	1.7
P_2O_5, %	22.8	14.7	22.7	22.0
SO_3, %	1.6	.6	1.6	1.4
Na_2O, %	* 9.4	.5	* 8.9	* 7.1

* Water soluble sodium ~.1%—Total sodium was determined by boiling deposit in hydrochloric acid.

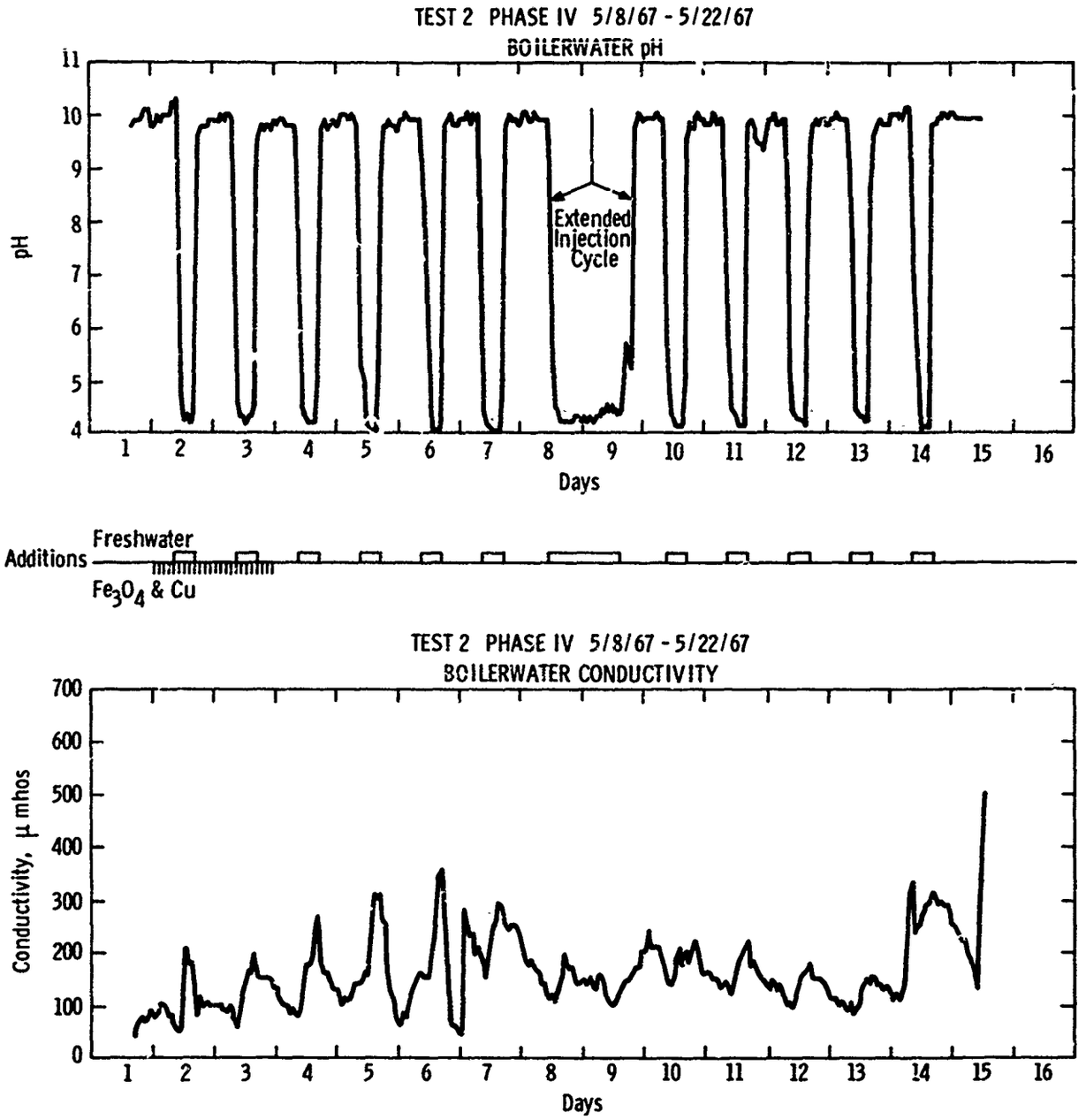

Fig. 18

calcium, phosphate compound. No pattern corresponding to the experimental X-ray diffraction pattern could be found in the ASTM card index. Figure 20 is a reproduction of the diffraction pattern obtained from a composite sample of this deposit. Attempts were made to purify this material by removal of the magnetic iron oxide. Subsequent X-ray analyses of the enriched deposit revealed increased intensity of the same lines that had previously eluded identification.

The purification process was not sufficiently effective to enhance making a positive identification on the basis of elemental analysis. Figure 21 shows the typical cross sectional structure of these deposits.

Deposits were removed from specimens with the standard chemical cleaning solution and the metal surfaces examined. Only widely dispersed minor pitting (1 to 2 mils) in both the A and B test sections was noted (Fig. 22). Subsequent testing and metallurgical evaluation proved that no hydrogen damage had occurred during this test.

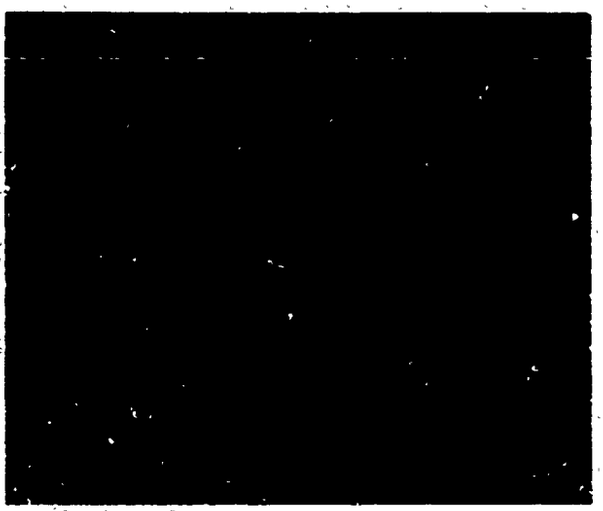

Fig. 19: Deposit on tube surface—Test 2

Fig. 21: Photomicrograph of deposit cross section—Test 2—unetched (original mag = 100x)

LOG-TEST 3, PHASE IV

Free Caustic Boiler Water Treatment — pH = 10.5 to 10.7

Dirty Boiler Conditions — Fresh Water Condenser Leakage

Because of the heavy deposition which occurred during the previous test, the test loop was acid cleaned prior to commencing Test 3. After start-up, the test loop was operated with normal free caustic treatment for two days before equilibrium hydrogen concentrations were achieved. The sequence of addition of iron oxide and copper contaminants as well as the injection of fresh-water-condenser leakage were begun on the third day of operation.

The variations in pH and conductivity and the plot of hydrogen evolution during pH excursions are shown in Figs. 23 and 24. Each pH depression, to values of approximately 4.0 to 4.5, produced a corresponding increase in corrosion rate as shown by the hydrogen data. The magnitude of each excursion varied considerably and no consistent pattern emerged. It is probable that, the affect of phosphate hide-out was

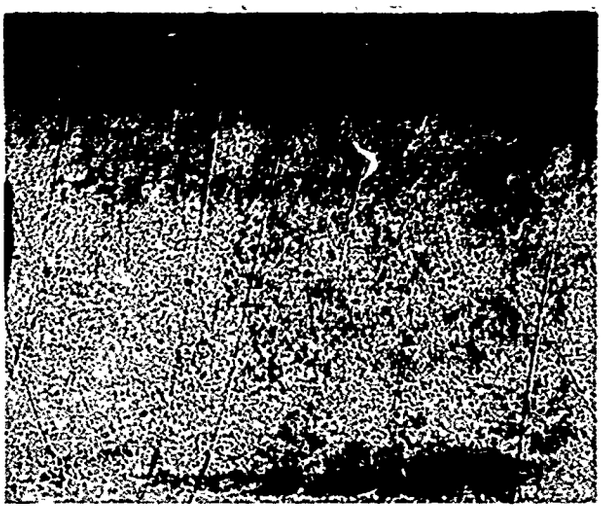

Fig. 22: Cleaned tube surface—Test 2

to provide a residual buffer which decreased the duration and severity of the corrosion cycles. Caustic corrosion sustained hydrogen concentrations at higher

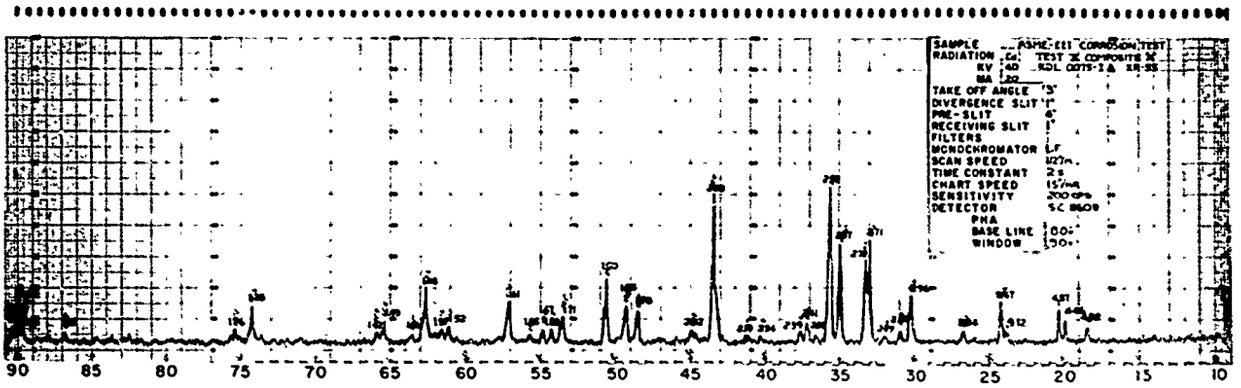

Fig. 20: X-ray diffraction pattern of "A" loop deposits—Test 2

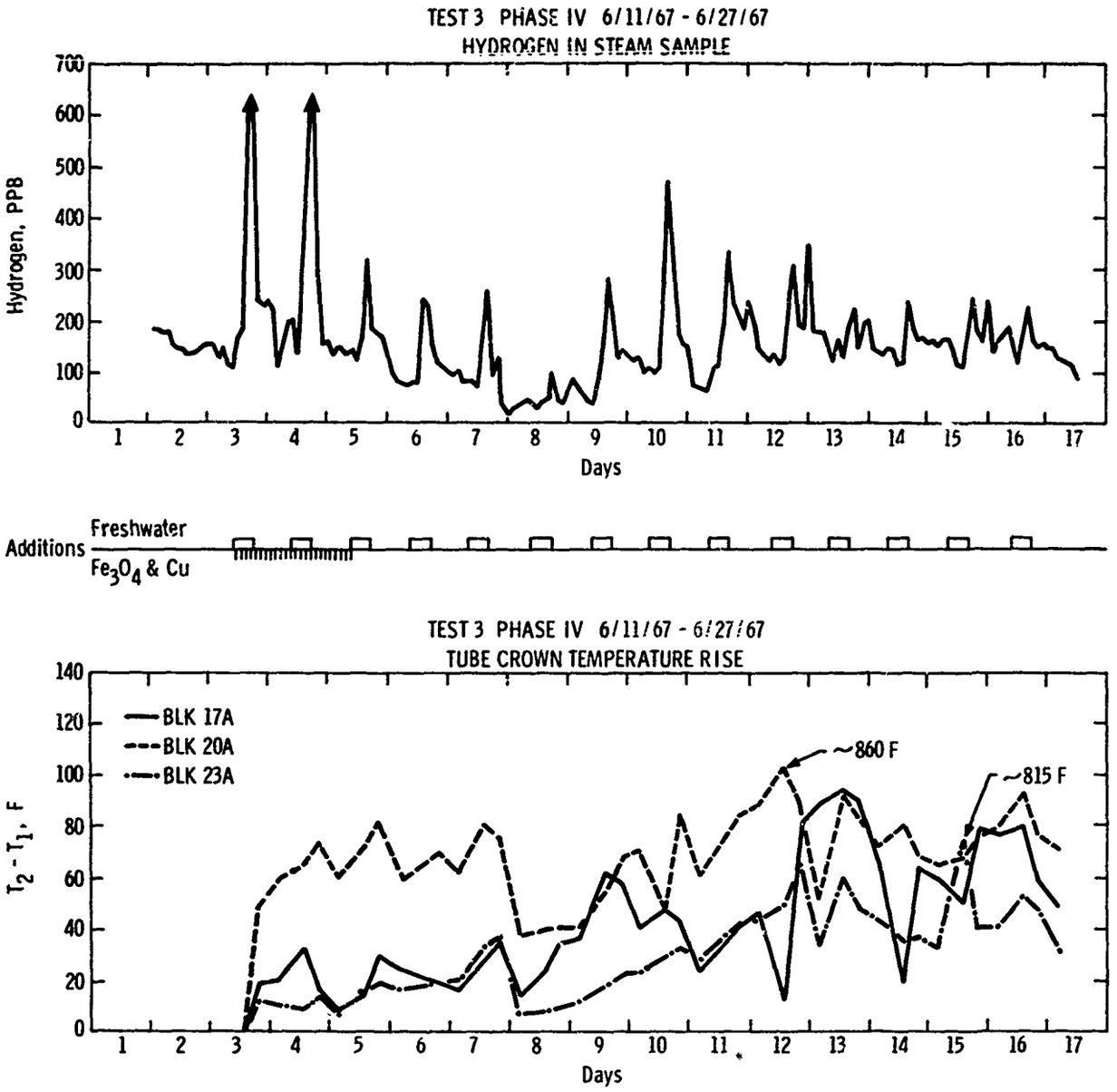

Fig. 23

than normal levels when control chemistry was maintained.

The results of water analyses performed on specimens taken throughout a daily leakage cycle are included in Table XI. Analyses of material filtered from the water are in Table XII.

Figure 23 illustrates the change in tube metal temperature which occurred during this test. The high-flux regions (block 17 through 20A and B) experienced rapid temperature increases which required flux adjustments to maintain temperatures under 920 F. The lower flux areas, blocks 21 through 24, experienced a less severe steady daily increase in tube metal temperature.

Phosphate hide-out data was accumulated during shutdown. Phosphate concentrations increased from 3.5 to 22 ppm, sulfate from 45 to 500 ppm, and sodium from 52 to 268 ppm. The pH remained unchanged.

Inspection of test surfaces revealed only light deposits, approximately 5 to 10 mils in thickness (Fig. 25). Analyses of these deposits are included in Table XIII. Specimens were cleaned in the standard acid solution and the surfaces were inspected. Only minor random pitting (4 to 5 mils) was noted throughout the A and B

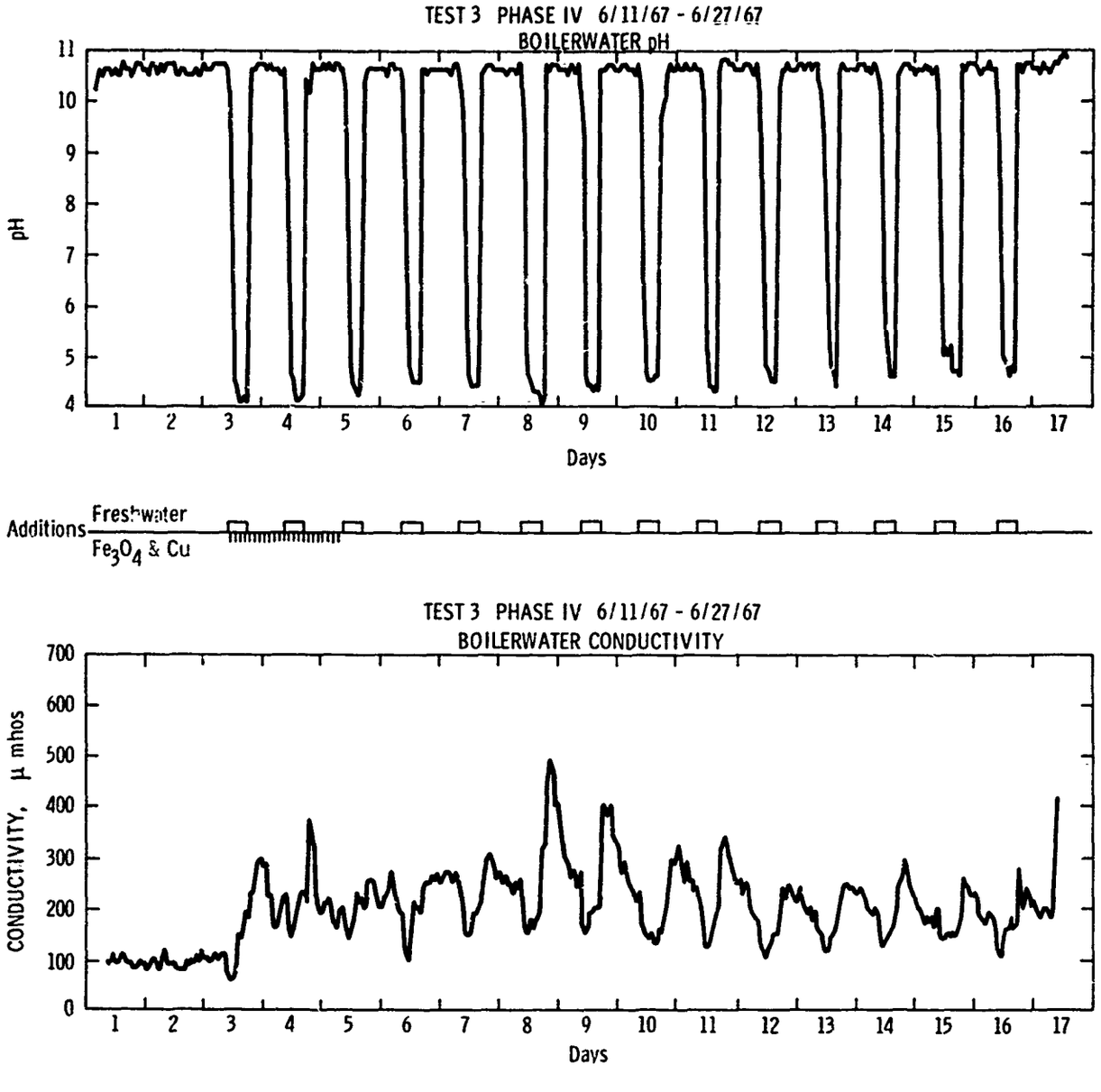

Fig. 24

test sections (Fig. 26). Metallurgical evaluation showed that no hydrogen damage occurred.

LOG-TEST 4, PHASE IV

Coordinated Phosphate Boiler Water Treatment — pH = 9.8 to 10.0

Dirty Boiler Conditions — Magnesium Chloride Contaminant

An equilibrium hydrogen concentration was achieved shortly after start-up. Injections of magnesium chloride solution were made on the second day of operation, prior to the addition of iron oxide and copper. As illustrated by Figs. 27 and 28, the pH decreased to a value of approximately 4.8 as the result of salt injection; however, with the exception of a short duration increase in hydrogen concentration, no appreciable corrosion was evident. After re-establishing control chemistry on the evening of the second day, injections of corrosion products were begun. These were continued until a total of 2200 grams of material had been introduced. On the third day, magnesium chloride injection was repeated, resulting in a rapid excursion in hydrogen concentration to values exceeding the full scale limits of the analyzer. On subsequent days, corrosion excursions declined. Since no increase in hydrogen concentration was experienced on the sixth operating day, it

TABLE XI
TEST 3, PHASE IV
BOILER WATER ANALYSIS
TEST DAY No. 10

Time	pH*	pH	Cond.* umhos	Total Alkalinity "P" Epm	Total Alkalinity "MO" Epm	SO_4 ppm	Cl ppm	PO_4* ppm	PO_4 ppm	Na ppm	Ca ppm	Mg ppm	Cu ppm	Fe ppm	H_2* ppb	SiO_2* ppm
0400	10.6	10.1	250	.12	.36	41.0	9.6	3.0	3.0	46.0	—	—	.017	.001	128	1.30
0900	10.3	10.1	165	.08	.20	31.3	6.8	1.1	1.1	31.0	.02	.01	.008	.002	105	.90
1000	6.7	5.4	120	—	.04	23.5	12.0	0.9	.9	23.0	.20	.09	.170	.040	96	1.10
1100	4.7	4.8	125	—	.04	25.0	15.2	0.1	.1	25.0	.10	—	.624	.043	84	1.60
1200	4.5	4.5	140	—	.04	17.0	17.4	—	—	21.0	.13	.110	.148	.041	108	1.60
1300	4.5	4.5	150	—	.04	15.5	18.4	—	—	23.0	.15	.120	.120	.070	183	1.70
1400	4.5	4.5	130	—	.04	13.0	18.6	—	—	22.0	.21	.130	.101	.041	273	1.20
1500	4.6	4.5	130	—	.04	12.0	22.6	—	—	21.0	.26	.130	.080	.025	383	1.70
1700	6.6	5.7	150	—	.04	18.5	20.8	0.1	—	24.0	.26	.120	—	—	490	—
1800	9.7	6.7	175	—	.12	26.5	18.0	0.8	.1	28.0	.19	.100	.009	.005	330	.70
1900	10.0	6.9	200	—	.12	38.5	16.4	0.7	.7	32.0	.15	.100	—	—	202	.38
2000	10.5	9.8	250	.12	.24	54.0	14.4	1.0	.5	41.0	.10	.090	.003	.004	170	.30
2100	10.7	10.2	295	.20	.32	62.5	11.2	1.2	.2	46.0	—	.010	—	—	160	.28
2200	10.6	10.4	285	.20	.32	62.0	5.2	2.4	2.4	44.0	—	.010	.014	.012	150	.38
2300	10.6	10.2	300	.16	.40	65.4	7.8	1.9	1.9	48.0	—	—	—	—	145	.76
2400	10.7	10.4	300	.24	.40	70.0	11.0	2.5	2.5	48.0	—	—	.025	.004	142	1.20

* Values determined at time of sampling. All other recorded values are from later lab analyses.

TABLE XII
TEST 3, PHASE IV
X-RAY DIFFRACTION ANALYSIS OF MATERIAL FILTERED* FROM BOILER WATER

Test Day	Time	Major	Minor	Trace
No. 10	1100**	—	Fe_3O_4	Fe_2O_3
	1200**	—	Fe_3O_4	Fe_2O_3
	1300	Fe_3O_4	Fe_2O_3	—
	1400	Fe_3O_4	Fe_2O_3	—
	1500	Fe_3O_4	Fe_2O_3	—
	1600	Fe_3O_4	—	Fe_2O_3, $Ca_5(PO_4)_3OH$
	1700	Fe_3O_4	$Ca_5(PO_4)_3OH$	Fe_2O_3
	1800	Fe_3O_4	$Ca_5(PO_4)_3OH$	Fe_2O_3
	1900	Fe_3O_4	$Ca_5(PO_4)_3OH$	Fe_2O_3
	2000	Fe_3O_4	$Ca_5(PO_4)_3OH$	Fe_2O_3

* 0.45 micron pore size.
** Amorphous phase present.

was decided that the magnesium chloride injection should be doubled. This started on the seventh day. Subsequently, daily hydrogen cycles became more severe both in concentration and duration. On the twelfth operating day of the test, a brittle tube failure was experienced at the Block 17A location.

Tables XIV and XV illustrate the variations in water chemistry which were experienced during an injection-corrosion cycle. It is interesting to note that calcium, presumably left in the loop from prior testing, became soluble in the boiler water at low pH. Hydrogen values listed in this table are calculated values from the steam sample concentrations using the characteristic relationship between steam and reflux condenser samples.

TABLE XIII
TEST 3, PHASE IV
DEPOSIT ANALYSIS

X-RAY DIFFRACTION ANALYSIS

Block No.	Loop "A" (17A-20A) Composite	Loop "B" (17B-20B) Composite
MAJOR	Fe_3O_4	Fe_3O_4
	Cu	Cu
MINOR	Fe_2O_3	Fe_2O_3
	$Ca_5(PO_4)_3OH$	$Ca_5(PO_4)_3OH$
TRACE	SiO_2	$NaFeSiO_6$

* Total sodium.

CHEMICAL ANALYSIS

Block No.	Loop "A" (17A-20A) Composite	Loop "B" (17B-20B) Composite	Loop "A" (17A-20A) Unheated Side Composite
IGNITION	GAIN	GAIN	GAIN
SiO_2, %	3.8	4.4	4.6
Fe_3O_4, %	72.7	61.0	53.1
Cu, %	11.8	22.0	14.0
CaO, %	1.0	3.3	9.0
MgO, %	4.6	0.7	2.5
P_2O_5, %	4.6	4.4	14.7
*Na_2O, %	.6	.5	.5

Fig. 25: Photomicrograph of deposit cross section—Test 3—(original mag = 250x)

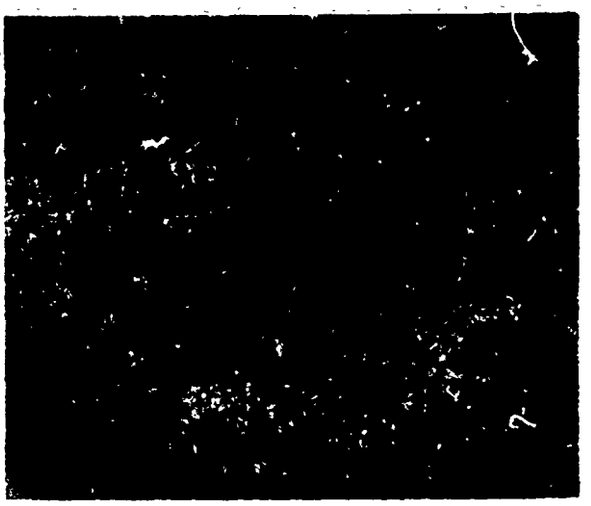

Fig. 26: Cleaned tube surface—Test 3

TABLE XIV
TEST 4, PHASE IV
BOILER WATER ANALYSIS
TEST DAY No. 9

				Total Alkalinity												
Time	pH*	pH	Cond.* umhos	"P" Epm	"MO" Epm	SO_4 ppm	Cl ppm	PO_4* ppm	PO_4 ppm	Na ppm	Ca ppm	Mg ppm	Cu ppm	Fe ppm	H_2* ppb	SiO_2* ppm
0400	10.0	9.2	275	.1	.20	—	45.5	8.0	9.0	47.8	—	.05	5.74	.20	99	.37
0800	9.9	8.6	215	.1	.16	—	35.4	10.0	6.6	39.2	—	.05	8.15	.16	74	.25
0900	5.0	5.1	200	—	.04	—	41.7	3.0	1	36.4	—	.95	6.92	.22	96	.17
1000	4.6	5.0	225	—	.04	—	48.0	2.5	1	35.0	—	3.0	6.79	.16	117	.18
1100	4.5	5.0	250	—	.04	—	49.3	2.5	1	30.0	3.1	1.8	6.06	.22	174	.20
1200	4.5	4.7	250	—	.04	—	45.4	1.5	1	29.0	2.9	1.44	7.61	.39	308	.18
1300	4.5	6.2	210	—	.04	—	40.5	1.2	1	21.6	3.0	1.85	7.98	.26	466	.14
1400	4.6	5.1	190	—	.04	—	39.2	0	—	16.6	3.5	4.6	6.59	.14	590	.14
1500	4.7	4.6	200	—	.04	—	41.2	0	1	17.9	4.9	6.2	.25	.04	620	.13
1600	4.6	4.7	260	—	.04	—	40.5	0	1	22.4	7.4	10.0	.06	.04	620	.16
1700	4.6	4.3	220	—	—	—	50.5	2.4	1	40.0	.25	.40	.06	.04	665	.33
1800	7.8	5.6	210	—	.04	—	34.8	3.5	6.2	32.9	—	.05	.06	.04	785	.14
1900	10.0	9.4	170	.1	.20	—	24.0	13.0	8.2	26.4	—	.05	.06	.04	865	.11
2000	10.0	6.4	130	—	.20	—	19.0	10.2	10.2	20.8	—	.05	.06	.04	940	.11
2100	10.0	7.0	100	—	.20	—	15.3	11.2	8.6	17.4	—	.05	.06	.02	768	.12
2200	10.0	6.4	95	—	.20	—	12.6	11.0	7.6	14.8	—	.05	.06	.01	761	.13
2300	10.0	6.8	95	—	.30	—	11.4	11.0	9.2	14.0	—	.05	.01	.01	712	.13
2400	9.9	7.1	70	—	.20	—	10.1	10.6	6.4	12.0	—	.05	.02	.01	698	.16

* Values determined at time of sampling. All other recorded values are from later lab analyses.

TABLE XV
TEST 4, PHASE IV
X-RAY DIFFRACTION ANALYSIS OF MATERIAL FILTERED* FROM BOILER WATER

Test Day	Time	Major	Minor	Trace
No. 9	0800**	—	—	—
	1000	Cu_2O	Fe_3C_4, Cu	Fe_2O_3
	1200	Cu_2O	Cu	Fe_3O_4, Fe_2O_3
	1400	Cu_2O	Cu	Fe_3O_4, Fe_2O_3
	1600	Cu_2O	Cu	Fe_3O_4, Fe_2O_3
	1800**	—	Cu	Cu_2O, Fe_3O_4
	2000**	—	—	Cu_2O, Cu, Fe_3O_4
	2200**	—	—	Cu_2O, Cu, Fe_3O_4
	2400**	—	Cu	Cu_2O

* 0.45 micron pore size.
** Amorphous phase noted.

Plots of tube-crown temperatures are shown in Fig. 27. These illustrate the rate of daily increase resulting from corrosion and deposition throughout the operating period. Erratic temperature cycling at various locations was observed during this test.

Following the failure, the A and B test sections were removed from the test loop for examination. Due to the violence of the failure, a major portion of the deposits, which were assumed to have been in place during operation, were lost. The remaining deposits are illustrated in Fig. 29. Their analysis is included in Table XVI.

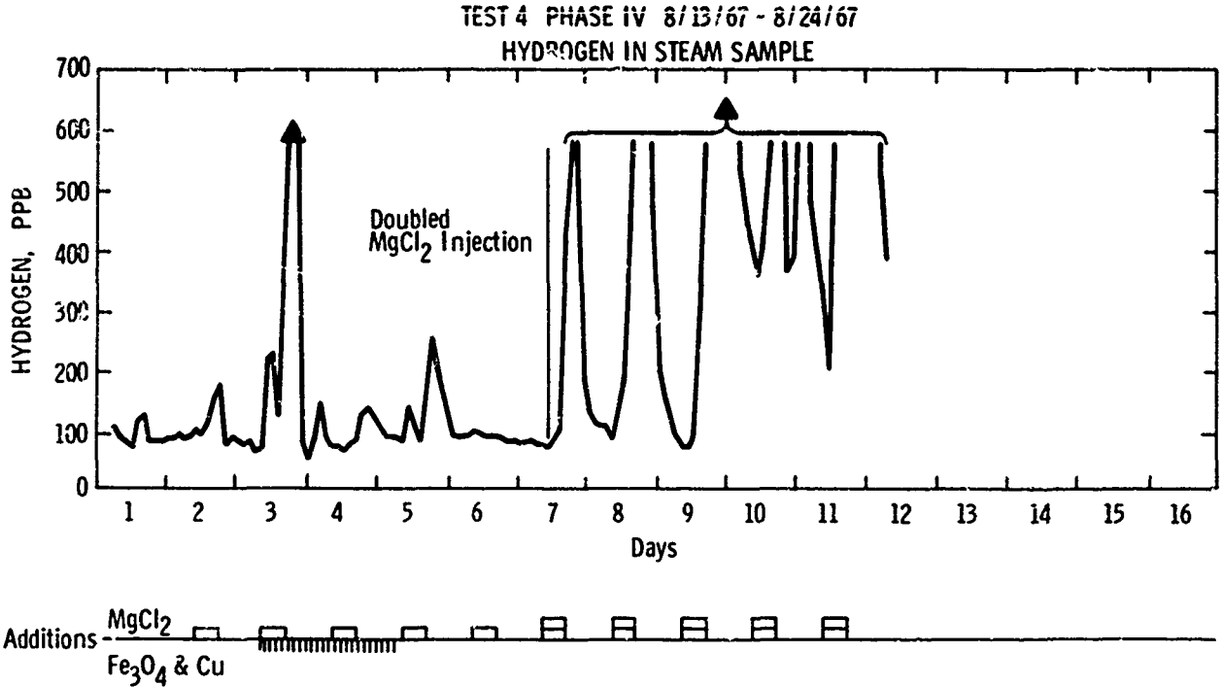

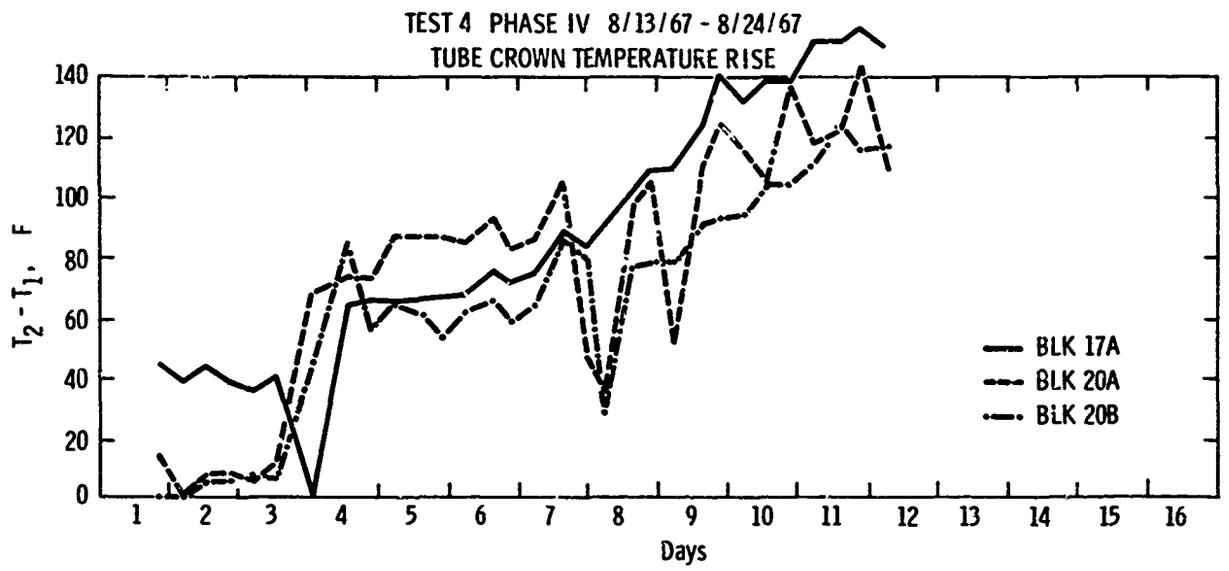

Fig. 27

TABLE XVI
TEST 4, PHASE IV
DEPOSIT ANALYSIS

X-RAY DIFFRACTION ANALYSIS

Block No.	20A	20B
MAJOR	Fe_3O_4	Fe_3O_4
MINOR	$Ca_4Mg_5(PO_4)_6$ $(Ca, Mg)_3(PO_4)_2$ $Ca_5(PO_4)_3OH$	$Ca_4Mg_5(PO_4)_6$ $(Ca, Mg)_3(PO_4)_2$ $Ca_5(PO_4)_3OH$
TRACE	Fe_2O_3 Cu $NaFeSiO_4$ $Mg(H_2PO_4)_2$ $MgHPO_4 \cdot 3H_2O$	Fe_2O_3 Cu $NaFeSiO_4$ $Mg(H_2PO_4)_2$ —

CHEMICAL ANALYSIS

Block No.	17A (Failure)	20A	20B
SiO_2, %	2.4	1.5	2.3
Fe_3O_4, %	95.6	59.8	65.3
Cu, %	0.6	1.1	TRACE
CaO, %	0.2	3.7	2.8
MgO, %	0.3	9.4	6.6
P_2O_5, %	—	19.3	15.4
*Na_2O, %	0.8	2.2	2.5

* Total sodium.

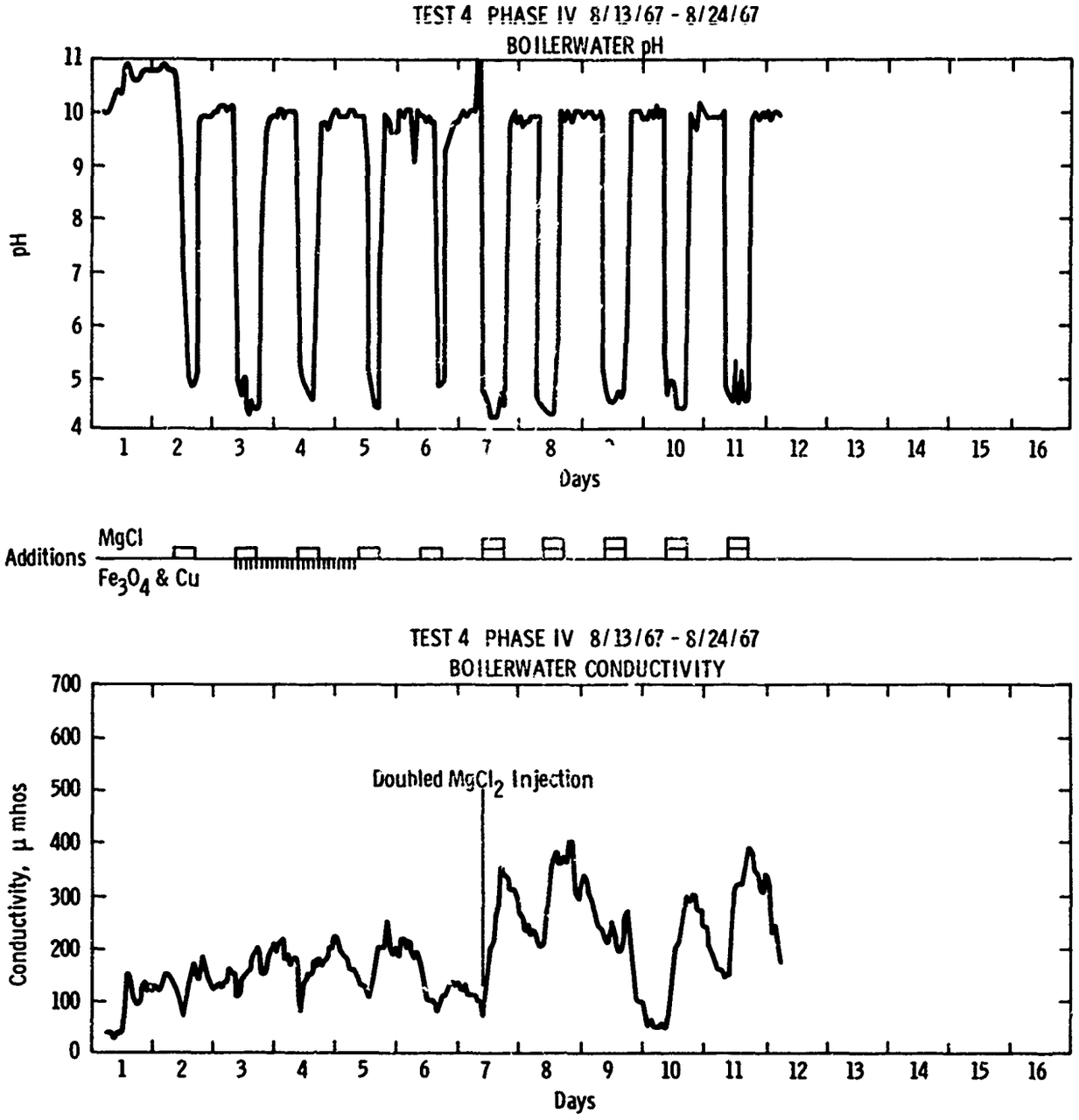

Fig. 28

Metallurgical examination and analysis of the failure revealed that the heated side of the tube was totally decarburized and fissured in an area approximately 6-in. long. Initial failure occurred by a brittle fracture along two lines at the edges of the heater block. The resulting stress was sufficient to result in a ductile shear failure of the unheated portion of the tube. The metal fragments shown in Fig. 30 were propelled from the tube as a result of the failure. In addition, the test section was detached from the lower tubing at this point and the entire upper length was propelled to one side (Fig. 31). Figure 32 is a close up of the failure location. Other sites of hydrogen damage are shown by bend test specimens shown in Fig. 33. Surface corrosion at sites of damage averaged only 10 mils in penetration. The appearance of a typical corrosion site is shown in Fig. 34.

Figure 35 is a photomicrograph of an unetched specimen showing the layered structure of the deposit and the fissuring of the tube metal at the site of the failure. It is typical of deposits seen with both preceding and subsequent incidents of hydrogen damage.

Fig. 29: Deposits on tube surface—Test 4

Fig. 30: Fragments of hydrogen damaged tube metal after brittle failure—Test 4

Fig. 31: View of damage to test loop after hydrogen damage failure—Test 4

Fig. 32: Close up view of tube end at site of brittle failure—Test 4

Deposits found at other locations had a less stratified structure and inclusions of salts were noted (Fig. 36). Some of this deposited salt was separated from the iron oxide matrix. X-ray diffraction anatysis revealed an amorphous structure.

LOG-TEST 5. PHASE IV

Free Caustic Boiler Water Treatment — pH = 10.5 to 10.7

Dirty Boiler Conditions — Magnesium Chloride Contaminants

Injection of preboiler corrosion products was begun once base-line hydrogen concentrations were established. Magnesium chloride injection was started on the second day of operation. Figures 37 and 38 show the response of hydrogen concentration and boiler water pH excursions resulting from the injection of

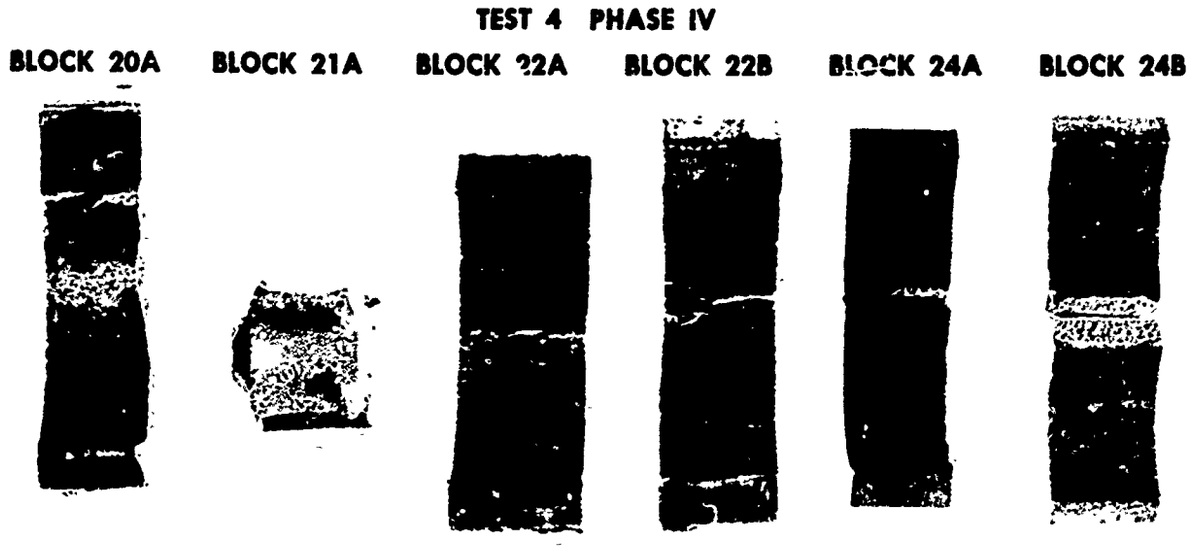

Fig. 33: Bend-test specimens—Test 4

Fig. 34: Cleaned tube surface—Test 4

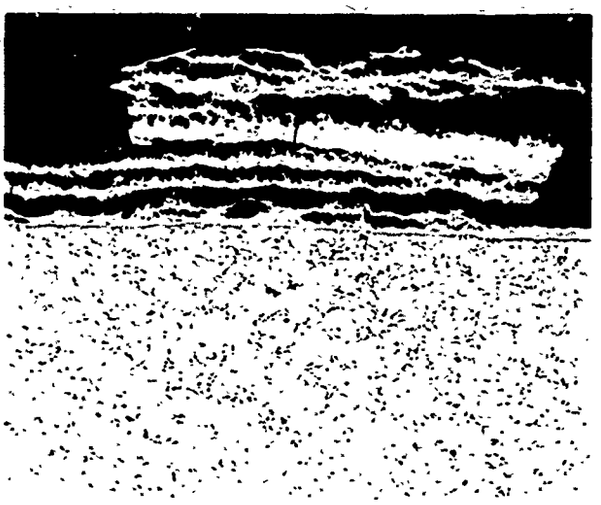

Fig. 35: Photomicrograph of deposit cross section and tube metal at site of hydrogen damage—Test 4—nital etch (original mag = 100x)

magnesium chloride. Water analyses from a corrosion cycle are listed in Tables XVII and XVIII. Hydrogen concentrations exceeded the full scale capability of the analyzer on each of the four days during which salt was added to the loop.

Test data show a marked similarity to those obtained from both Tests 1 and 4, during which hydrogen damage was experienced. The test was terminated seven days after start-up to preclude the occurrence of a tube failure similar to that which halted Test 4. This action was predicated upon the high rates of corrosion indicated by the hydrogen data and the erratic behavior of tube metal temperatures in various locations, which, in the past, accurately predicted the occurrence of hydrogen damage (Fig. 17).

Upon inspection of the test surfaces, relatively heavy plugs of deposit (30 to 65 mils) were noted at various locations (Fig. 39). Deposit analyses are included in Table XIX. Little magnesium was detected in these deposits. However, calcium salts resulting from the presence of residuals in the loop from previous tests were found. Water analysis revealed that at low pH (4.0 to 4.5) soluble calcium could be detected in the boiler water.

Test specimens were chemically cleaned using the standard acid solution. Corrosion plugs, 7 to 12 mils deep, were found at various locations (Fig. 40).

TABLE XVII
TEST 5, PHASE IV

BOILER WATER ANALYSIS
TEST DAY No. 6

				Total Alkalinity											
Time	pH**	pH	Cond.** umhos	"P" Epm	"MO" Epm	Cl ppm	OH ppm	PO_4** ppm	PO_4 ppm	Na ppm	Ca ppm	Mg ppm	Cu ppm	Fe ppm	H_2** ppb	SiO_2** ppm
0100	10.5	10.3	200	.24	.12	30.20	2.38	2.0	1.0	24.9	—	.01	.28	.17	348	.25
0200	10.5	10.2	160	.20	.10	24.65	1.00	2.0	.8	17.8	—	—	.10	.60	314	.23
0300	10.4	10.5	148	.34	.14	21.80	3.4	1.5	.8	23.4	—	—	*—	*—	296	.23
0400	10.6	10.4	150	.24	.12	18.60	2.7	2.3	1.2	19.1	—	—	.10	.22	285	.22
0500	10.5	10.3	150	.24	.08	16.35	3.06	2.2	1.6	15.6	—	—	—	—	256	.22
0600	10.4	10.2	125	.22	.08	15.15	.68	1.2	3.2	15.6	—	—	.09	.06	251	.20
0700	10.6	10.3	140	.24	.12	12.75	2.00	2.4	1.6	15.4	—	—	—	—	245	.20
0800	10.4	10.4	115	.24	.08	11.65	1.7	1.7	1.3	14.2	—	—	.23	.10	245	.19
0900	10.3	9.9	100	.12	.10	15.60	—	4.0	.4	10.8	—	—	—	—	273	.15
1000	9.7	6.2	80	—	.06	18.55	—	4.0	—	11.1	—	.05	.04	.10	268	.13
1100	6.4	5.4	80	—	.04	20.75	—	2.2	—	11.1	.40	.68	—	—	244	.14
1200	4.8	4.9	100	—	.04	25.30	—	—	—	10.7	.85	1.46	.81	.41	200	.15
1300	4.6	5.0	120	—	.04	28.35	—	—	—	10.7	1.15	1.71	—	—	198	.13
1400	4.5	4.8	140	—	.04	34.60	—	—	.4	13.6	1.70	1.82	.81	.23	426	.13
1500	4.5	4.8	150	—	.04	38.85	—	—	—	13.8	2.60	1.87	—	—	570*	.11
1600	4.5	4.8	170	—	.02	40.35	—	—	—	14.2	3.05	1.88	2.15	.39	570*	.15
1700	10.5	10.3	220	.22	.12	36.90	1.36	1.0	2.6	30.6	—	.05	—	—	570*	.085
1800	10.5	10.6	210	.40	.12	31.75	2.00	3.0	1.5	29.9	—	.01	3.07	.34	570*	.055
1900	10.6	10.5	230	.36	.10	30.35	3.06	2.8	.8	28.6	—	—	—	—	570*	.04
2000	10.7	10.5	220	.38	.12	28.65	2.00	3.4	.8	28.6	—	—	.7	.01	570*	.04
2100	10.6	10.5	200	.30	.10	26.90	2.70	3.2	.6	27.6	—	—	—	—	416	.045
2200	10.6	10.5	180	.30	.10	23.25	2.38	4.0	1.9	23.8	—	—	.7	.09	342	.06
2300	10.6	10.5	200	.36	.08	21.10	1.70	2.2	3.4	23.6	—	—	—	—	256	.06
2400	10.7	10.5	220	.30	.08	33.40	2.00	3.5	1.5	29.8	—	—	—	—	216	.084

* Sample taken every other hour.
** Values determined at time of sampling. All other recorded values are from later lab analyses.

Fig. 36: Photomicrograph of deposit cross section—Test 4—(original mag = 250x)

TABLE XVIII

TEST 5, PHASE IV

X-RAY DIFFRACTION ANALYSIS OF MATERIAL FILTERED* FROM BOILER WATER

Test Day	Time	Major	Minor	Trace
No. 4	0600	Fe_3O_4	Cu	Cu_2O, Fe_2O_3
	0800	Fe_3O_4	Cu	Cu_2O, Fe_2O_3
	1000	Cu, Cu_2O	Fe_3O_4	Fe_2O_3
	1250	Fe_3O_4, Cu, Cu_2O	—	Fe_2O_3
	1400	Cu_2O	Fe_3O_4	Cu, Fe_2O_3
	1600	Cu_2O	Fe_3O_4	Cu, Fe_2O_3
	1800	Fe_3O_4, Cu_2O	Cu	Fe_2O_3
	2000	Fe_3O_4	—	Cu
	2200	Fe_3O_4	Cu	O
No. 7	0200	Cu	Cu_2O	Fe_2O_3

* 0.45 micron pore size.

Bend testing (Fig. 41) and metallurgical evaluation revealed that the tube metal was completely embrittled at the Block 17 elevation in the "A" loop and was less severely effected at other locations. Figures 42 and 43 are photomicrographs of unetched specimens from the ID and OD of the tubing at Block 17A. Fissuring of the material existed uniformly through the entire tube wall. Failure was averted only by the reinforcement provided by the heater block and early termination of the test.

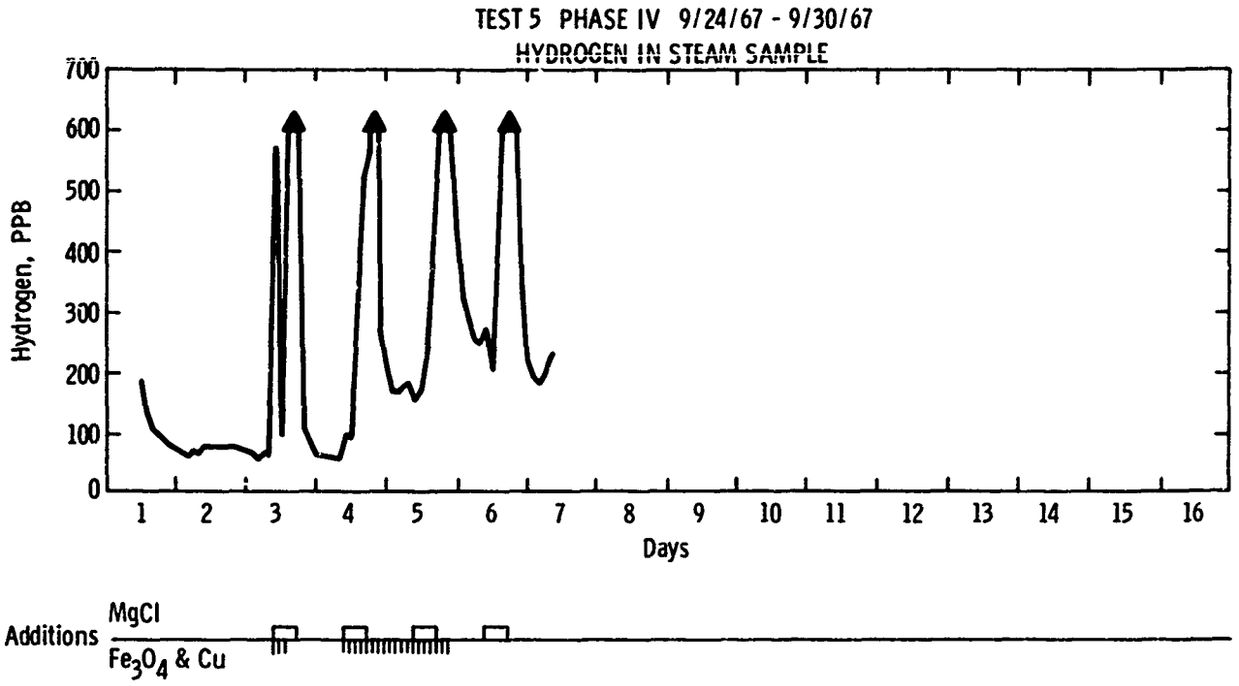

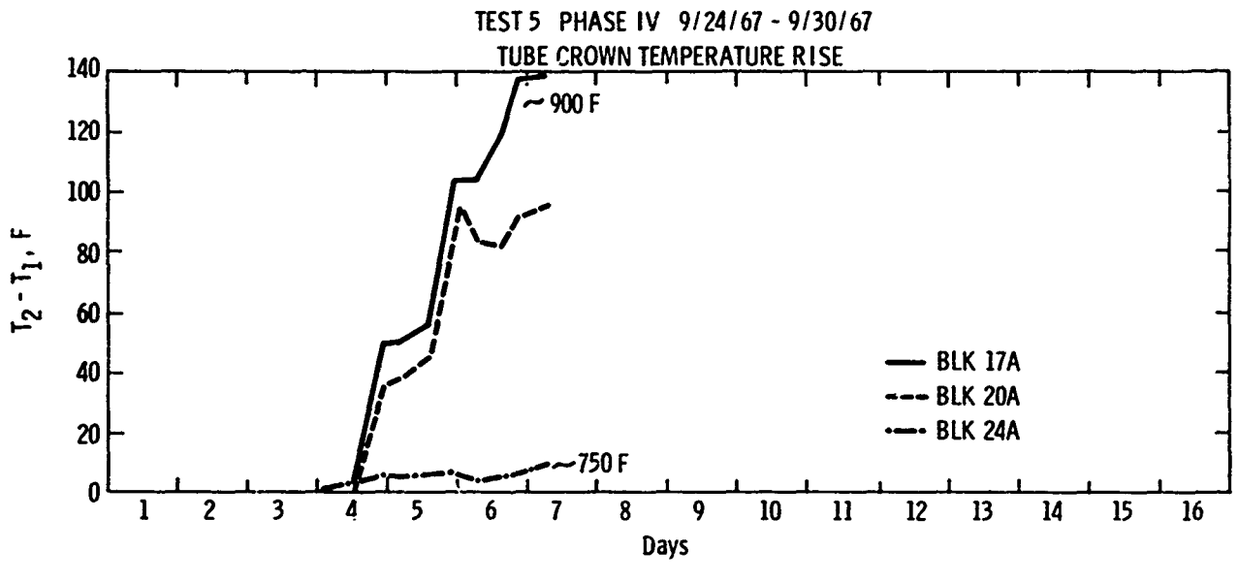

Fig. 37

TABLE XIX
TEST 5, PHASE IV
DEPOSIT ANALYSIS

X-RAY DIFFRACTION ANALYSIS

Block No.	20A	19B	20B
MAJOR	Fe_3O_4	Fe_3O_4	Fe_3O_4
MINOR	Fe_2O_3	Fe_2O_3	Fe_2O_3
	Cu		Cu
	$Ca_5(PO_4)_3OH$		

CHEMICAL ANALYSIS

Blocks	17A	19A	20A	17B	19B	20B
IGNITION GAIN	2.2	2.7	2.7	2.7	4.0	8.6
SiO_2, %	91.2	77.2	78.6	66.3	72.5	62.5
Fe_3O_4, %	2.6	6.8	7.8	6.9	14.0	11.8
Cu, %	1.2	1.3	1.6	1.9	1.3	1.6
CaO, %	0.2	5.2	4.5	12.1	4.8	7.7
Mg, %	—	2.4	1.9	7.5	2.8	6.9
P_2O_5, %	0.2	1.1	0.8	—	1.4	2.6
Na, %						

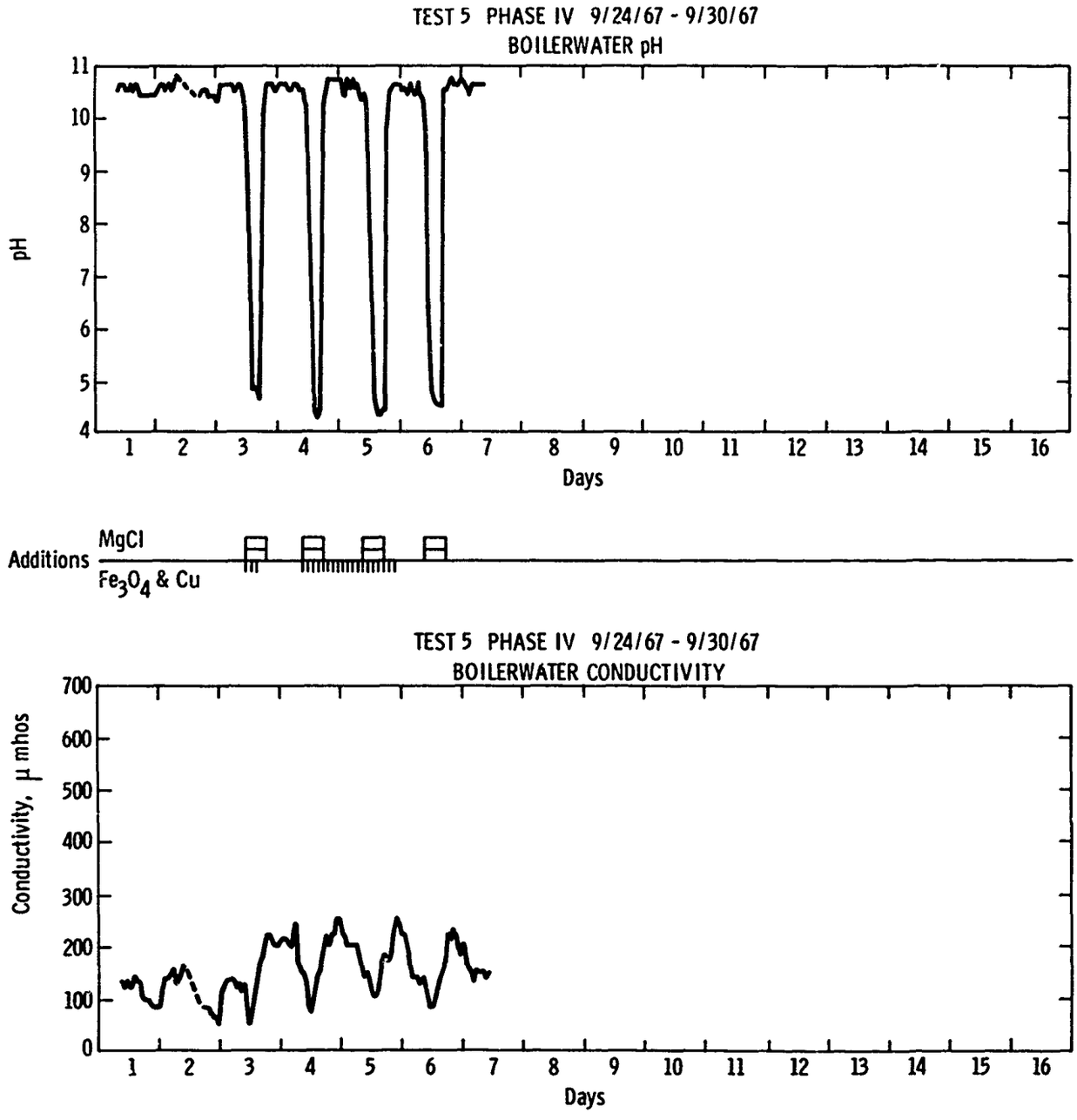

Fig. 38

The deposit structure shown in Fig. 44 is typical of that observed during previous tests at sites of plug-type corrosion and hydrogen damage. The layered structure of the deposit, which analysis showed to be almost entirely magnetite, appears to be characteristic of these sites. Some plated copper appears in the upper layers of the deposit.

LOG-TEST 6, PHASE IV

Coordinated Phosphate Boiler Water Treatment — pH = 9.8 to 10.0

DNB Operation With Clean and Dirty Boiler Conditions — No Condenser Leakage

Test 6 was conducted in a substantially different manner from the other tests of Phase IV. No simulated condenser leakage or chemicals other than sodium phosphate were added to the boiler water. The test, after establishing equilibrium hydrogen concentrations, was conducted entirely in the unstable temperature, transitional boiling region of DNB. In other words, the operating parameters exceeded the critical parameters which define the threshold of departure from nucleate

Fig. 39: Deposits on tube surface—Test 5

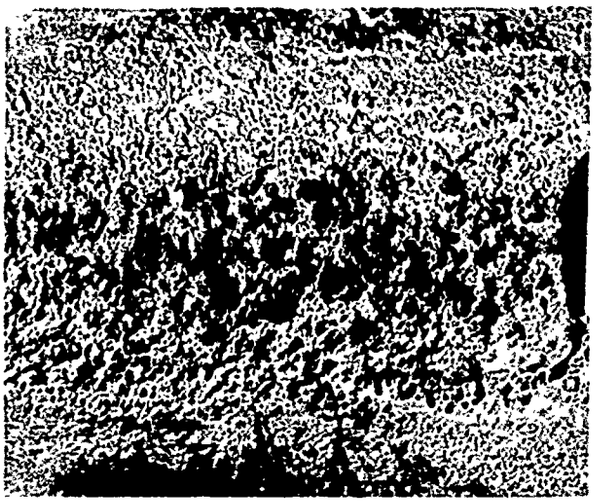

Fig. 40: Cleaned tube surface—Test 5

Fig. 42: Photomicrograph of tubing ID—Test 5—unetched (original mag = 250x)

boiling. For this test, mass velocity, heat flux, and pressure were maintained at the values employed during the previous 17 tests of the program, however, steam quality was elevated sufficiently for DNB operation. Only the "A" test loop was employed for this test.

Figure 45 and Tables XX and XXI show the boiler water chemistry maintained throughout the duration of the run. Figure 46 illustrates the hydrogen concentrations at the reflux condenser for the same period. Data (Fig. 46) show that no change in tube-metal temperature, other than the cyclical oscillations resulting from transitional boiling, occurred during clean surface testing. The amounts of chemicals required for boiler water treatment indicated that no phosphate hide-out occurred.

TEST 5 PHASE IV
BEND TEST FOR EMBRITTLEMENT

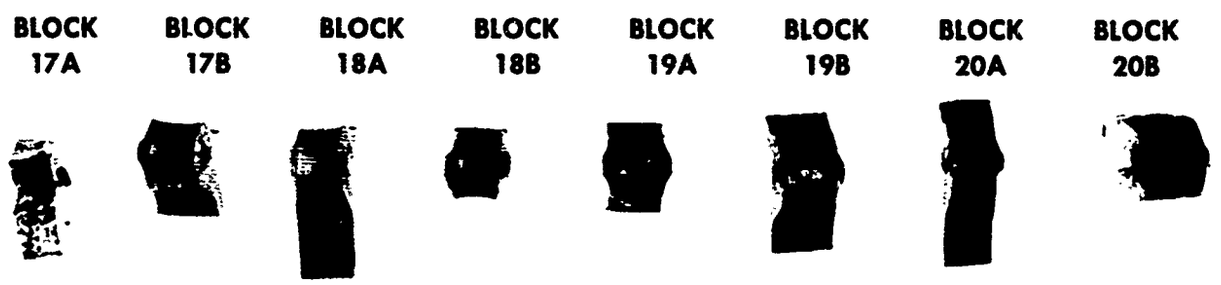

Fig. 41: Bend-test specimens—Test 5

TABLE XX
TEST 6, PHASE IV

BOILER WATER ANALYSIS

Test Day No.	Time	pH*	pH	Cond.* umhos	Alkalinity "P" Epm	Alkalinity "MO" Epm	PO_4* ppm	PO_4 ppm	Na ppm	Cu ppm	Fe ppm	H_2* ppb	SiO_2* ppm
1	2000	9.9	8.9	35	.04	.28	8.0	9.0	7.0	.06	.2	143	.84
2	2000	9.9	9.2	38	.04	.24	8.0	7.4	6.3	.22	—	152	.24
3	2000	10.0	7.3	36	—	.24	9.0	8.2	7.4	.34	.1	159	.14
4	2000	10.0	7.6	50	—	.24	10.0	6.4	8.0	.08	.1	213	.48
5	2000	9.9	7.4	40	—	.22	7.8	6.6	6.6	.08	.1	153	.96
6	2000	9.9	9.4	45	.04	.24	8.0	6.6	6.6	3.20	1.0	147	.86
7	2000	9.8	8.7	50	.04	.26	9.4	9.2	9.0	.04	.3	145	.23
8	2000	9.9	9.7	55	.04	.26	10.0	9.8	9.0	.02	.2	147	.16
9	2000	9.8	8.2	50	—	.24	8.8	8.5	9.0	.65	1.0	135	.16
10	0400	9.8	9.5	48	.04	.24	9.8	7.8	8.4	.02	.3	131	.15
11	0400	9.8	10.0	48	.14	.35	7.6	9.2	10.4	—	—	148	.15
12	1400	10.3	10.3	140	.26	.56	20.0	19.4	18.4	.08	.3	90	.18
13	0400	10.0	10.1	80	.18	.44	18.5	14.8	13.6	.02	.3	100	.12
14	0400	9.8	9.6	50	.05	.23	9.5	7.5	7.6	.02	.4	96	.11
15	0400	10.0	9.8	45	.06	.26	9.8	7.5	7.0	.02	.2	91	.098
16	0400	9.8	9.5	40	.04	.20	9.8	8.8	6.6	.02	.2	81	.14

* Values determined at time of sampling. All other recorded values are from later lab analyses.

TABLE XXI
TEST 6, PHASE IV

X-RAY DIFFRACTION ANALYSIS OF MATERIAL FILTERED* FROM BOILER WATER

Test Day No.	Time	Major	Minor	Trace
4	2000	Cu	—	Fe_3O_4, Cu_2O, CuO
6	0400	Fe_3O_4, Cu	—	Fe_2O_3, Cu_2O
7	1400**	—	—	—
14	1400**	—	Cu	Fe_3O_4

* 0.45 micron pore size.
** Amorphous phase noted.

Fig. 43: Photomicrograph of tubing OD—Test 5—unetched (original mag = 250x)

Fig. 44: Photomicrograph of deposit cross section—Test 5—unetched (original mag = 100x)

Reductions in operating quality were effected late on the third test day and corrosion products (iron oxide and copper) were added to the loop. Injections were made on a 2-hour cycle for the next 48 hours until 2,400 grams of contaminant had been injected. Subsequently, the quality was again elevated into the unstable DNB region. DNB occurred at a steam quality less than that required for clean tube conditions.

Operation in DNB was sustained during the following ten days. Hydrogen concentrations never exceeded 100

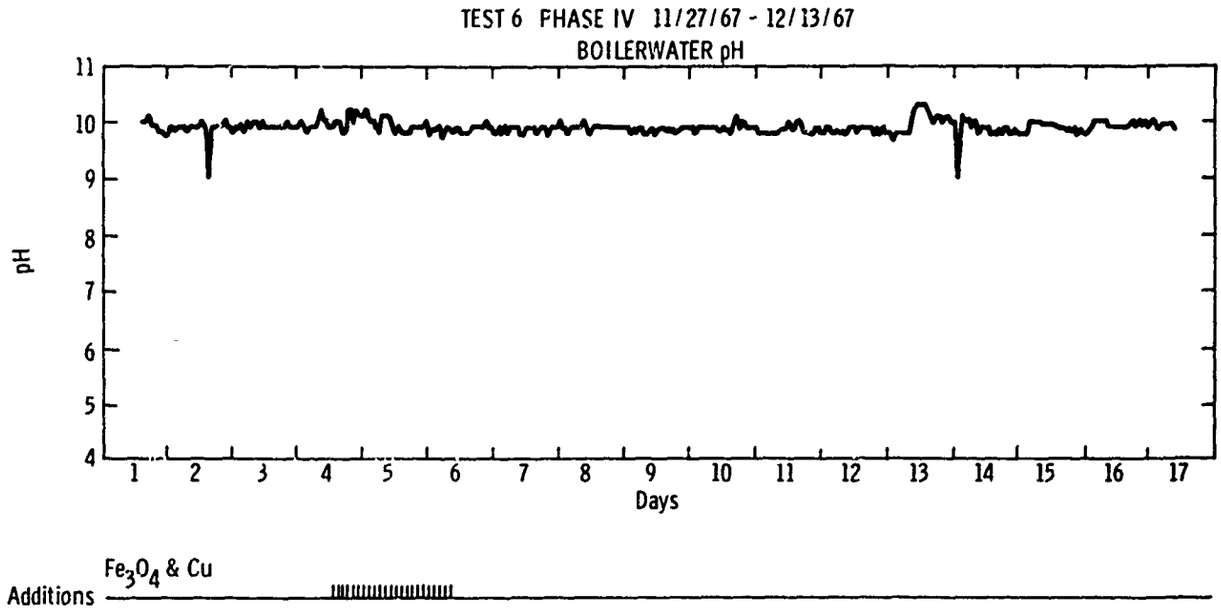

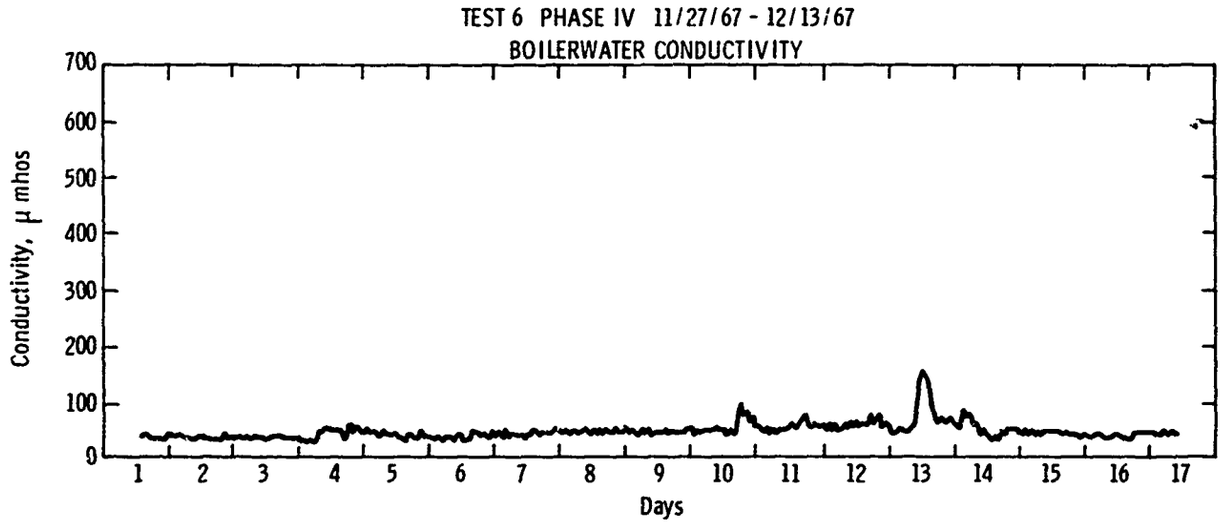

Fig. 45

TABLE XXII
TEST 6, PHASE IV
DEPOSIT ANALYSIS

	X-RAY DIFFRACTION ANALYSIS			CHEMICAL ANALYSIS		
Block No.	Composite of Blocks (17A-20A)	Composite of Blocks (21A-24A)	Water Soluble Extract from Composite (21A-24A)		Composite of Blocks (17A-20A)	Composite of Blocks (21A-24A)
MAJOR	Fe_3O_4	Fe_3O_4	Na_2HPO_4	IGNITION GAIN		
	Cu	Cu	—	SiO_2, %	0.4	1.1
	Unidentified	Unidentified	—	Fe_3O_4, %	47.7	43.1
MINOR	Fe_2O_3	Fe_2O_3	—	Cu, %	25.8	14.8
TRACE	Cu_2O	Cu_2O	—	P_2O_5, %	20.5	28.4
	$Na_4P_2O_7$	$Na_4P_2O_7$	—			
	$Cu_5(PO_4)_2(OH)_4$	$Cu_5(PO_4)_2(OH)_4$	—	Na_2O, %	7.9	12.4

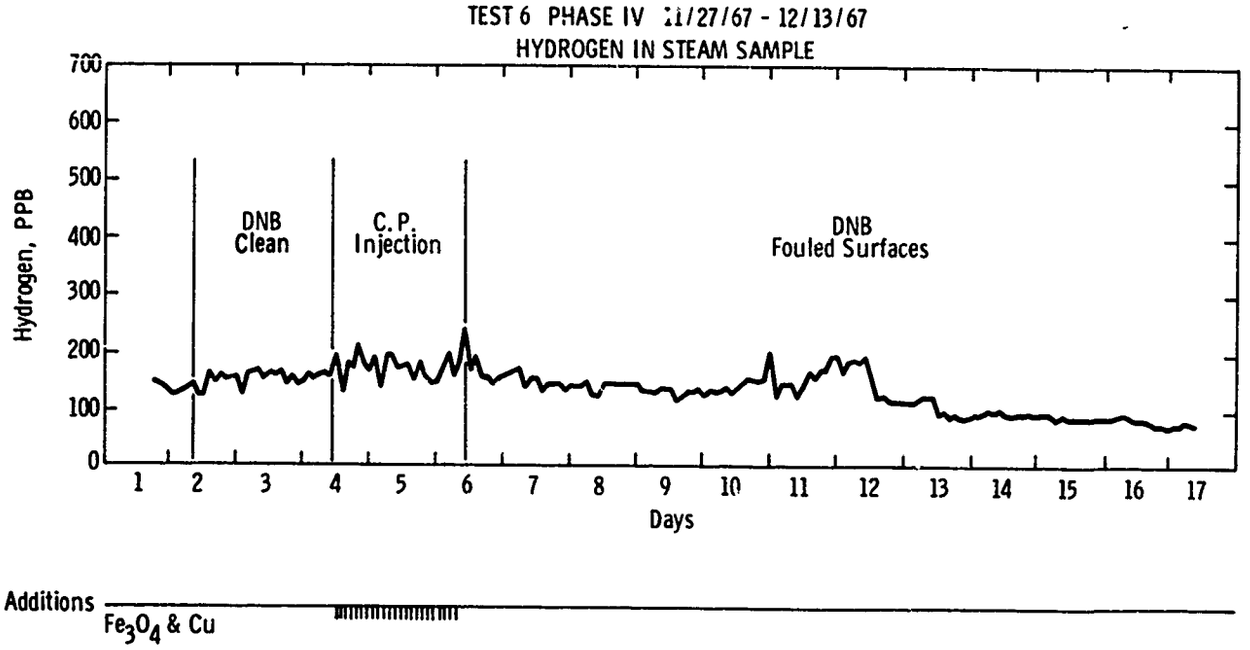

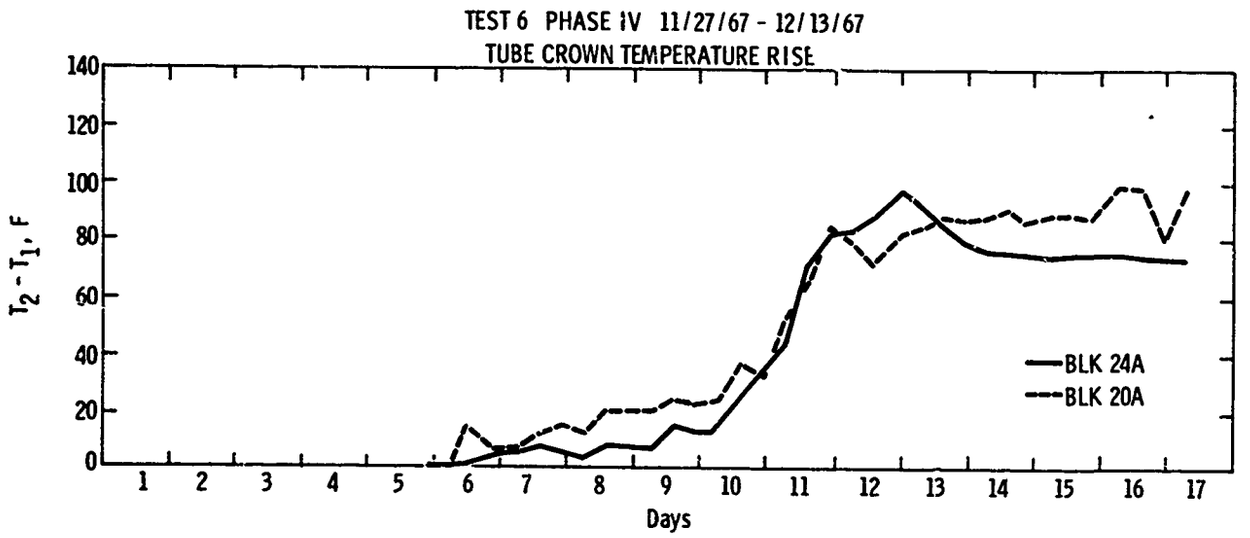

Fig. 46

ppb, which is a value considered to be the base line for the test apparatus. Temperatures did, however, increase during this period and, in fact, the outside tube metal temperatures were at or above 900 F during the last four days of testing. Some evidence of phosphate hide-out, as well as increases in silica concentration in the boiler water, were noted upon shutdown.

Relatively thin powdery deposits, not exceeding 25 mils in thickness and in most cases much less, were found on the test surfaces (Figs. 47 and 48). The deposits consisted primarily of iron oxide and copper with white salts randomly dispersed on the surface. Substantial proportions of sodium and phosphate were found in the deposits and X-ray diffraction suggested the presence of both sodium pyrophosphate, basic copper phosphate, and at least one other crystalline phase whose pattern was not identifiable from the 1967 ASTM diffraction card index. (This was similar to the unidentified phase in Test 2). Analyses of deposits are included in Table XXII.

The deposits were removed with the standard chemical cleaning solution and the surfaces examined. No corrosion was noted at any location in the test sections (Fig. 49). Draw marks and lines resulting from the wire brushing of the tube prior to testing were still in evidence on the metal surfaces. Bend tests and metallurgical evaluation revealed no decarburization or hydrogen damage.

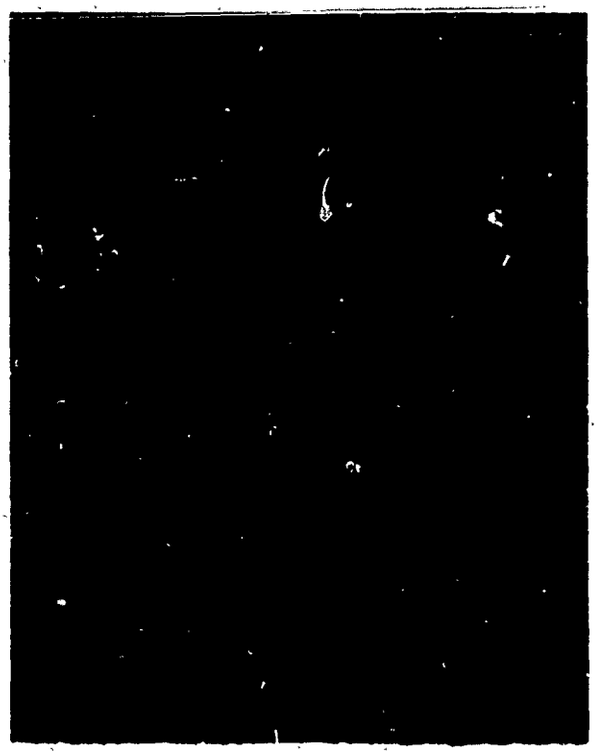

Fig. 47: Deposit on tube surface—Test 6

Fig. 48: Photomicrograph of deposit cross section—Test 6—unetched (original mag = 100x)

LOG-TEST 7, PHASE IV

Coordinated Phosphate Boiler Water Treatment — pH = 9.8 to 10.0

Dirty Boiler Conditions — Magnesium Chloride Contaminant (Continuous Injection)

Initial injections of contaminants were delayed until the third operating day due to difficulties with the hydrogen analyzer. After repair and calibration of the analyzer, preboiler corrosion product addition was begun.

Injection of magnesium chloride contaminant was started on the fourth day of operation. Salt solution was continuously added instead of the intermittent 8-hour cycle employed in earlier tests. The same total quantity of salt used in Tests 4 and 5, 77 grams of hydrated magnesium chloride in solution, was pumped into the loop each day. On the sixth day of operation, the rate was doubled to 154 grams of hydrated magnesium chloride during each 24 hour period. This rate of injection was maintained throughout the duration of the test.

Phosphate and pH concentrations were kept within normal specified control limits throughout the entire two-week operating period (Fig. 50). This differed from previous practice since during cyclical operations no attempt to maintain water chemistry specifications was made. Typical analyses of the boiler water during this two-week period are listed in Tables XXIII and XXIV.

Hydrogen data (Fig. 51) reveal that no substantial corrosion occurred during the test. The small hydrogen peaks which occurred during the injection of iron oxide and copper are typical for this operation. Other peaks on the hydrogen plot reflect deviations in reflux condenser operating conditions. When compared to previous data, the equilibrium hydrogen concentration which existed throughout most of the run was found to be one of the lowest experienced during the entire program. Chemical control of the boiler water was accomplished primarily with trisodium phosphate, although small amounts of caustic were occasionally required. Figure 51 shows the temperature change at various locations of the test sections. A maximum increase in tube-metal temperature of approximately 25 F was noted.

Fig 49: Cleaned tube surface—Test 6

TABLE XXIII

TEST 7, PHASE IV
BOILER WATER ANALYSIS

Test Day No.	Time	pH*	pH	Cond.* umhos	Alkalinity "P" Epm	Alkalinity "MO" Epm	Cl ppm	PO_4* ppm	PO_4 ppm	Na ppm	Mg ppm	Cu ppm	Fe ppm	H_2* ppb	SiO_2* ppm
3	0400	9.9	6.6	30	0	.20	.40	6.8	6.4	6.4	.01	.296	.002	30	.280
	1400	10.0	7.4	29	0	.20	.40	6.0	6.0	4.9	.01	.059	.007	45	.260
	2000	10.0	6.9	32	0	.24	.30	5.2	6.4	6.2	.01	1.80	.130	105	.540
5	0400	9.5	6.4	175	0	.16	39.40	5.6	4.5	31.60	.01	.118	.008	68	.670
	1400	9.9	6.6	220	0	.16	53.00	6.0	2.2	45.00	.01	.059	.009	60	.500
	2000	9.8	7.1	220	0	.28	50.00	10.0	10.4	46.00	.01	.094	.009	54	.326
7	0400	9.8	7.4	345	.04	.28	85.40	8.2	9.9	68.00	.015	.823	.176	47	.050
	1400	9.9	6.6	420	0	.12	98.80	7.4	5.4	78.00	.020	.070	.054	52	.050
	2000	9.8	6.6	440	0	.16	117.00	8.0	6.2	88.00	.010	.063	.002	52	.050
9	0400	9.6	6.7	—	0	.20	144.00	10.4	8.6	109.00	.015	.024	.001	49	.050
	2000	9.8	7.0	630	0	.24	169.60	11.0	8.3	136.00	.011	.046	.001	50	.160
11	0400	9.6	6.8	566	0	.20	167.00	5.9	5.4	127.00	.020	.094	.001	48	.100
	1400	9.6	6.8	655	0	.20	191.50	7.5	6.6	144.00	.020	.624	.024	47	.070
	2000	10.0	6.8	533	0	.20	152.50	9.8	7.3	102.00	.021	.118	.001	48	.090
13	0400	9.8	6.9	529	0	.29	138.00	7.2	5.0	112.00	.013	2.22	.637	52	.120
	1400	9.7	6.7	580	0	.20	156.00	9.8	6.2	125.00	.049	.212	.028	66	.112
	2000	10.0	7.3	510	0	.28	143.00	5.5	2.7	111.00	.011	.525	.074	54	.110
15	0400	9.8	7.0	560	0	.24	149.00	8.0	7.4	121.00	.018	.094	.021	48	.085
	1400	9.7	6.8	580	0	.24	150.00	7.2	7.3	109.00	.018	1.400	.147	55	.082
	2000	9.9	7.1	602	0	.28	160.00	5.8	5.8	112.00	.080	.070	.005	56	.110
16	0400	9.8	7.0	540	0	.28	141.50	10.4	7.3	100.00	.010	—	—	56	.093

* Values determined at time of sampling. All other recorded values are from later lab analyses.

TABLE XXIV

TEST 7, PHASE IV

X-RAY DIFFRACTION ANALYSIS OF MATERIAL FILTERED* FROM BOILER WATER

Test Day No.	Time	Major	Minor	Trace
10	2000	Fe_3O_4	Cu	Fe_2O_3, CuO
11	2000	Fe_3O_4	Cu	Fe_2O_3, CuO
12	0400	Fe_3O_4, Cu	Cu_2O, Fe_2O_3	—
13	2000	Fe_3O_4	—	Fe_2O_3, Cu_2O, Cu
14	1400	Fe_3O_4	—	Fe_2O_3, Cu_2O, Cu

* 0.45 micron pore size.

Inspection of the test surfaces revealed a very thin (~2 mils) powdery deposit (Fig. 52). Analyses showed that deposits consisted primarily of iron oxide and copper. Magnesium concentrations were surprisingly low (Table XXV). No corrosion was observed after acid cleaning with the standard solution. Draw marks as well as scratches resulting from wire brushing prior to testing were visible on the test sections (Fig. 53). Bend tests and metallurgical evaluations proved that no metallurgical damage had occurred.

TABLE XXV

TEST 7, PHASE IV
DEPOSIT ANALYSIS

X-RAY DIFFRACTION ANALYSIS

Block No.	17A
MAJOR	Fe_3O_4
	Fe_2O_3
MINOR	—
TRACE	—

CHEMICAL ANALYSIS

Block No.	20A	17B	20B	Drum Deposit
IGNITION	GAIN	GAIN	GAIN	GAIN
SiO_2, %	3.3	1.4	2.5	1.5
Fe_3O_4, %	92.3	66.2	68.6	51.4
Cu, %	<0.5	29.5	30.9	45.5
MgO, %	3.0	1.3	1.2	1.1
P_2O_5, %	<0.5	<0.5	<0.5	<0.5
Na_2O, %	1.0	<0.5	<0.5	<0.5

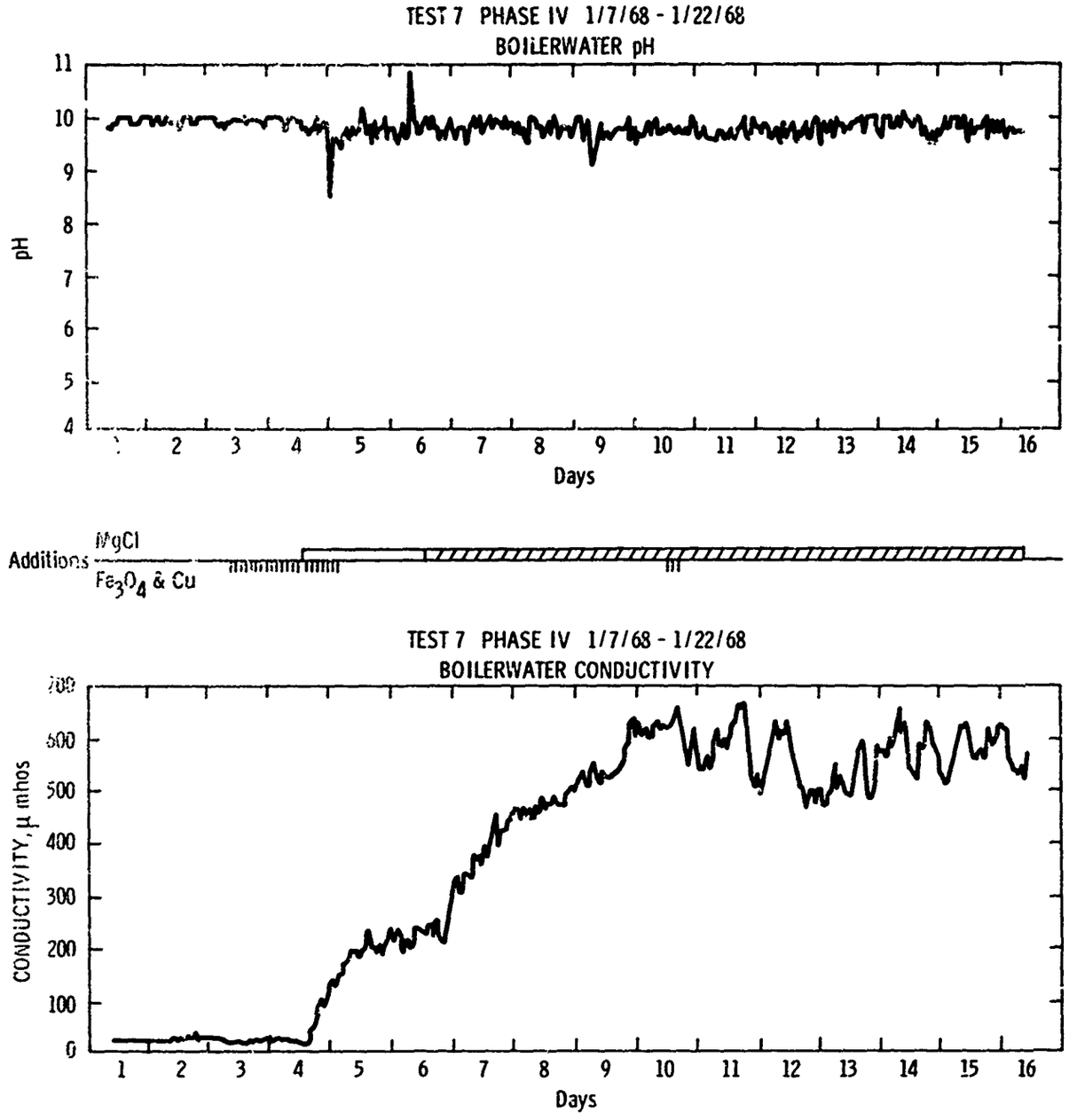

Fig. 50

LOG-TEST 8, PHASE IV

Coordinated Phosphate Boiler Water Treatment — pH = 9.8 to 10.0

Dirty Boiler Conditions — Calcium Sulfate, Calcium Chloride Contaminants

Acid cleaning prior to this test resulted in initially high hydrogen concentrations necessitating a period of seasoning operation. During seasoning, several circulating pump failures occurred. The period of operation shown in Figs. 54 and 55 constitutes the unaborted portion of the test.

Additions of iron oxide and copper were initiated approximately 24 hours after the start of the test, in spite of somewhat higher than normal hydrogen concentrations. Calcium sulfate solution was injected on the third operating day. Figure 54 illustrates the pH excursion which occurred from the introduction of salt solution. The hydrogen data indicate that no corrosion occurred during this period, in fact, concentrations

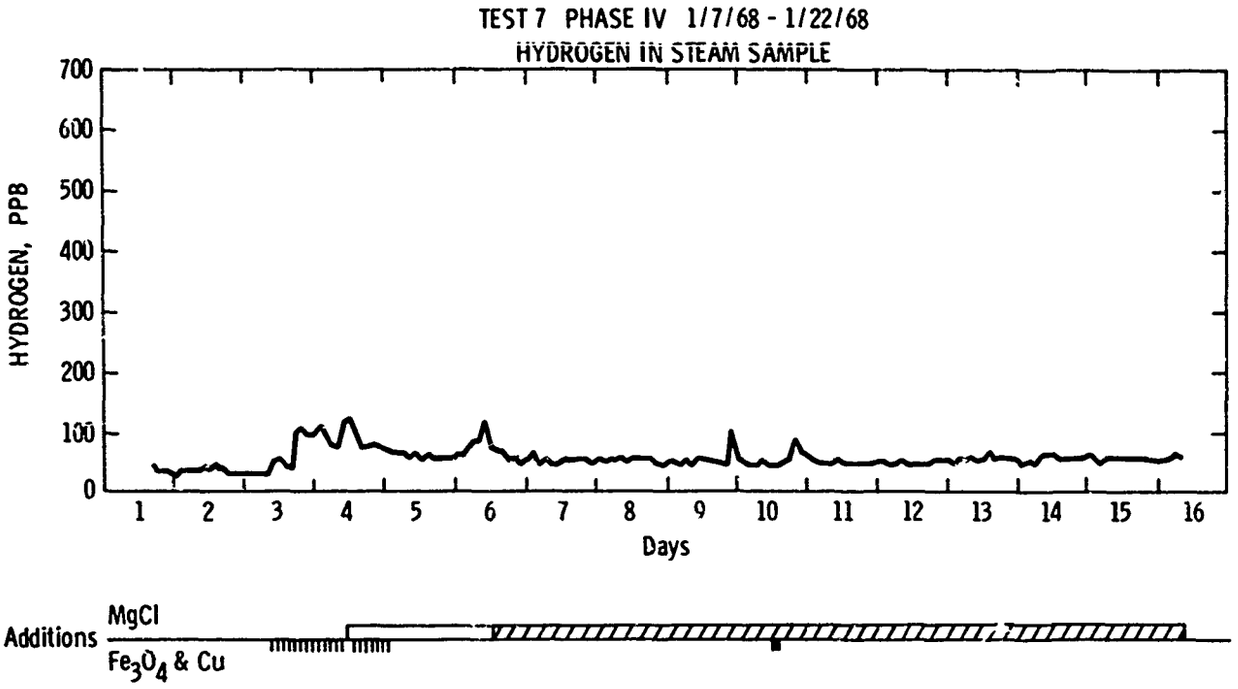

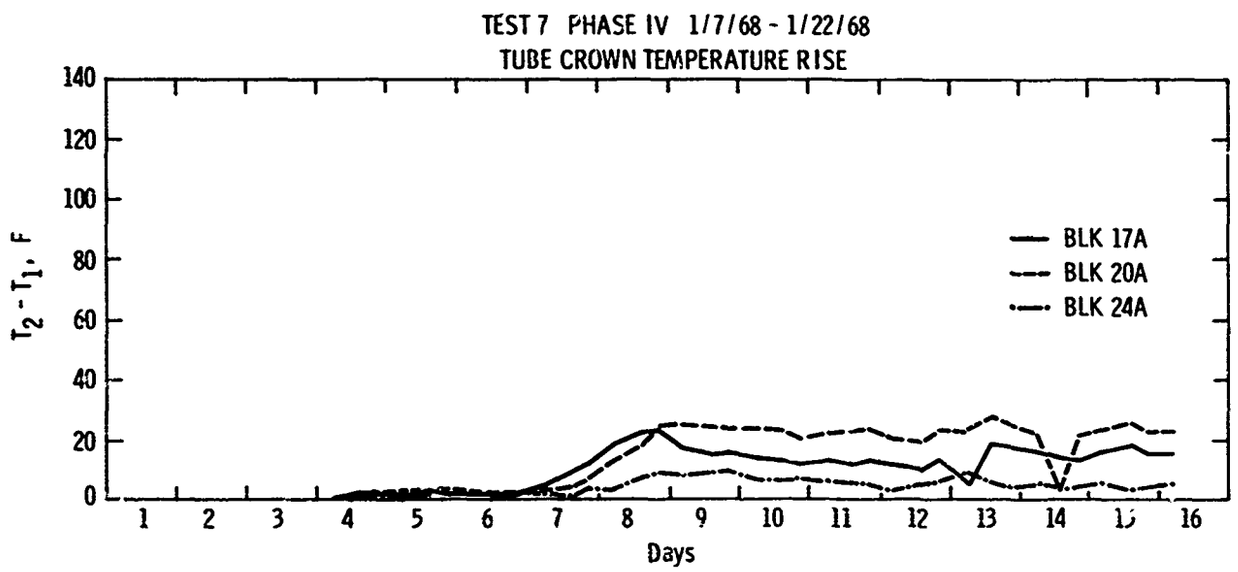

Fig. 51

continued to decrease as passivation progressed. A calcium sulfate injection cycle was made during the fourth day of operation, again resulting in no corrosion and only minimal temperature change. On the fifth day, calcium sulfate injection was extended beyond the normal 8-hour cycle for a total period of approximately 33 hours before control chemistry was restored. No change in hydrogen concentration or other indication of corrosion was experienced in spite of the low pH operation.

Several interesting phenomena were observed. Each injection of salt solution produced an immediate temperature rise and a decrease in pH. Once the pH had declined to values of from 5 to 6, the rising temperature reversed and began to decline. Another interesting observation is the unexplained increase in pH from values of approximately 4.2 to about 5.2 during the 32-hour period of calcium sulfate introduction. Table XXVI illustrates a daily cycle in water chemistry resulting from the introduction of calcium sulfate contaminant.

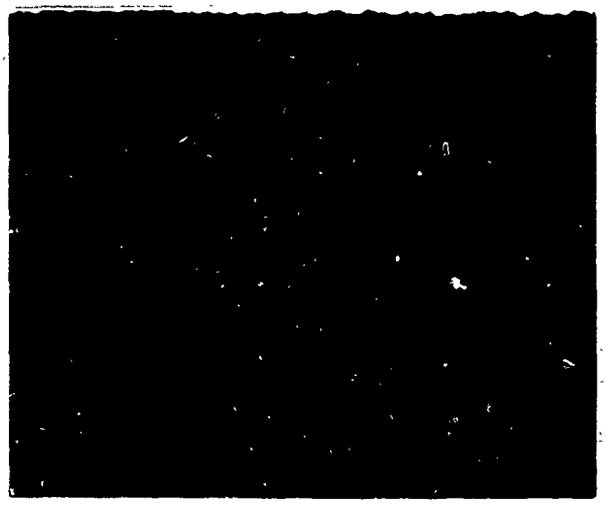

Fig. 52: Deposit on tube surface—Test 7

Since calcium sulfate did not produce corrosion, it was decided to evaluate the effects of calcium chloride. A substitution was made on the sixth operating day and an equivalent amount of calcium chloride was introduced to the test loop. The hydrogen concentrations resulting from the downward pH excursion can be seen on Fig. 55. The second, third, and fourth injections of calcium chloride produced decreasing hydrogen cycles and it was decided that further operation under these conditions served no useful purpose. The test was terminated on the twelfth operating day.

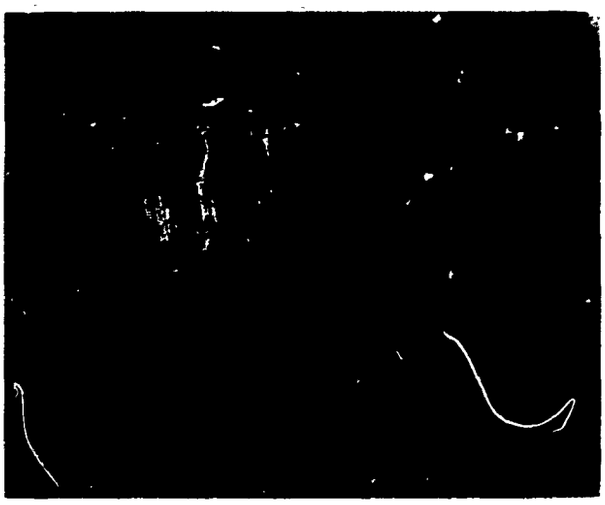

Fig. 53: Cleaned tube surface—Test 7

TABLE XXVI

TEST 8, PHASE IV
BOILER WATER ANALYSIS*
TEST DAY No. 4

				Alkalinity											
Time	pH**	pH	Cond.** umhos	"P" Epm	"MO" Epm	SO_4 ppm	Cl ppm	PO_4** ppm	PO_4 ppm	Na ppm	Ca ppm	Cu ppm	Fe ppm	H_2** ppb	SiO_2** ppm
0100	9.9	7.1	136	—	.20	39.2	<0.2	9.2	7.0	24.3	<.0	.70	.25	149	—
0200	9.8	7.0	134	—	.20	41.3	<0.2	10.1	7.0	25.8	<.01	.15	.25	168	—
0300	9.9	7.2	137	—	.21	42.2	<0.2	9.0	7.2	26.0	<.01	.40	.25	150	—
0400	9.8	7.1	125	—	.20	39.0	<0.2	7.6	6.1	23.8	<.01	.10	.25	188	.465
0500	10.0	7.2	127	—	.21	39.0	<0.2	9.2	6.9	24.0	<.01	.10	.25	181	—
0600	10.0	7.2	117	—	.22	38.1	<0.2	9.5	7.5	23.2	<.01	.80	1.80	195	—
0700	10.0	7.2	114	—	.22	34.3	<0.2	9.0	10.8	22.5	<.01	.08	.25	168	—
0800	9.9	7.2	104	—	.21	30.8	<0.2	9.6	8.5	21.4	<.01	.30	.50	188	—
0900	9.0	—	—	—	—	26.0	<0.2	5.0	3.0	17.5	.55	—	—	153	—
1000	6.0	5.6	85	—	.04	28.8	<0.2	5.0	2.0	15.8	.85	.50	.50	130	—
1100	4.9	4.9	—	—	<.01	29.4	<0.2	5.0	0.5	14.4	1.10	2.30	1.60	139	—
1300	4.6	4.7	102	—	<.01	29.8	<0.2	3.9	<0.2	15.4	.68	1.40	.80	127	—
1400	4.2	4.3	106	—	—	30.2	<0.2	0	<0.2	16.0	.91	1.40	.80	123	.55
1500	4.2	4.3	104	—	—	29.6	<0.2	0	<0.2	15.3	.87	1.20	.80	107	—
1600	4.4	4.6	102	—	<.01	29.7	<0.2	0	<0.2	15.3	1.18	1.20	.80	113	—
1900	9.9	7.5	210	—	.23	56.1	<0.2	9.0	11.0	31.3	.08	—	—	105	—
2000	10.0	9.2	236	.08	.30	71.6	<0.2	8.2	10.0	44.9	<.01	.15	.10	141	.40
2100	9.6	9.6	234	.14	.36	69.3	<0.2	9.0	8.5	43.3	<.01	—	—	143	—
2200	10.0	9.9	235	.16	.41	69.5	<0.2	8.0	11.2	43.8	<.01	—	—	173	—
2300	10.0	10.2	234	.20	.42	65.1	<0.2	8.0	10.8	42.9	<.01	—	—	168	—
2400	9.8	10.0	225	.15	.41	59.8	<0.2	8.6	9.8	37.8	<.01	—	—	177	—

* $CaSO_4$ injection.
** Values determined at time of sampling. All other recorded values are from later lab analyses.

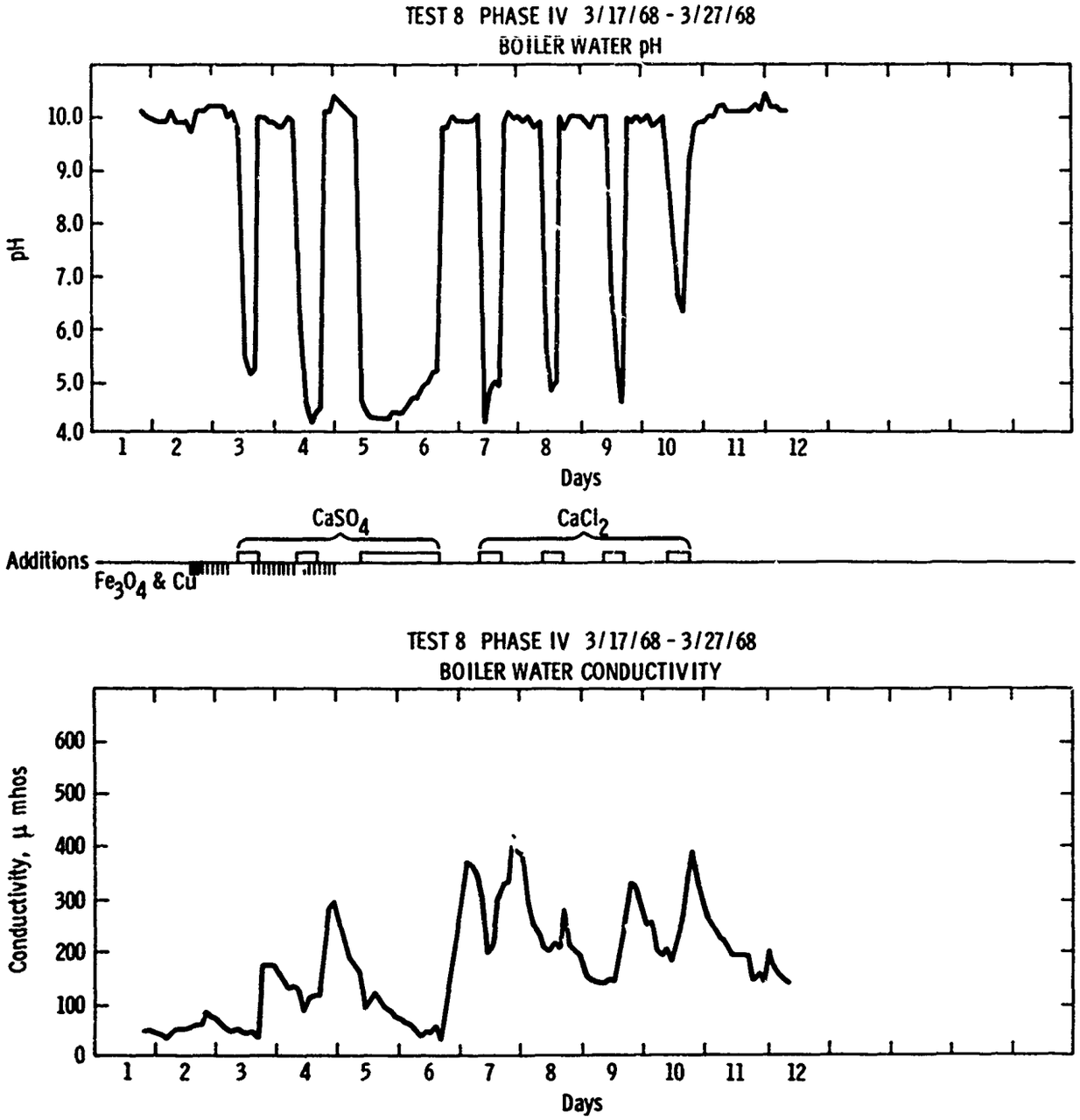

Fig. 54

Temperature plots during the period of calcium chloride injection reveal a response similar to that resulting from the injection of calcium sulfate; that is, cyclical increases and decreases in tube metal temperature occurred during contaminant addition periods. Table XXVII illustrates the changes in water chemistry experienced during a period of calcium chloride injection. Analyses of materials filtered from the boiler water from both portions of Test 8 are included in Table XXVIII.

Extensive hide-out testing was conducted during shutdown. The results of these tests are tabulated in Table XXIX and graphically displayed in Fig. 56. The pH values remained essentially constant during shutdown.

Thin, loose deposits (15 mils) were found on the test section surfaces after shutdown (Fig. 57). It was assumed that heavier deposits had been present during testing, however, most of this material sloughed off during the extended shutdown period. Analyses of the remaining deposits are included in Table XXX.

TABLE XXVII

TEST 8, PHASE IV
BOILER WATER ANALYSIS*
TEST DAY No. 9

Time	pH**	pH	Cond.** umhos	Alkalinity "P" Epm	Alkalinity "MO" Epm	SO_4 ppm	Cl ppm	PO_4** ppm	PO_4 ppm	Na ppm	Ca ppm	Cu ppm	Fe ppm	H_2** ppb	SiO_2** ppm
0100	9.9	9.5	150	—	—	—	58.0	8.0	5.6	52.0	<.01	—	—	136	—
0200	9.9	—	145	—	—	—	52.0	8.5	5.5	47.0	<.01	—	—	122	—
0300	9.9	—	140	—	—	—	45.0	8.5	4.0	46.3	<.01	—	—	129	—
0400	9.8	—	140	—	—	—	44.5	9.5	—	43.0	<.01	<.01	.10	123	.085
0500	9.9	9.3	130	.04	.18	16.0	40.0	8.0	6.3	42.9	<.01	—	—	128	—
0600	10.0	—	140	—	—	—	39.5	10.5	—	41.3	<.01	—	—	134	—
0800	10.0	9.4	140	.06	.18	—	35.0	8.5	5.4	36.3	<.01	—	—	134	—
0900	10.0	—	145	.00	.12	11.4	38.0	10.0	2.2	35.0	.12	—	—	132	—
1000	10.0	—	145	—	—	—	45.5	9.0	—	34.8	.55	—	—	132	—
1100	8.4	5.3	130	.00	.04	11.6	46.9	5.4	0.5	37.8	.58	—	—	149	—
1200	6.9	—	140	—	—	—	47.0	2.2	0.2	40.0	.63	—	—	143	—
1300	5.5	5.0	170	.00	.04	—	48.5	1.4	0.2	40.0	.49	—	—	133	—
1400	5.2	5.1	215	—	—	11.0	45.0	1.6	2.4	35.8	.10	.30	<.01	130	.083
1500	5.1	5.1	245	.00	.04	—	49.0	2.0	0.2	39.5	.56	—	—	138	—
1600	4.6	10.3	260	.28	.42	10.4	45.0	2.0	3.0	46.5	<.01	—	—	147	—
1700	4.6	9.5	300	.04	.20	—	42.0	2.0	6.8	42.8	<.01	—	—	222	—
2000	9.9	—	320	—	—	—	36.5	6.2	—	33.6	<.01	.15	<.01	131	.081
2100	10.0	9.6	310	.08	.22	—	34.5	8.5	7.7	36.0	<.01	—	—	133	—
2200	10.0	9.5	290	.06	.22	9.6	32.5	8.0	8.5	35.1	<.01	—	—	140	—
2300	9.9	9.5	270	.06	.18	—	29.0	7.5	5.1	29.0	<.01	—	—	141	—
2400	9.9	9.4	250	.04	.24	—	30.5	6.5	10.6	31.8	<.01	—	—	143	—

* $CaCl_2$ injection.
** Values determined at time of sampling. All other recorded values are from later lab analyses.

TABLE XXVIII

TEST 8, PHASE IV

X-RAY DIFFRACTION ANALYSIS OF MATERIAL FILTERED* FROM BOILER WATER

Test Day No.	Time	Major	Minor	Trace
4	0800	Cu	—	Fe_3O_4
6	0400	Cu	Fe_3O_4	—
7	0600	Cu	—	—
8	1400	Fe_3O_4	Cu	$Ca_5(PO_4)_3OH$, Cu_2O

* 0.45 micron pore size.

Minor pitting (~1 mil) was found at various sites in both test loops (Fig. 58). No hydrogen damage was observed.

DISCUSSION OF RESULTS

Deposits

In both of the two previous progress reports, observations and trends relating to the deposition of solids were indicated. The observations on deposits

TABLE XXIX

TEST 8, PHASE IV
BOILER WATER ANALYSIS
HIDE-OUT DATA

Test Day No.	Time	SO_4 ppm	Cl ppm	PO_4 ppm	Na ppm	Ca ppm
11	1030	8.6	25.0	8.4	25.8	<.01
	1130	8.6	23.0	9.4	23.4	<.01
	1250	8.6	21.0	7.4	26.4	<.01
	1410	8.0	21.0	6.6	25.8	<.01
	1520	9.0	17.0	11.2	24.0	<.01
	1620	8.6	19.0	14.6	27.0	<.01
	1740	9.0	17.0	10.8	22.0	<.01
	1900	13.8	17.0	16.6	26.4	<.01
	2020	13.6	14.0	14.0	24.0	<.01
	2140	13.8	12.0	12.6	22.4	<.01
	2300	13.2	12.0	25.4	34.0	<.01
12	0020	13.6	10.0	26.4	30.0	<.01
	0140	17.0	9.0	24.0	28.4	<.01
	0300	14.0	8.0	22.2	25.8	<.01
	0420	13.8	6.0	21.6	24.6	<.01
	0540	13.8	6.0	21.2	24.6	<.01
	0700	13.6	5.0	21.2	23.0	<.01
	082[illegible]	[illegible]8	4.0	20.8	22.4	<.01
	12[illegible]	1[illegible].6	3.0	19.4	18.0	<.01

TABLE XXX

TEST 8, PHASE IV
DEPOSIT ANALYSIS

X-RAY DIFFRACTION ANALYSIS

Block No.	17A	17B
MAJOR	Fe_3O_4 $Ca_5(PO_4)_3OH$	Fe_3O_4 $Ca_5(PO_4)_3OH$
MINOR	Cu	Cu
TRACE	—	SiO_2

* Water soluble sodium ~.1%—total sodium was determined by boiling deposit in hydrochloric acid.

CHEMICAL ANALYSIS

Block No.	17A	20A	24A	17B	24B
IGNITION	GAIN	GAIN	GAIN	GAIN	GAIN
SiO_2, %	1.3	0.5	1.5	0.3	0.1
Fe_3O_4, %	67.8	72.1	72.9	66.0	68.6
Cu, %	4.3	5.0	3.1	3.0	4.4
CaO, %	8.7	13.2	10.7	9.3	10.5
*Na_2O, %	1.9	1.1	0.5	1.9	1.1
P_2O_5, %	14.1	7.3	9.0	17.3	14.2

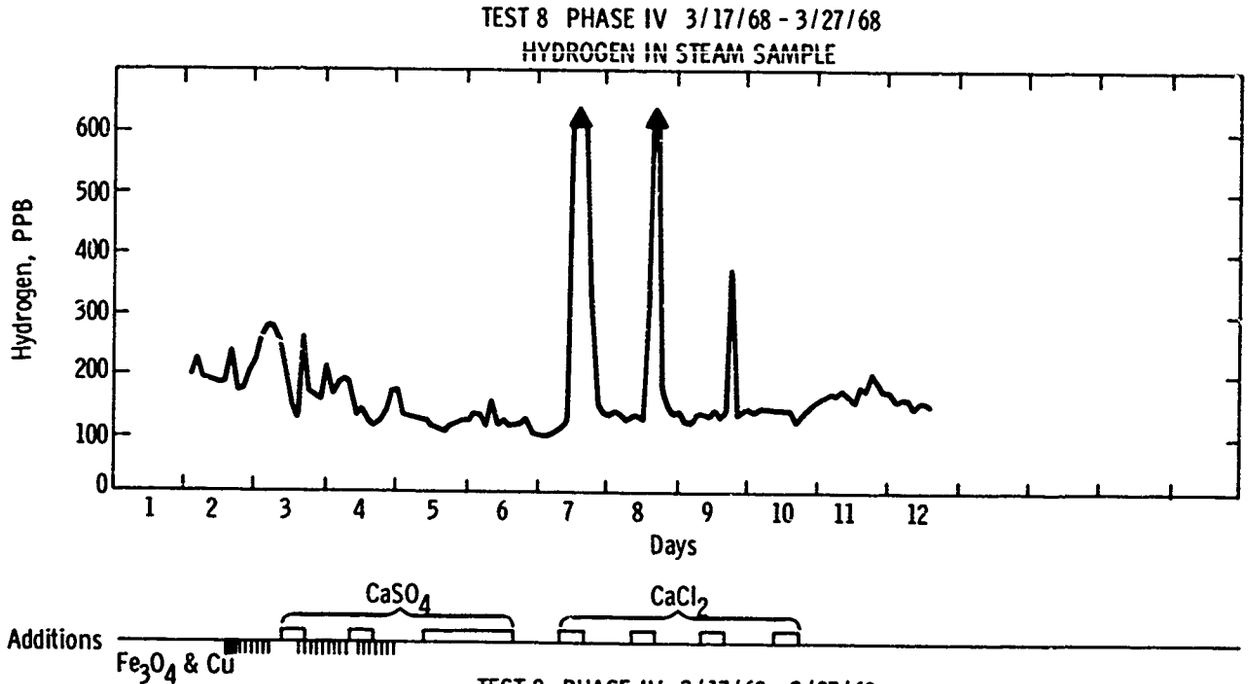

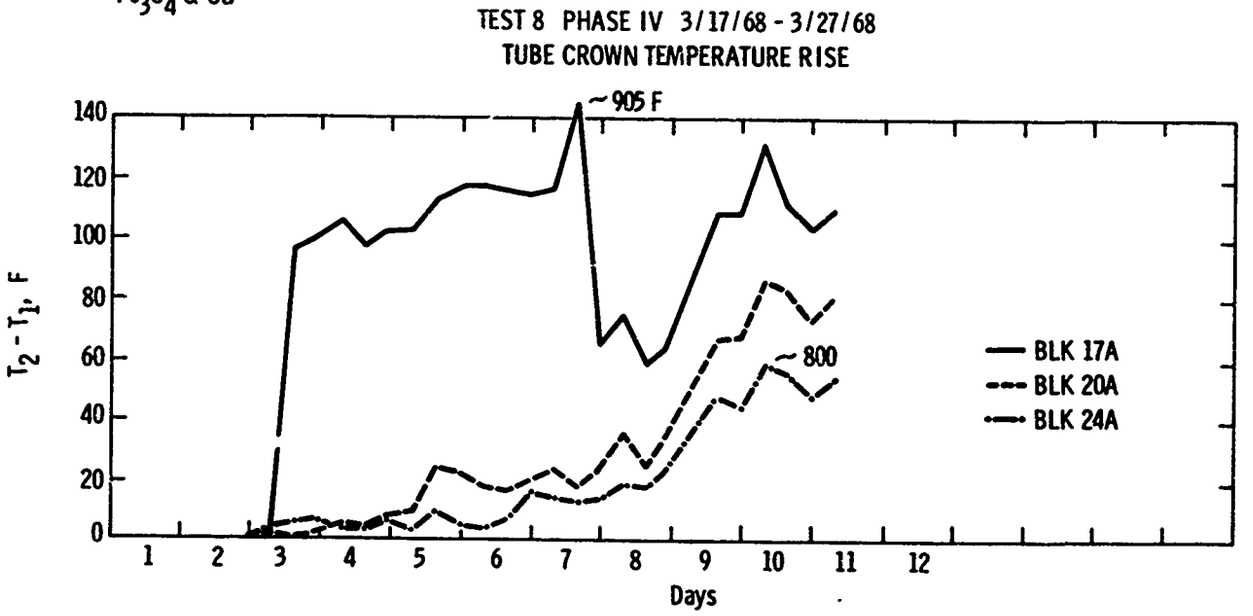

Fig. 55

made during Phase IV generally agree with these earlier results.

The reported relative increase in deposition with increasing heat flux was uniformly valid throughout the program. Aside from early tests in Phase II, which were run with corrosion products only, the steam quality of the circulating fluid appeared to have little effect on deposition. No significant differences in deposit accumulation was noted between the A and B test loops when both corrosion products and condenser leakage were injected in Phase III tests. Phase IV test conditions introduced another variable, mass-velocity, for evaluation. Within the range tested ("A" loop — .55 x 10^6 lb per hr-ft^2, "B" loop — .45 x 10^6 lb per hr-ft^2), this parameter had no discernable effect upon deposition or corrosion.

The increased amount of corrosion generally experienced during Phase IV made the trends of deposition more difficult to evaluate. In most cases, the large amount of corrosion products resulting from metal attack reduced the relative concentrations of material deposited from the boiler water although the absolute

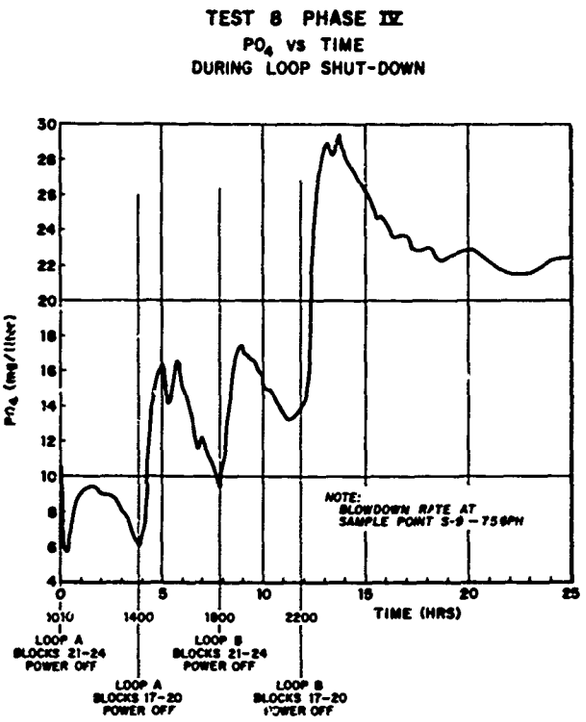

Fig. 56: Plot of phosphate hide-out data obtained during shutdown—Test 8

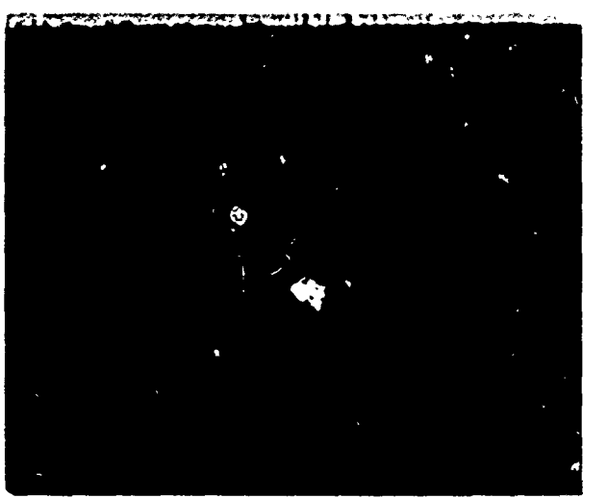

Fig. 57: Deposit on tube surface—Test 8

quantities of these materials were as great as those found after earlier tests.

The significance of surface fouling was emphasized during several tests in both Phases III and IV. It was found that with clean test surfaces no significant corrosion occurred under seemingly aggressive, low pH, boiler water conditions. Once corrosion products were injected into the loop the same contaminants produced accelerated attack.

Magnesium phosphate is generally assumed to be a "sticky" material which tends to deposit on heat-transfer surfaces. A test employing continuous injection of magnesium chloride into the boiler water with constant sodium phosphate control chemistry throughout the two-week operating period contradicts this assumption. Extremely small total amounts of deposit accumulated on heat transfer surfaces during this test. Chemical analyses of these deposits indicated less than 3 percent.

It was repeatedly found that preboiler corrosion products, added during testing, produced only small increases in tube-metal temperature. Various data also showed that phosphate hide-out did not occur with clean test surfaces even in DNB. Once surfaces were fouled with corrosion products, precipitation of various salts occurred within the porous matrix of these materials and significant increases in tube metal temperatures were observed. Test 6 of Phase IV, which was conducted in DNB, illustrates the above. Neither hide-out nor increases in metal temperature, other than the cyclical oscillation resulting from operation in the transitional boiling regime, occurred during the initial "clean tube" portion of the test. Once corrosion product fouling had been induced, phosphate hide-out occurred and the cyclical temperature oscillation became superimposed on a gradually increasing metal temperature resulting from the precipitation of salts within the deposit matrix.

Observations and data on deposition have substantially expanded our understanding of this subject. These same data, however, indicate the need for more detailed study of high-temperature surface phenomena. Various deposit analyses showed that both amorphous and unidentified crystaline phosphates, tied up as sodium, calcium, magnesium, iron, or complexes of these ions, frequently occurred. The existence of these

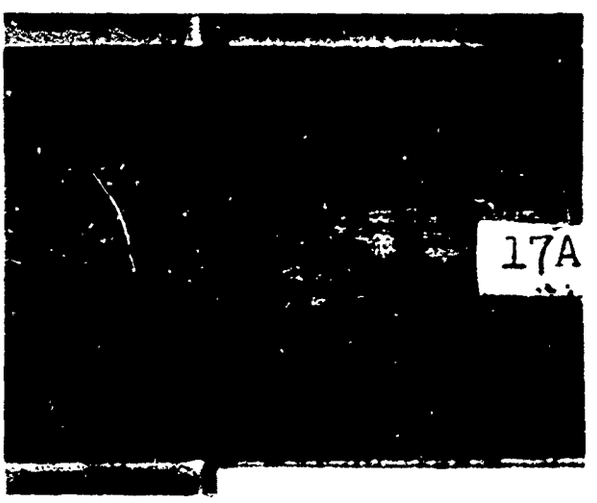

Fig. 58: Cleaned tube surface—Test 8

phases was established, their composition was not. The deposition of particulate matter on a boiling heat transfer surface was established. The mechanism producing this effect was not. Deposition of corrosion products from suspension in the boiler water was affected by water chemistry. The mechanism causing this remains to be established.

Corrosion

The data from the entire twenty-test program indicate that an active corrodent other than water was necessary to cause significant attack of the boiler tubing. Early Phase III tests under high-quality, high-flux, nucleate boiling conditions, both clean and with corrosion product fouling, resulted in no significant corrosion from the water itself. A Phase IV test conducted under unstable DNB heat-transfer conditions also showed that water by itself, even under these severe operating conditions, did not produce accelerated attack.

Of the three chemicals used for boiler water treatment (ammonia, sodium phosphate, and sodium hydroxide), only caustic proved to be aggressive. Caustic attack occurred during several tests. The most dramatic of these resulted in a gouging-type failure early in Phase III. Less severe caustic attack occurred during several other tests.

The extremely high corrosion rates which resulted in a gouging failure in the high-heat-flux-test section occurred when caustic was the major soluble constituent in the boiler water. When large concentrations of neutral salts were also present in solution, lesser rates of attack occurred. Data indicate that this type of attack resulted from the concentration of sodium hydroxide to aggressive levels within deposits on the heat transfer surface.

The solution concentration at a metal surface is a function of the thermal gradient across the deposit on the surface. The total salt concentration is, therefore, dependent upon three physical factors; local heat transfer rate, deposit thickness, and the thermal conductance of the deposit. In addition, the concentration of a specific soluble constituent is a function of its relative concentration in the bulk fluid. Hence, for a given ΔT, the concentration of caustic and the resulting rate of attack were highest when caustic represented the major fraction of the dissolved solids in the boiler water. In many of the tests which employed condenser leakage with caustic treatment, caustic corrosion occurred alternately with acid attack, the former during the 16-hour period of control chemistry and the latter during the period of condenser leakage injection. High corrosion rates, which occurred from acid attack, were reduced by caustic control chemistry. Reductions, however, were not to base-line zero corrosion values and often subsequent increases occurred as blowdown reduced contaminant salt concentrations in the boiler water. It may be seen from the hydrogen data that injections of condenser leakage and the initial decrease in pH values reduced corrosion rates to base-line zero values prior to the initiation of high rates of acid attack. Presumably, the caustic concentration at the deposit-metal interface was neutralized and diluted when condenser leakage was initiated.

Ammonium hydroxide was not aggressive. However, data showed that ammonia was ineffective in neutralizing acid attack caused by the reaction of condenser leakage contamination in the boiler water. In a number of tests, condenser leakage which normally produced pH excursions to the 4.0 to 4.5 range was initiated, but control chemistry (pH 9.0) was maintained with ammonia. In these instances, corrosion progressed unaffected by the ammonia concentration in the boiler water. This phenomenon is explained by the fact that ammonia exists as an undissociated (not ionized) molecule at high temperature and, thereby, provides no buffering action under these conditions (4).

Sodium phosphate treatment provided sufficient alkalinity to neutralize the effects of acid condenser leakage and to prevent corrosion. In many cases, phosphate hide-out provided stored buffer to the system which prevented corrosion from being initiated within the eight-hour period of condenser leakage normally employed. If, however, condenser leakage and the resulting aggressive conditions were maintained for sufficient time, corrosion commenced following the dissolution and reaction of precipitated phosphates from within the deposit matrix. As condenser leakage depleted phosphates from solution, the chemical equilibrium between the soluble and insoluble phases was upset and precipitated phosphates tended to redissolve in the boiler water. Since the rate of hardness injection equalled or exceeded the rate of dissolution of the phosphate hide-out, no appreciable concentrations of phosphate were detectable in solution.

A similar phenomenon was observed in the case of sulfates. The final test of Phase IV employed calcium sulfate contamination during the first week of operation and calcium chloride for the remainder of the run. During the period of sulfate injection, massive sodium sulfate deposition occurred. When the system equilibrium was changed by the blowdown of soluble sulfates and the injection of calcium chloride, dissolution of precipitated sodium sulfate occurred in quantities sufficient to sustain 5 to 15-ppm concentrations in the boiler water for the remaining week of the test. Calculated concentration decrease by blowdown indicates that the soluble sulfates should have declined to the limit of detection within a 24-hour period following their last addition. Upon shutdown, the balance of the sodium sulfate hide-out returned to solution producing

30-ppm water concentrations. These data are consistent with the findings of earlier tests in which it was observed that sodium sulfate hide-out was normally five to ten times greater than sodium phosphate.

Earlier progress reports described three characteristic types of corrosion failures which constitute the most severe problem in high-pressure boilers. These were:

1. Ductile gouging
2. Hydrogen damage or embrittlement
3. Plug-type oxidation

As previously noted, ductile gouging was induced and studied in this program. Plug-type oxidation, which describes the physical appearance of the corrosion site, has been observed during numerous tests and was previously reported. Attempts to induce hydrogen damage so that the phenomenon could be studied were unsuccessful during Phase II and Phase III, however, three of the Phase IV tests resulted in hydrogen damage of the test tubing. Test 1 with fresh water condenser leakage, Test 4 with magnesium chloride contamination, and Test 5 also with magnesium chloride all experienced hydrogen damage at some locations and plug-type corrosion without damage at other sites.

The environmental conditions which produced each incident of plug-type corrosion and each incident of hydrogen damage were basically similar. Corrosion product contamination, and condenser leakage which induced a pH depression from control conditions to a range of from 4.0 to 5.0, brought about these results.

Sea-water condenser leakage, Phase IV fresh-water condenser leakage, magnesium chloride solutions, and calcium chlorides solutions, all produced pH excursions and accelerated attack which resulted in plug-type corrosion sites. In the case of fresh-water condenser leakage with ammonia treatment, incipient hydrogen damage sites were found randomly distributed at corrosion plugs in both the "A" and "B" loops in the 150,000-Btu per hr-sq ft and 110,000-Btu per hr-sq ft zones. Two subsequent tests with the same contaminants, but with sodium phosphate and sodium hydroxide treatment, respectively, resulted in corrosion without hydrogen damage of the tube metal.

Two tests (sodium phosphate and sodium hydroxide treatment) with magnesium chloride contamination resulted in total fissuring of the tube metal at the Block 17 location in the "A" loop and varying degrees of damage randomly located in other areas. In both cases, high corrosion rates existed only for a period of approximately 48 hours, after which, in the first instance, a brittle failure occurred and, in the second, an early shutdown was executed to avoid failure. Corrosion rates in the fresh-water ammonia test were not as great as the two magnesium chloride runs, but all were significantly higher than tests which resulted in plug-type corrosion alone. A valid comparison of these three experiments to the Phase III sea-water test with volatile treatment is not possible, since this run was terminated after only one major corrosion cycle.

The occurrence of pH excursions as a result of the injection of soluble salts to the test loop is fairly clear cut where a single salt was injected. Magnesium chloride produced reductions in boiler water pH by reacting with and precipitating phosphate and hydroxyl ions. Once the soluble phosphates were depleted, magnesium hydroxide precipitation reduced the pH to values of 4.0 to 5.0. Continued injection of magnesium chloride at these minimum pH values resulted in increasing concentrations of soluble magnesium in the boiler water. Similar excursions accompanied the injection of calcium chloride. The minimum pH reached was approximately equal to that resulting from magnesium chloride injection. The reactions are considered to be similar. These reactions may be written as follows:

$$MgCl_2 + 2\ HOH \rightleftharpoons Mg(OH)_2 + 2\ HCl$$

$$CaCl_2 + 2\ HOH \rightleftharpoons Ca(OH)_2 + 2\ HCl$$

In both cases, the high-corrosion rates which occurred indicated that hydrochloric acid was ionized at operating conditions and that the acid was concentrated within the deposit at the metal surface. Hydrogen and temperature data indicate that each daily corrosion cycle produced an increase in deposit thickness and a corresponding higher thermal differential across the deposit, which resulted in increasing corrodent concentrations at the surface and corrosion rates. This effect is generally true except when phosphate hideout progressively increased with deposit growth, and the duration and magnitude of corrosion cycles decreased within the fixed period of contaminant injection.

Calcium sulfate also brought about pH excursions in the 4.0 to 5.0 range, however, no corrosion occurred even when the injection period was extended to approximately 32 hours. This extended injection period was maintained to determine whether phosphate hideout could be suppressing the initiation of corrosion. Data suggest that calcium hydroxide precipitation occurs, leaving an acid sulfate (HSO_4) in solution. The acid sulfate is apparently not ionized at operating temperature and, therefore, does not constitute an active corrodent. Upon cooling the boiler water sample, ionization occurs, giving the measured low-pH indication and, thereby suggesting an aggressive boiler-water condition.(5)

The deposits found in all plug-type corrosion sites were physically similar. The tube metal was coated with a dense, brittle, and adherent layer of corrosion products formed from the tube wastage. Over this layer or series of layers, a relatively loose deposit composed of externally generated corrosion products

interspersed with precipitates of various salts was normally found. Chemically, the inner deposits next to the metal were almost entirely magnetite in all cases. The outer deposit varied in composition depending upon the type of contaminants and the boiler water treatment employed. At all sites of hydrogen damage and at many of the plug-type corrosion sites, the inner deposit was composed of multiple strata of magnetite separated by partial voids. Crystallites of magnetite were identified in these void spaces, and in some cases, small amounts of plated copper were noted in the voids furthest from the tube-metal surface. From these observations, it appears that neither the composition of the outer deposit nor the presence of copper plays a major role in the corrosion process which produces both plug-type corrosion and hydrogen damage.

In all of the previously referenced tests, pH excursions were permitted to occur. Particularly aggressive conditions resulted from the injection of magnesium chloride when control chemistry was not maintained. In order to determine whether corrosion could be successfully controlled during magnesium chloride leakage, a test was run with sodium phosphate treatment and contamination for a two-week period. Neither corrosion nor significant deposition was observed after two weeks of continuous (24 hours per day) addition of magnesium chloride when sodium phosphate control chemistry was maintained.

Data indicate that the occurrence of hydrogen damage is directly related to corrosion rate. Corrosion rate controls the rate of hydrogen-ion reduction which controls the hydrogen diffusion rate through the metal within the narrow range of metal temperature of these experiments. The random occurrence of decarburized and fissured metal at some corrosion sites and not at others, and in some tests and not others with similar environmental conditions, is explained on the basis of local rates of attack. When local attack was sufficiently great, diffusion rates and corresponding hydrogen concentrations in the steel increased to the point at which hydrogen-carbon reactions were initiated and continued until significant decarburization and fissuring occurred.

Equally high corrosion rates were experienced with caustic attack as well as the acid attack discussed above. Hydrogen damage was not found under these conditions. This apparent contradiction is explained by the location of the cathode in the electro-chemical cell. Figure 59 illustrates the concentration gradient which occurs across deposits on heat transfer surfaces and the electro-chemical cells set up in the corrosive environments being discussed. Since both types of corrosion involve hydrogen ion reduction, hydrogen-ion concentration has a direct effect upon the site of the cathode. In the case of acid attack, the hydrogen ion concentration is highest under the deposit where the boiler water contaminants are concentrated. In the caustic corrosion situation, the hydrogen ion concentration is highest in the bulk stream since sodium hydroxide is concentrated within the deposit. With the cathode at a localized corrosion site under the deposit, sufficiently high hydrogen concentrations and diffusion rates are possible for the induction of hydrogen damage. These conditions were less likely to occur with the cathode at a location exposed to the bulk fluid.

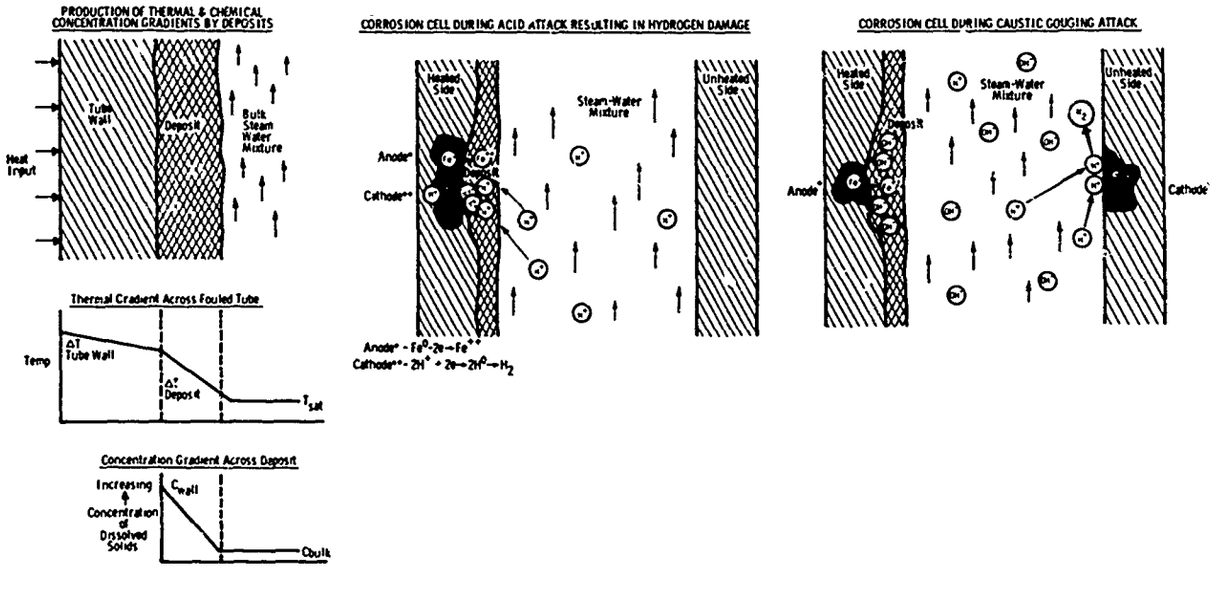

Fig. 59: Illustration of (a) temperature and concentration gradient at a fouled heat transfer surface (b) local corrosion cell in an acid environment (c) local corrosion cell in a caustic environment

Heat Transfer

Figures 4 and 5 indicate that departure from nucleate boiling can be characterized by either a critical heat transfer rate, $(Q/A)_{crit}$, or a critical local flowing mass quality, X_{crit}, sometimes listed as XDNB. An interpretation of the trends of these critical parameters can be developed by a review of the various physical phenomena leading to the critical conditions.

Observations of the boiling and nucleation phenomena on a heat-transfer surface show that there are only a few sites producing bubbles at low-heat-transfer rates. As the heat-transfer rate is increased, the number of nucleating sites also increases. It is found that, at higher heat-transfer rates, the steam being released from the now closely spaced nucleating sites no longer separates from the surface as bubbles, but forms a semi-stable blanket of steam. The heat-transfer process becomes severely limited by the formation of the steam blanket. This restriction to the heat-transfer system shows up as a significant increase in the temperature of the heat-transfer surfaces; *i.e.*, the boiler tubing being discussed here. The relative magnitude of this temperature increase is indicated on Fig. 4, where the tube metal temperature under conditions of DNB is compared to an assumed extrapolated condition of nucleate boiling.

The occurrence of steam blanketing, or DNB, can be correlated by an analysis of the rate of steam generation on the one hand and bubble release factors on the other. In general, the rate of steam generation, as a function of Q/A, can be characterized by physical phenomena: number of nucleating sites, size of bubbles, frequency of bubble release, and surface temperature. However,

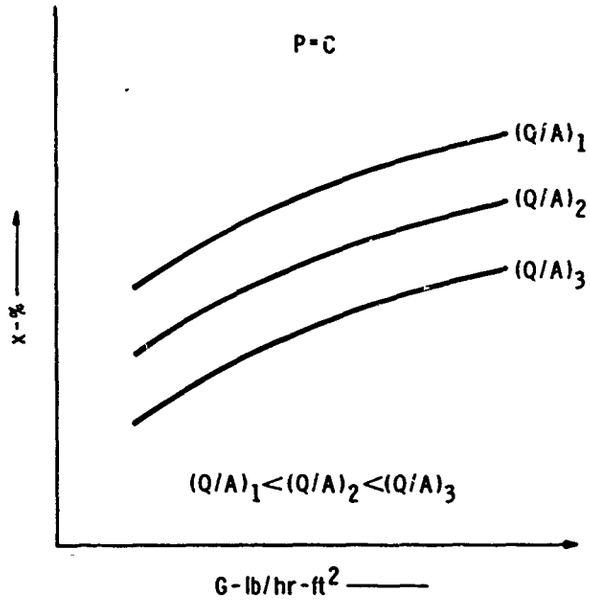

Fig. 60: Effect of heat-transfer rates on other critical DNB parameters

bubble size and release frequency are strongly controlled by the momentum of the bubble, fluid surface tension, and buoyancy. These factors will subsequently be described.

The momentum force is generated as the bubble grows through the resultant movement of its center of mass with respect to the surface. This force is perpendicular to the heat-transfer surface. Surface tension provides the primary control of the bubble size, but also contributes a release force when the bubble is pinched off. Buoyancy is, of course, a strong bubble release force, but is modified by surface orientation with respect to gravity. All of these factors are operative in non-flowing or "pool" boiling-heat-transfer systems. An additional factor which must be considered, in commercial steam generating equipment, is the beneficial momentum effect of the bulk fluid as it flows past the steam release surfaces. An overall interpretive analysis indicates that nucleate boiling exists when the bubble release mechanisms are capable of removing the volume of steam being produced.

The DNB data format presented in Fig. 5 has been expanded in Fig. 60 to include the relative effects of increasing heat transfer rates, (Q/A). The trends of Fig. 60 can be interpreted with respect to the above described phenomena.

At a given mass flow rate, G, the total weight of fluid flowing past a reference location, must be constant. That is, the weight of water *plus* the weight of steam is a constant irrespective of the local mass quality. Assuming a constant value of G, an increasing mass quality results in an increase in the mass flow of the steam phase and a corresponding reduction in mass flow of the liquid phase. Reducing the liquid mass flow rate then reduces the bulk fluid momentum effect in the bubble release system. The result is that $(Q/A)_{crit}$ must decrease with increasing steam quality at a constant mass-flow rate. It may also be seen from the above that increasing the total mass flow, G, of the mixture produces a beneficial effect on the critical DNB parameters, but not to the extent that might be expected. An interpretation of this data trend will be presented later.

Most of these processes which are related to the occurrence of DNB are periodic phenomena. The initiation of DNB, or steam blanketing, is, therefore, unstable because cyclic changes between nucleate boiling and steam blanketing occur. This periodic change of boiling mode produced the fluctuations in tube-metal temperature reported and illustrated in Figs. 6 and 61.

Phase I testing produced two other interesting results. First, the quality at which DNB was initiated was significantly higher than most of the data reported in the literature at that time. Second, as noted pre-

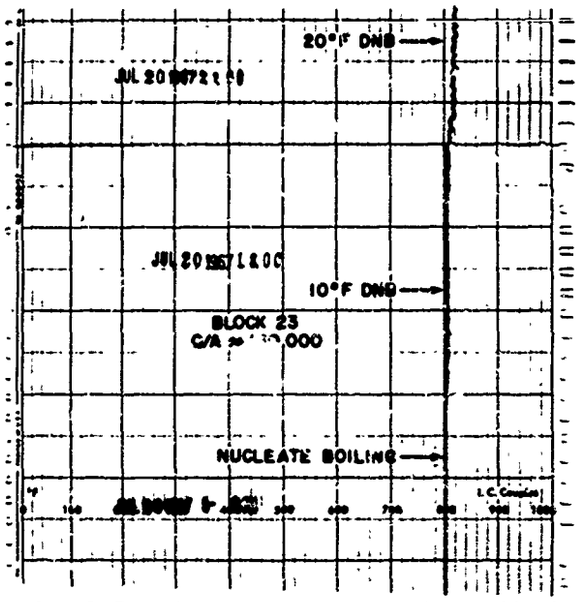

Fig. 61: Typical temperature response with control levels on DNB

viously, variations in mass flow did not have a very strong effect on the critical parameters.

Many sources have reported on the importance of the physical distribution of the steam and water phases in the boiling heat transfer system. Some consistency in the correlation of boiling heat transfer data was obtained by an evaluation of the two-phase flow regime. Flow regimes are typically described as subcooled boiling, babble flow, slug flow, annular flow, and mist flow. The interpretation derived from the results of Phase I was that commercial steam generating boiler tubing operates predominantly in the annular flow regime. In annular flow, most of the water moves along the inside surface of the boiler tube and most of the steam moves as a high-velocity core through the center of the tube. The steam phase can move through the boiler tube at a velocity two to five times faster than the water. A thermodynamic analysis shows that the steam quality in the boiling film of water on the tube walls can be significantly less than that indicated by a simple heat balance. In addition, the mass velocity of the mixture does not necessarily describe the mass velocity of the boiling film of water on the tube wall. The indications of the results of Phase I are that the imposed variations in mass flow primarily affected the high velocity steam core and, therefore, produced only a minimal effect on the DNB phenomena within the annular film of water on the tube wall.

Phase I test data indicated that the nucleate-boiling film temperature drop was in the range of 5 to 15 F for the heat transfer rate (Q/A) = 150,000 Btu per hr-sq ft. Hence, the equivalent heat transfer film coefficient, h, for this system ranges from h = 10,000 to 30,000 Btu per hr-sq ft-F. Published data indicate that the film coefficient associated with film boiling and DNB is in the range of from h = 500 to 1,000 Btu per hr-sq ft-F. The resultant temperature drop across the "boiling" film in DNB at the same heat flux is 150 F to 300 F. Table XXXI lists calculated metal temperatures for film boiling at the corrosion test conditions. These values are found to be consistent with the temperature trends shown by Fig. 6. The data indicate that, at $(Q/A)_{crit}$ or (XDNB), nucleate boiling conditions predominate on a time average basis.

TABLE XXXI

	Nucleate Boiling	Range to be Expected in Film Boiling or DNB (min)	(max)
t bulk fluid	674 F	674 F	674 F
Δt film	15 F	150 F	300 F
Δt tube wall	88 F	88 F	88 F
t outside tube surface	777 F	912 F	1062 F

Phase I established the normal boiling and critical heat-transfer parameters for clean boiler tubing. Phase III test procedures required that preboiler corrosion products, in the form of a slurry of black magnetic oxide and copper, be added to the loop. Shortly after the first introduction of the slurry, the "A" loop test section experienced DNB at the 30 to 35 percent operating quality conditions shown in Table III. It was found that the top quality, X_2 of Table III, had to be reduced to 26 to 29 percent to eliminate DNB. This condition was not expected on the basis of the Phase I results.

Figure 62 illustrates the variations in XDNB which occurred as a result of additions of corrosion products to the test loop. The initial reduction of the value XDNB increased to some intermediate level, but was subsequently reduced by further batch additions of contaminants.

A loop upset was experienced at 11:00 AM during the second day as shown in Fig. 62. The loop upset was initiated by a low-water condition in the drum and a

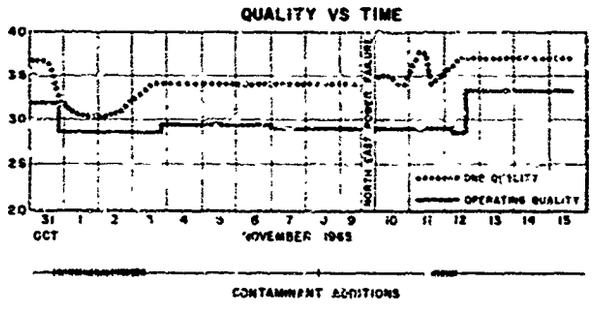

Fig. 62 History of critical quality with a "blac water" environment

TABLE XXXII

CORROSION SUMMARY

	Phase II			Phase III						Phase IV										
				A			B			C										
	1	2	3	1	2	3	1	2	3	1	2	3	1	2	3	4	5	6	7	8
No corrosion	X	X	X	X	X	–	–	–	–	–	–	–	–	–	–	–	–	X	X	–
Caustic attack	–	–	–	–	–	Total	Trace	Trace	Trace	–	–	X	–	–	X	–	X	–	–	–
Plug-type oxidation	–	–	–	–	–	–	–	–	–	X	X	X	X	X	X	X	X	–	–	Trace
Hydrogen damage	–	–	–	–	–	–	–	–	–	–	–	–	X	–	–	Total	Total	–	–	–

subsequent flow surge in the test sections. Contaminant materials, which had dropped out in the quiescent spaces of the drum, were re-entrained in the boiler water producing a massive black-water condition. The flow surge then produced a transient quality level in both of the test sections which at that time approached clean tube DNB quality.

The combined conditions of high quality and black water produced DNB which required immediate reduction in loop quality to prevent the occurrence of excessive tube-metal temperatures. X_1 had to be reduced to a 20 percent quality level to eliminate the DNB in the "A" loop. Once out of DNB, it was found that quality could then be immediately increased to the normal operating level of $X_1 = 28$ to 29 percent.

The data, produced by the loop transient, indicated the existence of a strong hysteresis effect. As a check, X_1 in the "A" loop was increased to produce DNB, which occurred at 35 percent quality. DNB could not then be eliminated until the quality was reduced to 31 percent. This last check was repeated several times with the same results, showing that a significant quality reduction was required to eliminate DNB with this black-water condition. On the basis of these results the operating levels of Fig. 62 were established.

Black-water DNB and the observed hysteresis effects are interpreted on the basis of the existence of a porous deposit on the heat-transfer surface. Apparently, nucleate boiling occurs under the porous deposit at normal conditions. However, a porous deposit creates a restraint on bubble release. Thus, DNB will occur at a lower gross quality than an equivalent clean-tube system. Further, once DNB is initiated, the steam film becomes stabilized by the deposit producing a more severe increase in temperature. The steam film is essentially trapped within the deposit and a significant reduction in quality is required to permit release of the steam. This gross reduction in quality is the observed hysteresis effect.

SUMMARY OF RESULTS OF PHASES II, III, AND IV

Table XXXII lists the results in terms of corrosion of the 20-test research program. Significant observations, many of which have previously been reported, are summarized below:

1. Deposition of boiler water contaminants, both simulated preboiler corrosion products and condenser leakage, occurred primarily on the heated portions of the test surfaces.
2. With few exceptions, preboiler corrosion products deposited from suspension.
3. The amount and location of preboiler corrosion-product deposition was affected by boiler-water treatment and the presence of condenser leakage.
4. Deposition of preboiler corrosion products was greater in the "A" loop (23 to 35 percent quality) than in the "B" loop (8 to 20 percent quality) at identical conditions of water chemistry, heat flux, mass velocity, and pressure. The formation of deposits resulting from condenser leakage was not appreciably affected by mixture quality; approximately equal amounts of these materials having been found at similar locations in both the "A" and "B" loops.
5. Within a four-block test section, deposition of preboiler corrosion products increased with mixture quality at constant heat flux (*i.e.*, block 20 > 19 > 18 > 17 and block 24 > 23 > 22 > 21). Deposition of condenser leakage constituents was not clearly affected by increasing mixture quality within each section.
6. Within each test section, the deposition of both preboiler corrosion products and condenser leakage was greater in the high-heat-flux zone (blocks 17 to 20, at 150,000 Btu per hr-sq ft) than in the low-heat-flux zone (blocks 21 to 24, at 110,000 Btu per hr-sq ft).
7. Within the range tested (0.45×10^6 to 0.55×10^6 lb per hr-sq ft), mass velocity had no discernible effect upon deposition or corrosion.
8. Volatile treatment permitted the formation of difficult to remove deposits. The deposits formed with this type boiler water treatment had higher concentrations of precipitated hardness and silicon compounds than with coordinated phosphate or free caustic boiler water.
9. Coordinated phosphate and free caustic treatment reduced the amount of deposition and resulted in less objectionable deposits from the standpoint of

cleaning when fresh-water condenser leakage was introduced to the test boiler.

10. No objectionable deposits, from the standpoint of quantity or composition, were formed on heat-transfer surfaces with continuous magnesium hardness injection when sodium phosphate control chemistry was maintained.
11. In all cases, when corrosion was experienced, prior fouling of heat-transfer surfaces was necessary for the initiation of attack. When heat-transfer surfaces were free of deposits, no corrosion occurred independent of heat-transfer conditions and water chemistry.
12. No corrosion occurred within a wide range of test conditions when sodium phosphate control chemistry was employed. Neither fouled surfaces and magnesium chloride injection nor fouled surfaces and DNB operation induced any attack.
13. When volatile treatment was employed with fouled heat-transfer surfaces and without condenser leakage, no corrosion occurred.
14. With free caustic boiler water treatment, the initial deposition of preboiler corrosion products on heated tube surfaces initiated caustic attack. Subsequent formation of additional deposits resulting from corrosion of the metal sustained and finally accelerated the corrosion rate.
15. Plug-type corrosion, and in some cases plug-type corrosion with hydrogen damage, occurred when acid producing condenser leakage was employed with fouled heat-transfer surfaces.
16. The pH reduction of boiler water resulting from condenser leakage caused corrosion and damage with all types of chemical treatment. However, corrosion rates could be effectively reduced by elevating the pH with sodium phosphate or sodium hydroxide. Once the heat-transfer surfaces had become sufficiently fouled, the introduction of sodium hydroxide to arrest corrosion resulted in caustic attack.
17. Phosphate hideout became more pronounced with the accumulation of deposits on heat-transfer surfaces. No corrosion was associated with its occurrence.
18. The chemical composition of deposits on heat-transfer surfaces varied significantly from those found on unheated areas.
19. Deposition of contaminants resulted in DNB where nucleate boiling had been experienced with clean test surfaces. This effect was temporary since it was observed that the depressed value of critical quality recovered over a period of several hours subsequent to the addition of contaminant.

CONCLUSIONS

Based upon the results of this "Research Study on Internal Corrosion of High Pressure Boilers" the following conclusions have been made:

1. The contamination of boiler water by condenser leakage can result in attack and corrosion failures of boiler tubing after relatively short periods of operation. The corrosivity of specific condenser coolants may be evaluated on the basis of data and observations presented in this report. Selection of methods of boiler water treatment, instrumentation for detection, automatic control and alarm systems, and a planned course of corrective action should be engineered based upon these factors.
2. Acid-producing condenser leakage can result in accelerated attack of boiler metal. If local corrosion rates are sufficiently high, hydrogen damage failures are likely. Ductile failures resulting from overheating at "plug-type" corrosion sites will occur in the same environment when local corrosion rates are less severe.
3. Ammonia is applicable for boiler water treatment only when there are no soluble boiler water contaminants. Volatile treatment provides little or no buffering action at high temperature, therefore, even low contaminant concentrations may create a corrosive environment. pH measurements are not valid control parameters under these conditions.
4. Sodium hydroxide solutions, when sufficiently concentrated, are aggressive to carbon steel boiler tubing. Normal caustic concentrations employed for boiler water treatment are not corrosive, but the concentrating effect of internal deposits can lead to accelerated attack.
5. Sodium phosphate proved to be the most effective boiler water treatment chemical evaluated in this research program. Maintenance of boiler water pH in the range of 9.5 to 10.0 and phosphate concentrations of from 5 to 10 ppm provided corrosion protection from potentially aggressive condenser leakage and minimized the deposition of calcium and magnesium compounds. Sodium phosphate was not aggressive to boiler metal even when concentrated to the limit of its solubility and hideout occurred within the matrix of deposits on heat-transfer surfaces.
6. Aggravated heat-transfer and flow conditions do not cause attack of boiler metal in the absence of an active corrodent. No detectable evidence of corrosion was found nor increases in corrosion rate observed after testing in the transitional boiling region beyond the threshold of departure from nucleate boiling for a two-week period

7. Major corrosion damage of high-pressure boiler tubing occurs as a result of fouled heat-transfer surfaces and an active corrodent in the boiler water. The thermal gradient across deposits produces increased corrodent concentrations within the deposit and corresponding increased rates of metal attack. The susceptibility of high-pressure boilers to major corrosion damage may be reduced by minimizing the ingress of deposit forming materials with the feedwater and by performing periodic removal of internal deposits.
8. Deposition of corrosion products on heat-transfer surfaces can produce an impairment to the normal boiling processes. Under this condition, a departure from nucleate boiling can be initiated below measured clean tube DNB parameters.

REFERENCES

1. H. A. KLEIN and J. K. RICE; "*A Research Study on Internal Corrosion of High Pressure Boilers*"; Transactions of the ASME, Journal of Engineering for Power, Volume 38, Series A, Number 3, July 1966.
2. P. GOLDSTEIN, I. B. DICK, and J. K RICE; "*Internal Corrosion of High Pressure Boilers*": ASME Paper No. 66-WA/BFS-10, Transactions of the ASME, Journal of Engineering for Power, Volume 89, Series A, No. 3, July 196[illegible].
3. P. GOLDSTEIN; "*A Research Study on Internal Corrosion of High Pressure Boilers*": ASME Paper No. 67-PWR-2; Transactions of the ASME; Journal of Engineering for Power. Volume 90. Series A. No. 1, January 1968.
4. M. E. MEEK: "*The Calculated pH of Aqueous Boric Acid Solutions as a Function of Temperature and Added Base Content*": U.S. A.E.C. Report WCAP-3265-51.
5. W. L. MARSHALL and E. V. JONES: "*Second Dissociation Constant of Sulfuric Acid from 25-350°C Evaluated from Solubilities of Calcium Sulfate in Sulfuric Acid Solutions*": Journal of Physical Chemistry, Vol. 70, No. 12, pp 4028-4040.
6. W. M. ROHSENOW; "*Developments in Heat Transfer*": MIT Press 1964. Chapter 8, Heat Transfer with Boiling.
7. F. KREITH; "*Principles of Heat Transfer*": International Textbook. 1967. Section 10-1. Fundamentals of Boiling Heat Transfer.